

UC Irvine

UC Irvine Electronic Theses and Dissertations

Title

C-H Activation for Use in Total Synthesis and Tandem Oxidation-Dehydroformylation

Permalink

<https://escholarship.org/uc/item/3wm8235q>

Author

Burt, Craig McLaughry

Publication Date

2015

Copyright Information

This work is made available under the terms of a Creative Commons Attribution-NoDerivatives License, available at <https://creativecommons.org/licenses/by-nd/4.0/>

Peer reviewed|Thesis/dissertation

UNIVERSITY OF CALIFORNIA,

IRVINE

**C–H Activation for Use in Total Synthesis and
Tandem Oxidation-Dehydroformylation**

THESIS

submitted in partial satisfaction of the requirements

for the degree of

MASTER OF SCIENCE

in Chemistry

by

Craig McLaughry Burt

Thesis Committee:

Professor Vy Dong, Chair

Professor James Nowick

Professor Suzanne Blum

2015

Table of Contents

Table of Contents	ii
List of Abbreviations.....	iv
List of Tables.....	viii
List of Figures	ix
List of Schemes	x
Acknowledgements	xii
Abstract	xiii
Chapter 1: Total Synthesis via C–H Activation-Desymmetrizing Hydroacylation	1
1.1 Introduction	1
Review of Total Synthesis via Ring Forming C–H Functionalization.....	1
Desymmetrization of α -Quaternary Stereocenters by Intramolecular Olefin Hydroacylation	16
Total Synthesis of (+)-Tanikolide	18
Total Synthesis of (-)-Adalinine.....	24
1.2: Results and Discussion	31
Efforts Towards the Total Synthesis of (+)-Tanikolide	31
Efforts Towards the Total Synthesis of (-)-Adalinine	35
1.3: Conclusions:	40
1.4 Supporting Information	41
General Experimental Information.....	41
General Procedures.....	42
Synthesis of Tanikolide Substrates.....	43
Synthesis of Adalinine Substrates	49
1.5 References.....	52
Chapter 2: Tandem Oxidation-Dehydroformylation of Alcohols	55

2.1 Introduction.....	55
2.2 Results and Discussion:	58
2.3 Conclusions:	67
2.4 Supporting Information	68
General Procedures.....	68
Synthesis of Substrates:.....	69
2.5 References.....	78
Appendix A: Spectral Information	79

List of Abbreviations

δ	chemical shift
$^1\text{H-NMR}$	proton NMR
$^{13}\text{C-NMR}$	carbon 13 NMR
BINAP	2,2'-bis(diphenylphosphino)-1,1'-binaphthyl
Bn	benzyl
Boc	<i>tert</i> -butyloxycarbonyl
br	broad
Bz	benzoyl
CDCl_3	deuterated chloroform
CI/MS	chemical ionization/mass spectroscopy
cod	1,5-cyclooctadiene
coe	cyclooctene
COSY	homonuclear correlation spectroscopy
Cp^*	pentamethylcyclopentadienyl
Cy	cyclohexyl
d	doublet
DavePhos	2-dicyclohexylphosphino-2'-(<i>N,N</i> -dimethylamino)biphenyl
dba	dibenzylideneacetone
DBU	1,8-diazabicyclo[5.4.0]undec-7-ene
dd	doublet of doublets
DCE	1,2-dichloroethane

DCM	dichloromethane
DMAc	dimethylacetamide
DMF	dimethylformamide
DMAP	4-dimethylaminopyridine
DMSO	dimethylsulfoxide
DPEN	diphenethylenediamine
DPEPhos	bis[(2-diphenylphosphino)phenyl] ether
dppp	1,3-bis(diphenylphosphino)propane
DTBM	di- <i>tert</i> -butylmethoxyphenyl
EDCI	1-ethyl-3-(3-dimethylaminopropyl)carbodiimide
Et	ethyl
EtOAc	ethyl acetate
g	grams
Gly	glycine
h	hours
Hex	hexanes
HMBC	heteronuclear multiple bond correlation
HMDS	hexamethyldisilazane
HMPA	hexamethylphosphoramide
Hz	hertz
<i>i</i> Pr	isopropyl
J	coupling constant
μg	micrograms

μL	microliters
M	molar
mCPBA	<i>meta</i> -chloroperoxybenzoic acid
Me	methyl
MeOBIPHEP	(R)-(-)-2,2'-bis[di(-4-methoxyphenyl) phosphino]-6-6'-dimethoxy-1,1'-biphenyl
mg	milligrams
mL	milliliters
mmol	millimoles
MSH	<i>o</i> -mesitylenesulfonylhydroxylamine
Nixantphos	4,6-bis(diphenylphosphino)phenoxazine
NMR	Nuclear Magnetic Resonance
NMO	N-methylmorpholine N-oxide
Ac	acetyl
PDP	(2S,2'S-(-)-[N,N'-bis(2-pyridylmethyl)]-2,2'-bipyrrolidinebis(acetonitrile)
PGME	phenylglycine methyl ester
Ph	phenyl
Piv	pivaloyl
ppm	parts per million
q	quartet
quinox	2-(4,5-dihydro-2-oxazolyl)quinoline
rt	room temperature
s	singlet

t	triplet
TBHP	<i>tert</i> -butylhydroperoxide
TBS/TBDMS	<i>tert</i> -butyldimethylsilyl
TLC	thin layer chromatography
THF	tetrahydrofuran
TFA	trifluoroacetic acid
TPAP	tetrapropylammonium perruthenate
Ts	tosyl
t-Bu	tertiary-butyl
<i>t</i> Bu-Xantphos	9,9-dimethyl-4,5-bis(di- <i>tert</i> -butylphosphino)xanthene
Walphos	(<i>R</i>)-1-[(<i>R</i>)-2-(2'-diphenylphosphinophenyl)-ferrocenyl]-ethyl-di-bis(3,5-trifluoromethylphenyl)phosphine
Xantphos	4,5-bis(diphenylphosphino)-9,9-dimethylxanthene

List of Tables

Table 1: Initial Parameter Screening for Reaction Optimization.....	59
Table 2: Base and Temperature Screening	62
Table 3: Preliminary Substrate Scope.....	65

List of Figures

Figure 1: Mechanistic Cycle for Desymmetrizing Olefin Isomerization-Hydroacylation	17
Figure 2: Proposed Alternative Desymmetrizing Hydroacylation.....	18
Figure 3: Proposed Mechanism for the Tandem Oxidation-Dehydroformylation.....	61

List of Schemes

Scheme 1: Srikrishna Synthesis of Angular Triquinanes	3
Scheme 2: Wang Synthesis of Cannabinol	4
Scheme 3: Brown Synthesis of Gracilioether F	5
Scheme 4: Cheng Synthesis of Arborinine	6
Scheme 5: Dictyodendrin B	7
Scheme 6: Knölker Strategy for the Synthesis of Carbazole Cores.....	8
Scheme 7: Structure of Murrayaline C, Murrafoline A, and Clauszoline-H	8
Scheme 8: Koert Synthesis of Fulcineroside	9
Scheme 9: Fröhlich Synthesis of Alternariol and Alternariol-Methyl Ether	10
Scheme 10: Li Synthesis of (±)-Goniomitine	12
Scheme 11: Cheng Synthesis of Papaverine	13
Scheme 12: Cheng Synthesis of Oxychelerithrine.....	14
Scheme 13: Baudoin Syntheses of Aeruginosins 98A-C and 298A	15
Scheme 14: Structure of Tanikolide	19
Scheme 15: Tanikolide Dimer	19
Scheme 16: Ogasawara Synthesis of Tanikolide	21
Scheme 17: Zhai Synthesis of Tanikolide	22
Scheme 18: Alternative Zhai Synthesis of Tanikolide	22
Scheme 19: Deng Synthesis of Tanikolide	23
Scheme 20: Retrosynthetic Analysis of Tanikolide	24
Scheme 21: Structure of (–)-Adalinine	24
Scheme 22: Biosynthesis of (–)-Adaline	26

Scheme 23: Biosynthesis of (–)-Adalinine	26
Scheme 24: Kibayashi Synthesis of Adalinine	28
Scheme 25: Honda Synthesis of Adalinine.....	29
Scheme 26: Retrosynthesis of Adalinine	30
Scheme 27: Synthesis of Aldehyde 79	31
Scheme 28: Hydroacylation of 79.....	32
Scheme 29: Initial Synthetic Approach to Tanikolide.....	32
Scheme 30: Revised Synthetic Strategy towards Tanikolide	33
Scheme 31: Baeyer-Villiger Oxidation of Pinacolone Model System	34
Scheme 32: Attempted Baeyer-Villiger Oxidation of Ketone 76.....	34
Scheme 33: Hydroacylation of Aldehyde 102.....	35
Scheme 34: Attempted Beckmann Rearrangement of Pinacolone Model System.....	36
Scheme 35: Beckmann Rearrangement of Pinacolone Model System.....	36
Scheme 36: Wacker Oxidation of 2-Octene Model System.....	38
Scheme 37: Projected Synthesis of Adalinine	38
Scheme 38: Rh-Catalyzed dehydroformylation of aliphatic aldehydes.....	55
Scheme 39: Oxidation-Dehydroformylation of Alcohols.....	56
Scheme 40: Generation of Odd-Numbered Olefins from Even-Numbered Acids	57
Scheme 41: Standard Conditions in Initial Screening	59
Scheme 42: Conditions for Tandem Oxidation-Dehydroformylation Following Initial Screening	60

Acknowledgements

First, I would like to thank Professor Vy Dong for accepting me into her group and providing me the opportunity to study organometallic C–H activations. Vy and Wilmer have been very helpful and supportive of me during my time in the group. I really appreciate their support throughout my journey in the group.

I would also like to thank my committee for taking time to read my thesis and for their advice along the way. Professor Nowick has always been a friendly source of advice and support. My experiences in his spectroscopy class have made me a far more confident chemist and I would like to thank him for his help. Professor Blum has also been friendly and supportive, and I appreciate her taking the time to help with my thesis. Phil Dennison and John Greaves also provided a great deal of help in the NMR facility and the mass spectrometry facility. I would also like to thank Professor Liz Jarvo for her help, her advice, and her recommendations. Professor Jen Prescher and Professor Chris Vanderwal also have my thanks for their advice in this transitional period.

I also need to thank the members of the Dong group for their support and help along the way, especially my mentors: Aaron, Qing-An, Faben, and Jung-Woo; you guided me and provided great feedback through my time in the group. The entire group has been supportive and I appreciate all of your help. Zhiwei and Jan have always been willing to discuss ideas and have been very supportive. Thank you Dan, Diane, and Faben for being role models and for providing helpful advice along the way. In addition, I would like to thank the NIH for their funding for our research.

Thank you to all of my friends and fellow graduate students at UCI. I have enjoyed your company in the lab and out. Tyler and David, thank you for always being there to grab a coffee and bounce ideas around. Roy, thank you for getting me to laugh and think at the same time. Thank you all for going hiking with me while still thinking about chemistry and coming up with new ideas while getting some fresh air.

Finally, I need to thank my family for their support. David, you are the best brother I could hope to have, and even three time zones away you are still there for me with a joke to lift my spirits. Mom and Dad, I cannot even begin to thank you enough for everything you do for me. You have always been behind me, supporting me in my goals and your love is invaluable. Aunt Ellen, thank you so much for everything: dinners, advice, walks, and everything else. You have been a huge help throughout this past year and I cannot fully express my gratitude to you for all you have done and continue to do. Aunt Sarah and Uncle Mario, thank you so much for your support and help, I have really enjoyed being able to spend more time with you over the past year and you have always lifted my spirits, thank you. I could not have reached where I am without all of you.

Abstract

C–H Activation for Use in Total Synthesis and Tandem Oxidation-Dehydroformylation

By

Craig McLaughry Burt

Master of Science in Chemistry

University of California, Irvine, 2015

Professor Dong, UC Irvine, Chair

Chapter 1 focuses on the use of C–H activation in total synthesis and the strategies that these methods enable. Following a review of recent total syntheses using C–H activation to form a variety of rings, we discuss our efforts towards two total syntheses using C–H activation methodology. In this instance, desymmetrizing olefin hydroacylation offers a method to generate quaternary stereocenters on cyclic ketones in a rapid manner with high atom economy. The resulting cyclic scaffolds were used to develop a formal synthesis of the natural product (+)-tanikolide, a cyanotoxin from *lyngbya majuscula*, and in efforts towards the total synthesis of (–)-adalinine, an alkaloid natural product isolated from *adalia bipunctata* and *adalia decempunctata*.

Chapter 2 describes recent efforts to use aldehyde C–H activation in a tandem oxidation-dehydroformylation reaction that we have worked to develop. This new methodology offers the ability to directly transform primary alcohols directly to olefins while cleaving a carbon-carbon bond, a previously undocumented transformation.

Chapter 1: Total Synthesis via C–H Activation-Desymmetrizing

Hydroacylation

1.1 Introduction

Review of Total Synthesis via Ring Forming C–H Functionalization

The activation of C–H bonds has been a major focus of research in transition metal-catalysis and in synthetic methodology. While C–H bonds are typically viewed as relatively inert, the ability to activate these bonds chemoselectively offers the opportunity to rapidly increase functionality from simple C–H bonds without the need for other complex functionalities to be present in the molecule. Thus, C–H activation strategies in synthesis offer the possibility to improve efficiency by decreasing the number of steps, improving atom economy, and avoiding many of the unnecessary functional group interconversions that are necessary in traditional synthetic strategies.¹

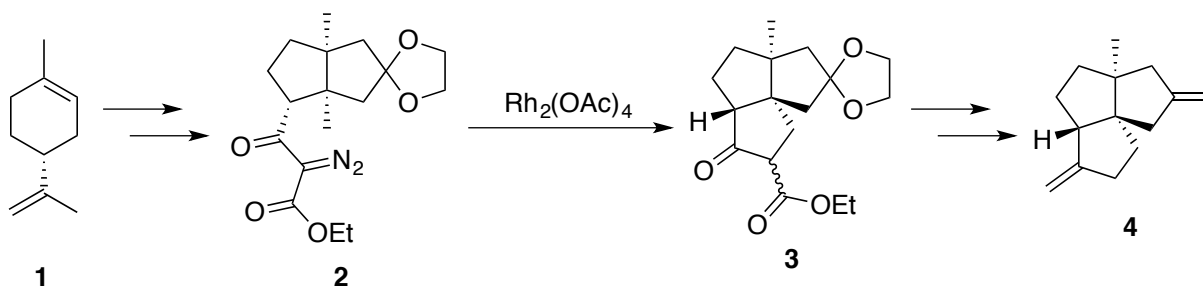
C–H activation has been a topic of study in total synthesis since 1909 with the Löffler synthesis of nicotine, which used radical decomposition of N-haloamines to activate aliphatic C–H bonds for subsequent halogenation.² However, C–H activation only began to be used frequently in total syntheses beginning in the 1970's and 1980's with the advent of organometallic reagents for C–H activation; Trost and others developed a number of transition metal catalysts to activate aryl C–H bonds for intramolecular cyclizations during this period.³ Subsequent expansion of C–H activation methodology has led to an explosion in the number of syntheses featuring these methods in recent years. These syntheses use C–H activation for rapid

increases in the complexity in early stages of their synthetic routes, and also to generate functionalities that would otherwise be difficult to establish in the late stages of the syntheses.¹

Carbocycles and heterocycles are key structures in many natural products and drug candidates, and, as such, are of great interest as targets in C–H activation.⁴ The ability to form these rings via C–H activation is of great interest in synthesis and has been a major focus of recent methodological development. In addition, many of these new methods have been applied in the total synthesis of natural products to generate the cyclic cores of these structures. These syntheses feature a number of strategies to form the desired rings, including oxidative cyclizations of diazo compounds, aryl-aryl linkages, annulations, alkenylations, lactonizations, and aminations. A variety of inter- and intramolecular strategies can be used to generate these rings. Over the past five years, these C–H activation methods have been implemented in a large number of syntheses, demonstrating the development of a large number of new synthetic strategies that have only become possible in the last few years with the development of these methods.

Oxidative cyclization via C–H activation provides rapid access to rings in previously unactivated systems, making the generation of carbon-carbon bonds to close carbo- and heterocycles. Unlike many other C–H activation methods, this method does not require heteroatoms in the ring and can activate sp^3 -hybridized carbons without the need for a directing group. This type of method was recently highlighted in the Srikrishna synthesis of the cores of angular Triquinanes (Scheme 1).⁵ The key to the core of this class of natural products, diazo-ketoester (**2**), was generated from limonene (**1**) in 11 steps. Diazo-ketoester **2** was used in the key sp^3 -hybridized C–H activation oxidative cyclization reaction to generate cyclopentanone **3** and complete the core of the desired natural products. Deprotection and Wittig olefination of **3**

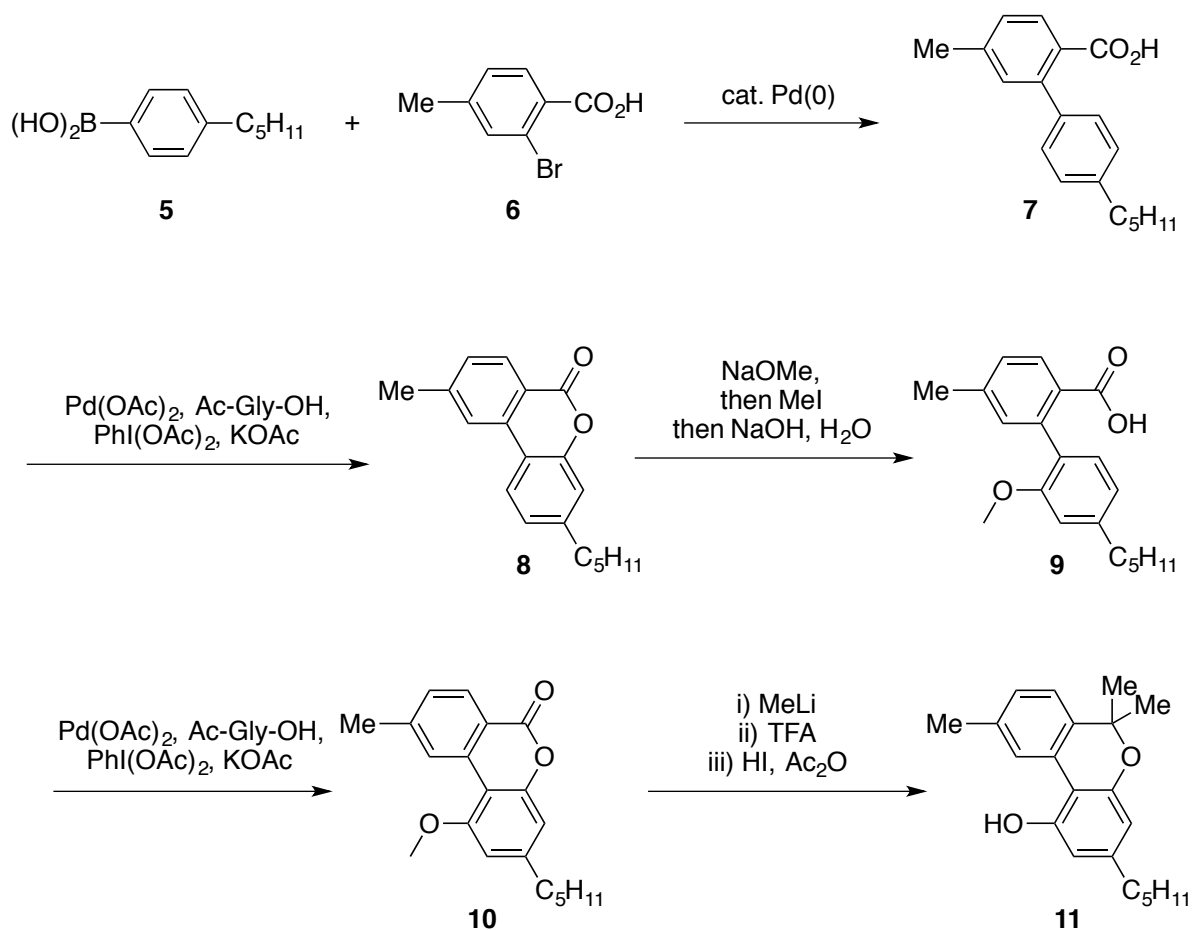
afforded diene **4**, which is both norsilphiperfolane and norcameroonane, and could be used to generate a number of sesquiterpene natural products and derivatives via methylations.



Scheme 1: Srikrishna Synthesis of Angular Triquinanes

This synthesis of sesquiterpene cores demonstrates the value of oxidative cyclization methods to establish carbocycles in total synthesis strategies with relatively high atom economy and high selectivity for a difficult C–H activation.

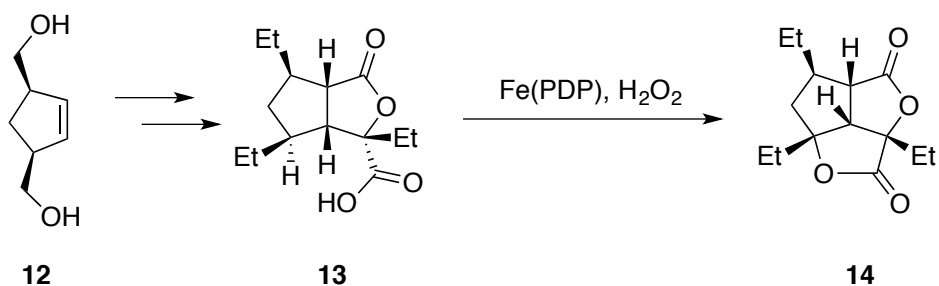
Lactones are commonly featured structures in a wide variety of natural products. However, these rings are frequently unstable, and require late-stage installation in traditional synthetic methods, often through inefficient routes. However, C–H activation-lactonization methods from carboxylic acids have recently been developed and applied in a number of total syntheses, including the Brown synthesis of gracilioether F and the Wang synthesis of cannabinol (Scheme 2).⁶ This methodology only requires generation of a carboxylic acid in the desired location for the lactone ring, requiring no additional functional group interconversions and maintaining a high degree of atom economy compared to traditional lactonization methods.



Scheme 2: Wang Synthesis of Cannabinol

In the Wang synthesis, cannabinol, **11**, was synthesized via a Suzuki-cross coupling of **5** and **6**, followed by a palladium-catalyzed lactonization of **7** via C–H activation of an aryl ring to generate **8**. One-pot ring opening, methylation, and hydrolysis afforded acid **9**, which could then undergo lactonization again via C–H activation, generating **10**. Subsequent dimethylation, dehydration, and deprotection afforded **11** in a longest linear sequence of 7 steps and an overall yield of 18%.^{6b}

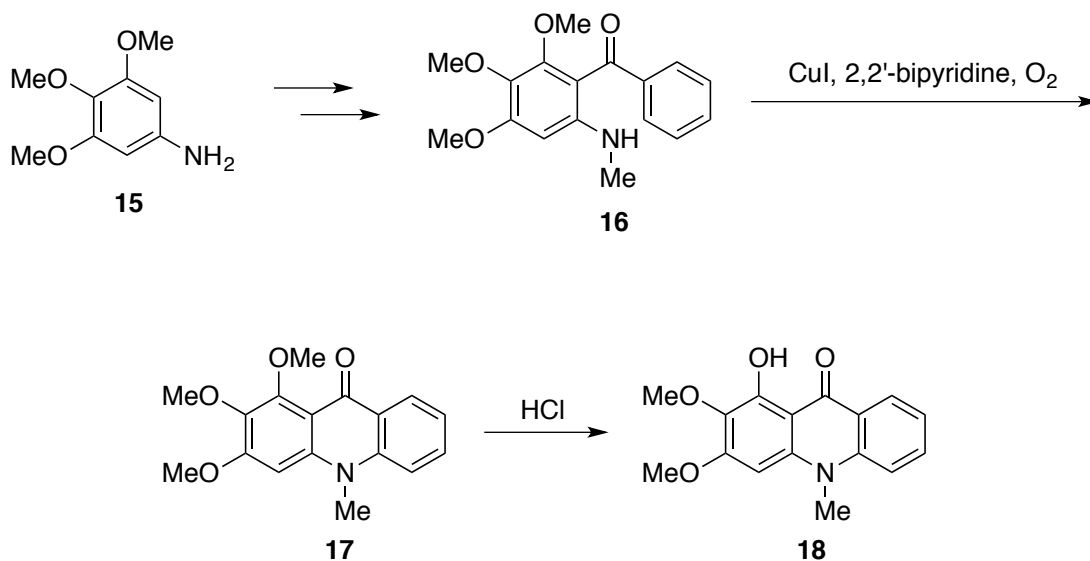
Similarly, Brown established a route to gracilioether F (**14**) via an iron-catalyzed C–H activation-lactonization from carboxylic acid **13** at an sp^3 -hybridized carbon center without loss of stereochemistry to generate gracilioether F (**14**), as shown in Scheme 3.^{6a}



Scheme 3: Brown Synthesis of Gracilioether F

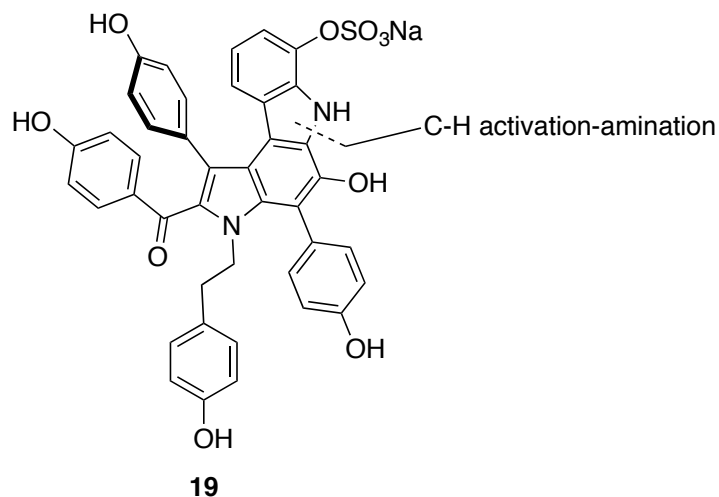
Although the yield for the reaction was generally quite low, this was mainly due to steric limitations from the substrate preventing high conversion. The reaction generally maintained high yields based on recovered starting material, as well as high selectivity, preferring the desired C–H selectivity based on its greater electron density and tertiary position. This method provided a concise route to gracilioether F in a longest linear sequence of 8 steps and an overall yield of 9.3%.

The ability to activate C–H bonds to form amines is of significant interest for synthetic chemists, as amines and other nitrogen-containing heterocycles are featured prominently in many natural products and drug candidates.⁴ While oxidative cyclizations between aryl rings are commonly used to generate nitrogen-containing heteroaromatics, C–H activation-amination methods such as the Buchwald-Hartwig amination are also frequently used to generate heterocycles in total syntheses.⁷ The Cheng synthesis of arborinine also uses a ring-closing C–H activation-amination methodology.⁸ This route to arborinine begins with the synthesis of bis-aryl ketone **16** from aromatic amine **15**. Ketone **16** can then be used in a copper-catalyzed intermolecular amination to rapidly generate 2-aminobenzophenone **17**. Finally, selective deprotection of the *ortho* methyl ether of **17** to reveal the alcohol afforded arborinine (**18**) in a longest linear sequence of 6 steps with an overall yield of 43% (Scheme 4).



Scheme 4: Cheng Synthesis of Arborinine

Another significant recent total synthesis prominently featuring C–H activation-amination is the Gaunt synthesis of dictyodendrin b (**19**) (Scheme 5).⁹ The Gaunt synthetic route relies heavily on a variety of different C–H activations, including C–H arylation, borylation, and amination, demonstrating the versatility of these methods in synthesis. By using these C–H activations, Gaunt quickly built complexity while avoiding the need for protecting groups or functional group interconversions in the manner that would be necessary in traditional synthetic routes.

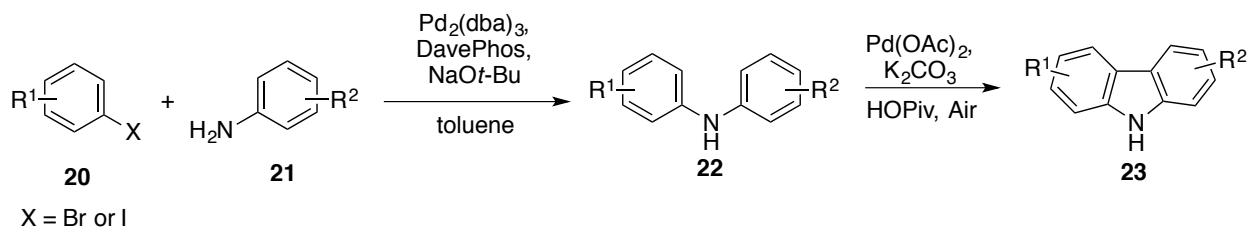


Scheme 5: Dictyodendrin B

The dense aryl core of **19** would be difficult to generate via traditional coupling reactions with any control. However, this C–H activation strategy allowed Gaunt to generate dictyodendrin b in a total of 13 steps longest linear sequence and an overall yield of 0.7%.

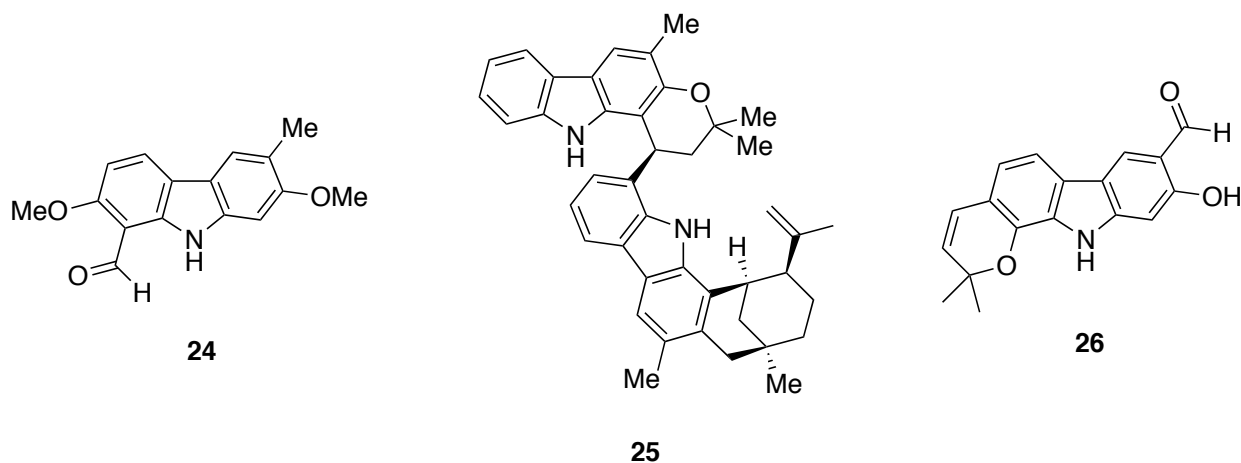
The most commonly used C–H activation-cyclization strategy used in total synthesis in the past five years is aryl-aryl linkage to generate extended aromatic systems. This strategy offers far greater atom economy than traditional cross-couplings can offer, since it does not require stoichiometric organometallics. One of the most commonly employed strategies using these methods in recent total syntheses is the generation of dibenzopyrrole and dibenzofuran rings via C–H activation-dehydrogenation. This strategy is a particularly useful route to heterocycles since it allows for a high degree of convergency in the synthesis of natural product cores. Over the past five years, the Knölker group has been particularly prolific using this strategy, performing the total synthesis of fifteen different heterocyclic natural products with their methodology (Scheme 6).¹⁰ The Knölker strategy to access the core of these natural products is based on a cross-coupling Buchwald-Hartwig amination of **20** with **21** followed by a

dehydrogenative ring-closing aryl linkage between the two benzene rings in **22** using air as the terminal oxidant, producing carbazole **23**.



Scheme 6: Knölker Strategy for the Synthesis of Carbazole Cores

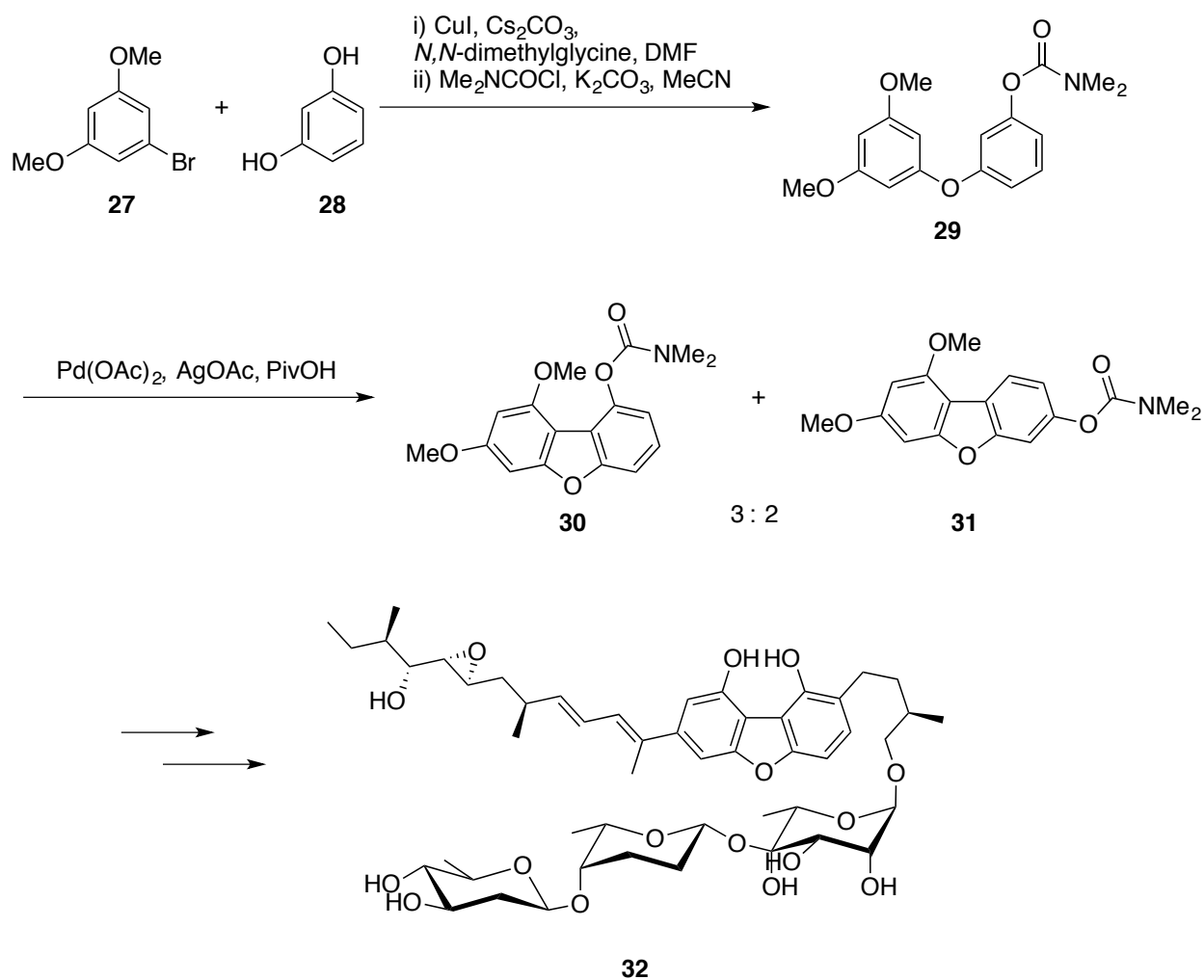
This strategy is particularly robust, allowing the Knölker group to generate products with a variety of substitution patterns rapidly before installing other functionality. Included in these latest fifteen natural products are murrayaline C (**24**), murrayaline A (**25**), and clauszoline-H (**26**), shown in Scheme 7.



Scheme 7: Structure of Murrayaline C, Murrayaline A, and Clauszoline-H

These natural products demonstrate the versatility of this synthetic strategy to generate carbazole cores of natural products with a variety of different substitution patterns. In the case of the murrayaline family of natural products, the Knölker group was able to use this strategy twice for each natural product to generate both carbazole rings, making these synthetic routes highly economical in terms of both steps and atoms. The Knölker synthetic strategy is an excellent example of C–H activation for aryl-aryl bond formation in the total synthesis of natural products.

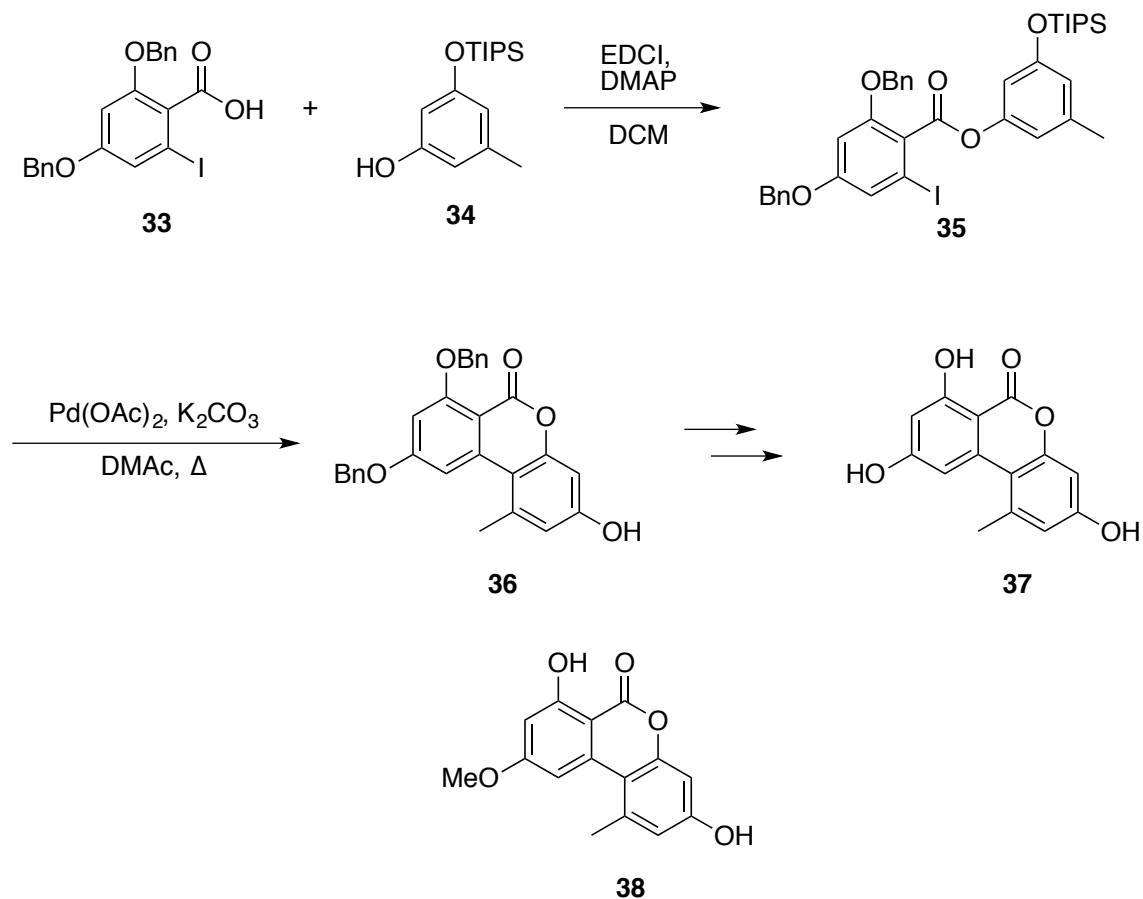
The Koert synthesis of fulcineroside (**32**) used a similar strategy to generate the core of the natural product.¹¹ Ullman-type coupling of alcohol **28** with bromide **27** and subsequent carbamate protection of the free phenol produced bisaryl ether **29**, which was then closed via a dehydrogenative double C–H activation using silver acetate as the terminal oxidant to generate a mixture of the desired product, **30** and the undesired regioisomer **31** (Scheme 8). Although this reaction only demonstrates moderate regioselectivity, the ability to link the two halves of the core allows for rapid increases in complexity while maintaining atom economy to a far greater extent than traditional synthetic strategies would allow.



Scheme 8: Koert Synthesis of Fulcineroside

Following the synthesis of **30**, which completed the core of fulcineroside, the Koert group used a variety of transformations to complete the synthesis in fourteen more steps via a highly convergent strategy, generating separate polyketide and glycosidic chains for attachment to the central aromatic core. This synthetic strategy generated the desired natural product, fulcineroside (**32**), in a longest linear sequence of 21 steps with an overall yield of 3.0%.

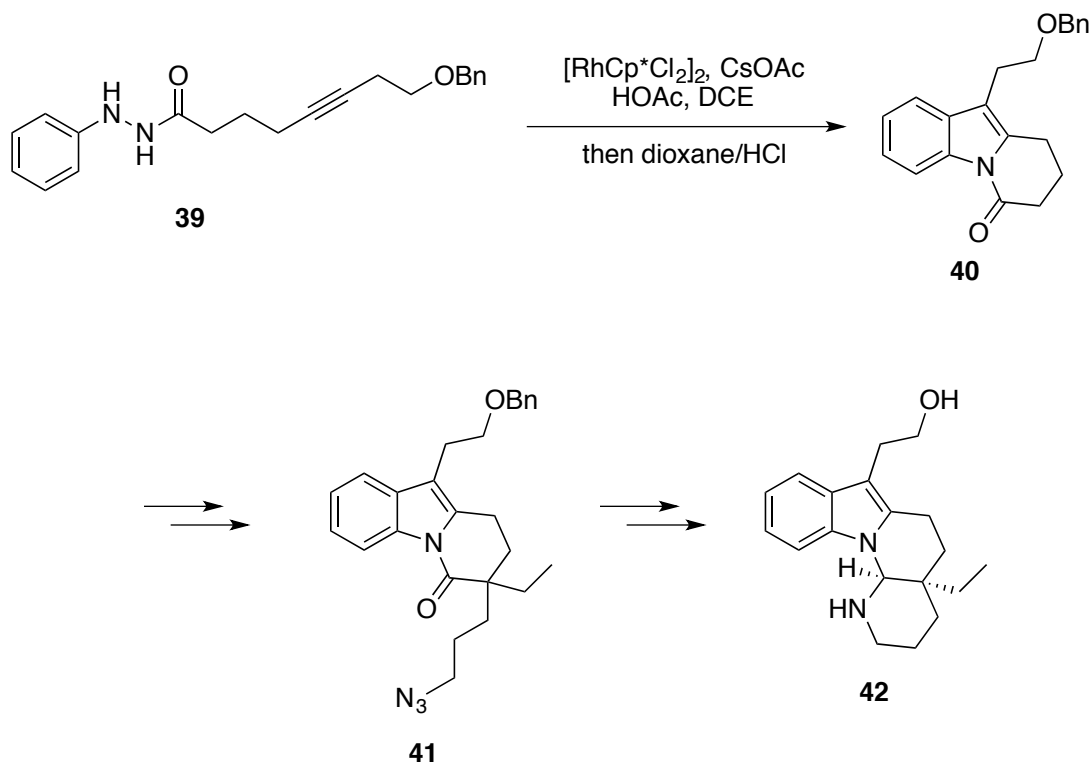
Another class of aryl-aryl linkage via C–H activation is the generation of lactone rings from bis-aryl esters. This synthetic strategy was recently used in the Fröhlich syntheses of alternariol and alternariol-methyl ether, two natural products featuring six-membered, bis-aryl lactone rings.¹² Linkage of alcohol **34** and acid **33** via esterification provided a simple way to link the two aryl systems, forming ester **35** (Scheme 9).



Scheme 9: Fröhlich Synthesis of Alternariol and Alternariol-Methyl Ether

Use of ester **35** in the key C–H activation ring-closing transformation afforded lactone **36**, which formed the core of the two natural products. Deprotection afforded the desired natural product, alternariol (**37**), demonstrating the value of this strategy to generate lactone cores containing two aryl rings rapidly, with high atom and step economy. Alternariol-9-methyl ether (**38**) was also synthesized using this strategy, with the only difference being the use of a different protecting group strategy to allow for the selective generation of the methyl ether in the natural product.

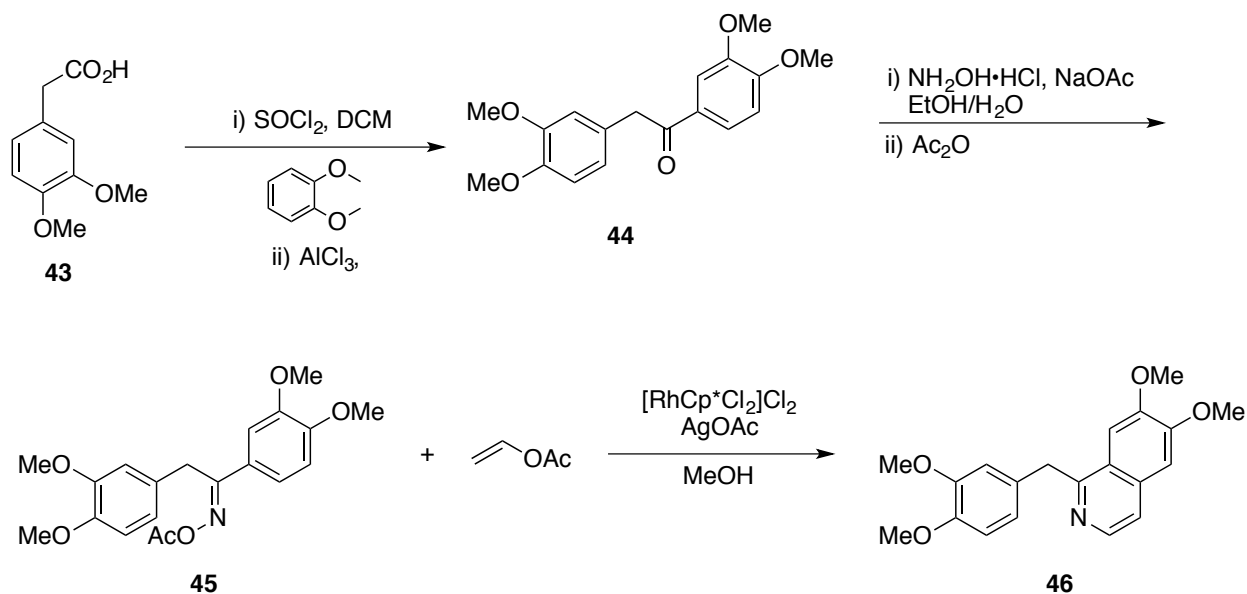
Over the past five year, alkene and alkyne annulation has become a common C–H activation strategy to form a variety of rings, offering a route to build hetero- and carbocycles with high atom efficiency and step economy. This strategy has been featured prominently in a number of total syntheses in the past five years. Of particular note, these annulation reactions develop nitrogen-containing heterocycles such as indoles, indolizines, and isoquinoline rings, which have been used extensively in total syntheses over the past several years. Alkyne annulation to form indoles offers a route to generate valuable heterocycle cores with convergency and the ability to prefunctionalize these aryl rings with a high degree of control over site selectivity. The synthetic strategy enabled by these types of C–H activation-annulation methods can be seen clearly in the Li synthesis of (±)-goniomitine, which used an intramolecular C–H activation to generate indoles from alkynes in a highly efficient manner (Scheme **10**).¹³ In the Li synthesis, diazoamide **39** was converted to indole **40** via their annulation methodology, simultaneously generating two of the rings in the core.



Scheme 10: Li Synthesis of (±)-Goniomitine

Functional group conversions and two enolate additions generated the quaternary center of (±)-goniomitine and allowed for the formation of azide **41**. Reductive ring closing of **41** via lithium aluminum hydride and deprotection of the alcohol afforded (±)-goniomitine, **42**. In total, the Li synthesis of **42** had a longest linear sequence of seven steps with an overall yield of 9%.

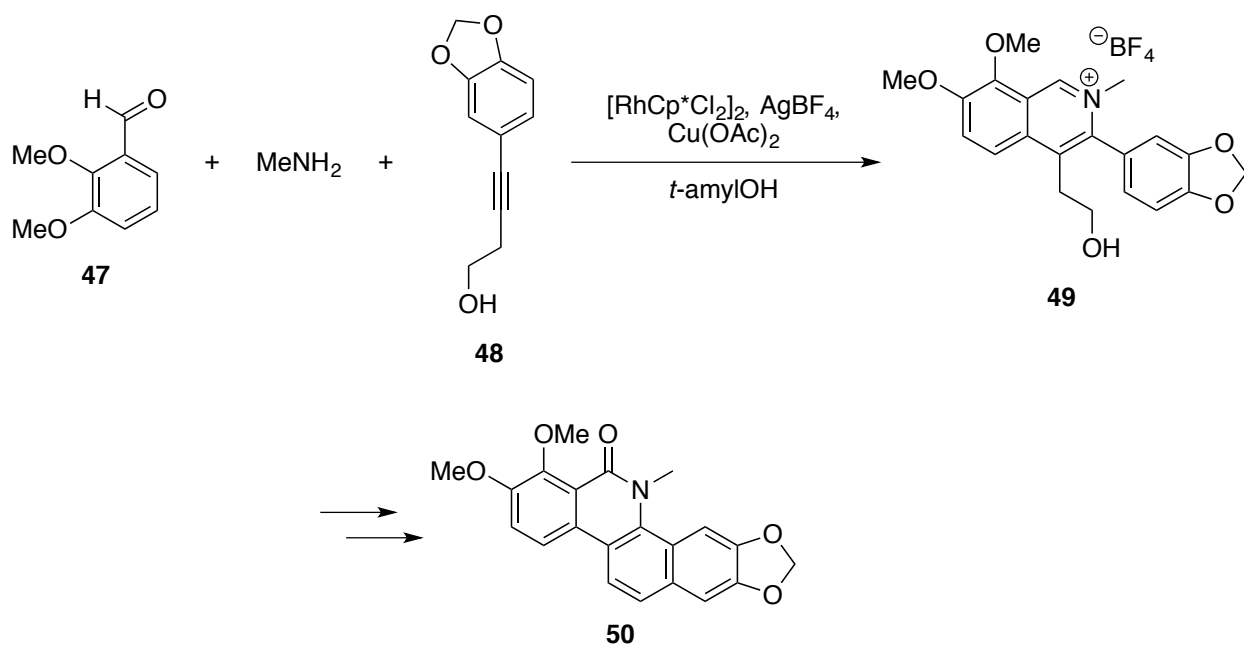
Isoquinoline rings can be easily generated via C–H activation-annulation strategies to introduce convergency and build complexity rapidly. Annulations to generate isoquinolines have been used in a number of recent total syntheses, including the J. Cheng synthesis of papaverine and the C.-H. Cheng synthesis of oxychelerithrine (Scheme **11**).¹⁴ The J. Cheng synthesis of papaverine began with the generation of aryl ketone **44** from acid **43** via Friedel-Crafts acylation. Ketone **44** was then condensed with hydroxylamine and acetylated to generate oxime acetate **45**.^{14a}



Scheme 11: Cheng Synthesis of Papaverine

The key annulation step of the synthesis was then performed using vinyl acetate and oxime acetate **45** to generate the isoquinoline **46**, completing the synthesis of papaverine in a longest linear sequence of 5 steps and an overall yield 32.5%.

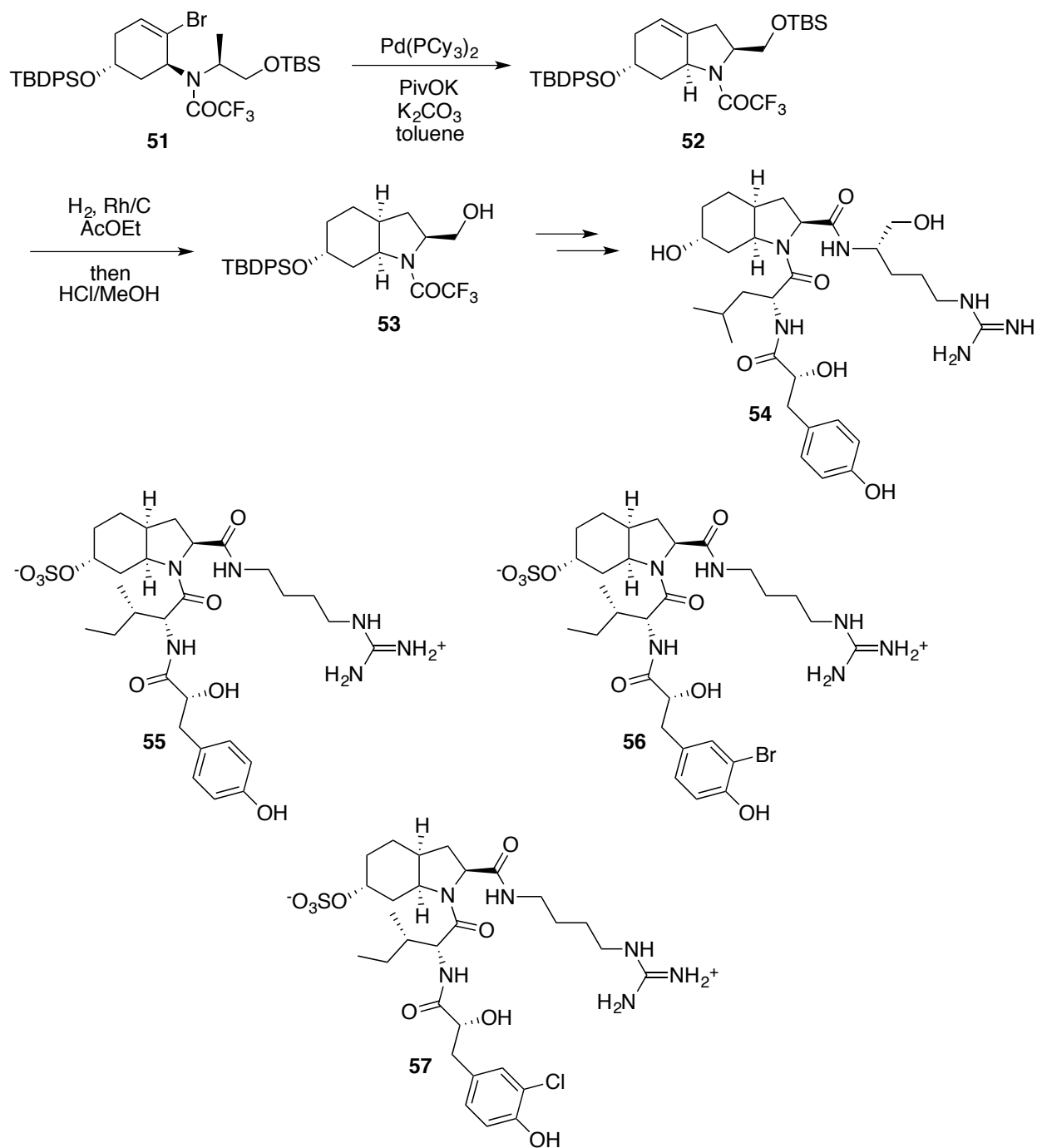
Unlike the synthesis of papaverine, the C.-H. Cheng synthesis of oxychelerithrine used an early stage isoquinolinium-forming C–H annulation to rapidly generate the core of their compound rapidly (Scheme **12**).^{14b} One-pot condensation of methylamine into aldehyde **47** and rhodium-catalyzed alkyne annulation with alkyne **48** formed isoquinolinium salt **49**.



Scheme 12: Cheng Synthesis of Oxychelerithrine

Functional group interconversion and acid-catalyzed dehydration-aromatization generated oxychelerithrine, **50**, in a longest linear sequence of four steps and an overall yield of 38.2%. This synthesis demonstrates the value of C–H activation-annulation strategies to rapidly build the core of a target compound early in a synthesis.

Ring formation via C–H activation-alkenylation is a highly desirable strategy for the generation of rings in total synthesis. The ability to use olefins to generate rings is a highly desirable transformation, particularly if these transformations result in the generation of new stereogenic centers. C–H activation-alkenylation methods have been used in the Baudoin synthesis of aeruginosins 98A (**57**), 98B, (**55**), 98C (**56**) and 298A (**54**).¹⁵ These four total syntheses all rely heavily on an intramolecular C–H activation-alkenylation of **51** to generate the common hexahydroindole ring **52** which was then hydrogenated to yield the octahydroindole core of the natural products (**53**), as shown below in Scheme **13**.



Scheme 13: Baudoin Syntheses of Aeruginosins 98A-C and 298A

This core was then joined to various peptide side chains to generate these natural products efficiently and with high selectivity. The C–H activation used in this synthesis is notable for its ability to activate C–H bonds attached to sp^3 -hybridized carbons to generate a new C–C bond

without the need for a directing group while tolerating protected amines and alcohols. The Badouin syntheses of aeruginosins were able to generate the desired core for the natural products rapidly.

Recent developments in C–H activation-cyclization methodologies have allowed for significant advances in the ability of synthetic chemists to perform highly economical synthesis, particularly in the formation of rings. Many of the examples above were the shortest syntheses of these natural products to date, usually due to the significant increases in complexity that are possible with C–H activation methodologies. Although some of these C–H activations have low yields or only moderate selectivity for the desired product, the increases in complexity and the atom economy of these strategies still make many of them valuable tools to plan and accomplish a synthetic route.

Desymmetrization of α -Quaternary Stereocenters by Intramolecular Olefin

Hydroacylation

Recently, our group has developed an olefin hydroacylation method that activates aldehydic C–H bonds and hydroacylates olefins to form chiral cyclopentanones via desymmetrization.¹⁶ α -Bis-allyl aldehydes are activated by a rhodium (I) catalyst with a chiral bisphosphine ligand to generate an acyl-rhodium (III)-hydride. This rhodium hydride then isomerizes one of the olefins preferentially via an insertion and a rare endocyclic β -hydride elimination to desymmetrize the stereocenter and generate an internal olefin. This olefin acts as a directing group, binding to the regenerated rhodium hydride and promoting insertion of the rhodium into the other olefin. Subsequent reductive elimination regenerates the rhodium (I) catalyst and forms the cyclopentanone product.

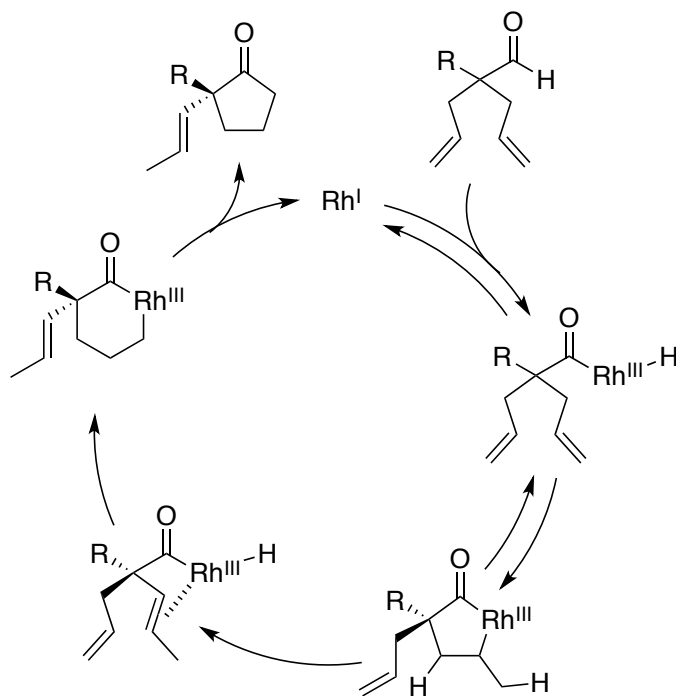


Figure 1: Mechanistic Cycle for Desymmetrizing Olefin Isomerization-Hydroacylation

Interestingly, the mechanism seems to vary slightly depending on the identity of the non-allyl substituent at the α -position. In the case of aromatic substituents, the olefin isomerization always occurs early in the mechanism, as outlined in the mechanism in figure 1. However, aliphatic substituents show a mixture of isomerized and non-isomerized olefin products, indicating that the transformation can take place through an alternative mechanistic cycle that does not require initial isomerization to generate the internal olefin, shown below in figure 2.

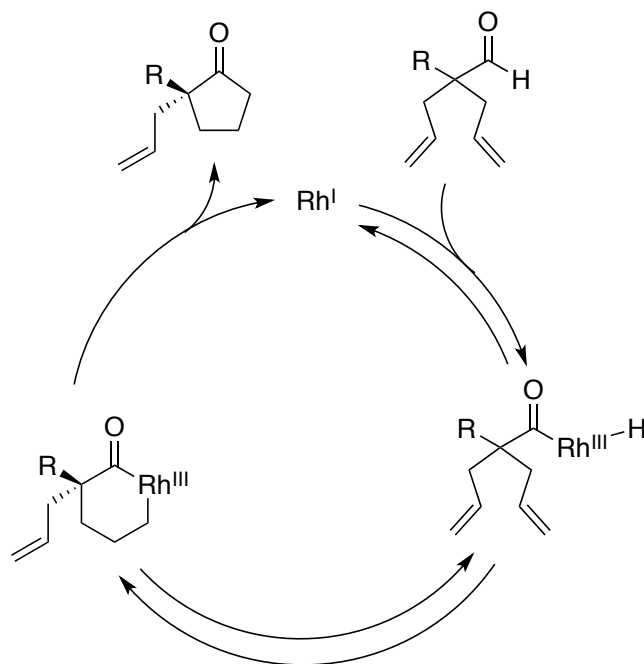


Figure 2: Proposed Alternative Desymmetrizing Hydroacylation

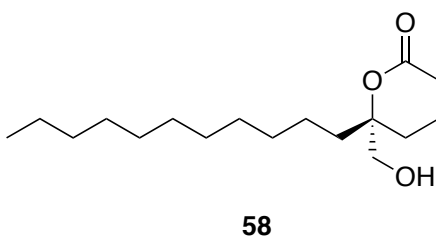
In this instance, it is possible that the mixture of products may occur solely via the mechanism shown in figure 2, followed by isomerization of the olefin. Alternatively, the catalyst may be able to undergo both the mechanistic cycles shown in figures 1 and 2, producing a mixture of the two products.

During the development of this method of C–H activation, we realized that the possibility of using this reaction to form chiral cyclopentanones could be used to rapidly generate the cores of chiral natural products with high enantioselectivity.

Total Synthesis of (+)-Tanikolide

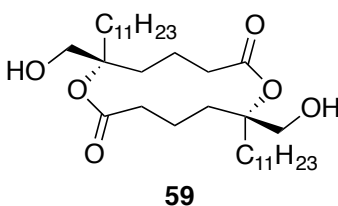
The first target for total synthesis via our C–H activation-hydroacylation strategy was tanikolide. Tanikolide (**58**) is a marine natural product isolated from the cyanobacterium *Lyngbya majuscula* (Scheme 14).¹⁷ Tanikolide was first identified as a target of interest

following brine shrimp bioassays showing strong toxicity of 100% death at a concentration at 10 ppm and an LD₅₀ of 3.6 µg/mL, while showing no toxicity towards goldfish. Further assays demonstrated that tanikolide is also a potent antifungal agent when tested against *Candida albicans*, inhibiting fungal growth in a 13 mm diameter zone when treated with 100 µg per disk.



Scheme 14: Structure of Tanikolide

The naturally occurring tanikolide dimer **59** also shows potentially useful bioactivity, demonstrating significant SIRT2 inhibition (Scheme 15).¹⁸



Scheme 15: Tanikolide Dimer

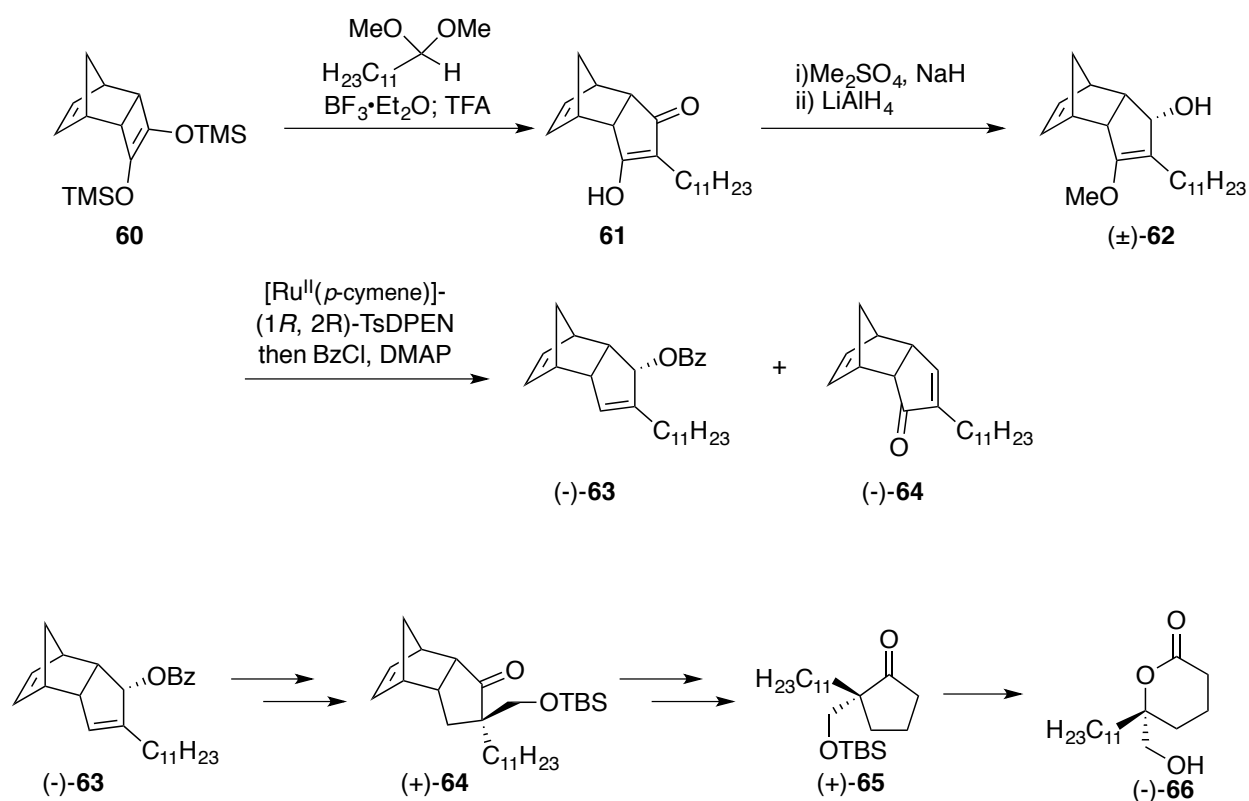
NAD-dependent deacetylase sirtuin-2 (SIRT2) is a NAD⁺-dependent protein that deacetylates p53, and thus prevents p53 from binding to DNA. Since p53 binding plays a significant role in the mediation of apoptotic responses in human cells, the ability of SIRT2 to silence these responses is a potential method to treat human cancers: lymphoma in particular. As such, SIRT2 inhibitors are of significant interest as potential anticancer drugs.¹⁹

Tanikolide's structure contains a δ -lactone core linked to *n*-undecane and methanol chains at the C₁ position. The structure of tanikolide was determined via a combination of high-resolution mass spectrometry, CI/MS, IR spectroscopy, ¹H NMR, ¹³C NMR, DEPT, ¹H-¹H COSY, and HMBC experiments.¹⁷ Once the main structure of tanikolide had been determined

via these methods, the Gerwick group determined the absolute configuration of the C₁ stereocenter by synthesizing (*R*)- and (*S*)- PGME derivatives of tanikolide.¹⁷ These PGME derivatives were then studied using a variety of NMR experiments in order to determine the relationship between the two stereocenters of the derivatives and thus to find the absolute stereochemistry.

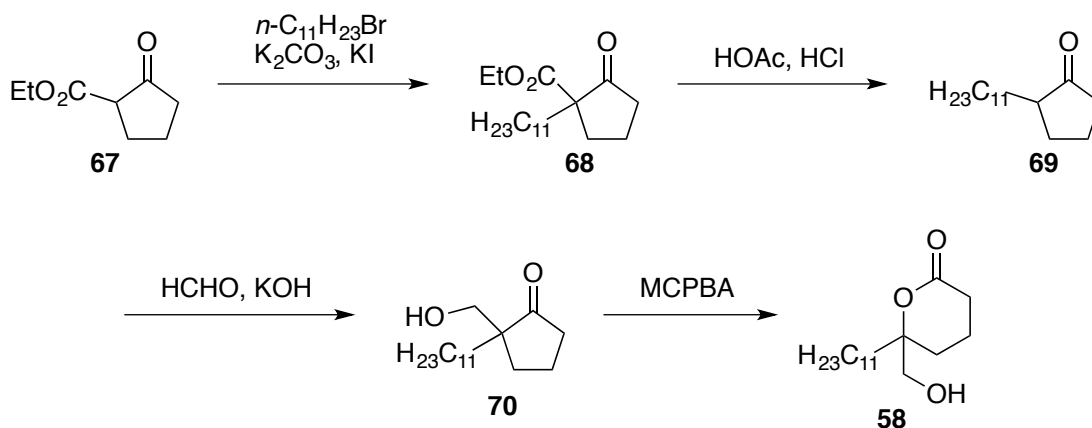
The biosynthetic origins of tanikolide have not been examined in previous studies. However, based on the structure of the natural product, it is likely formed via fatty-acid synthases in a polyketide-type synthesis followed by a final lactonization to close the ring and generate the natural product.

Tanikolide has been previously synthesized via a number of different routes over the past sixteen years since its discovery. The first total synthesis of tanikolide was achieved in 2000 by the Ogasawara group.²⁰ The Ogasawara group achieved the synthesis of tanikolide with high stereoselectivity using a norbornadiene derivative-based strategy with an enol-silane ring expansion and a catalytic asymmetric hydrogen transfer reaction resolution as the key step in their synthetic strategy. Overall, the Ogasawara synthesis of (+)-tanikolide was successful in a longest linear sequence of 12 steps from commercially available starting material (Scheme **16**). However, in their manuscript and supporting information, the Ogasawara group only provided yields for three of their steps, preventing general knowledge of the overall yield.



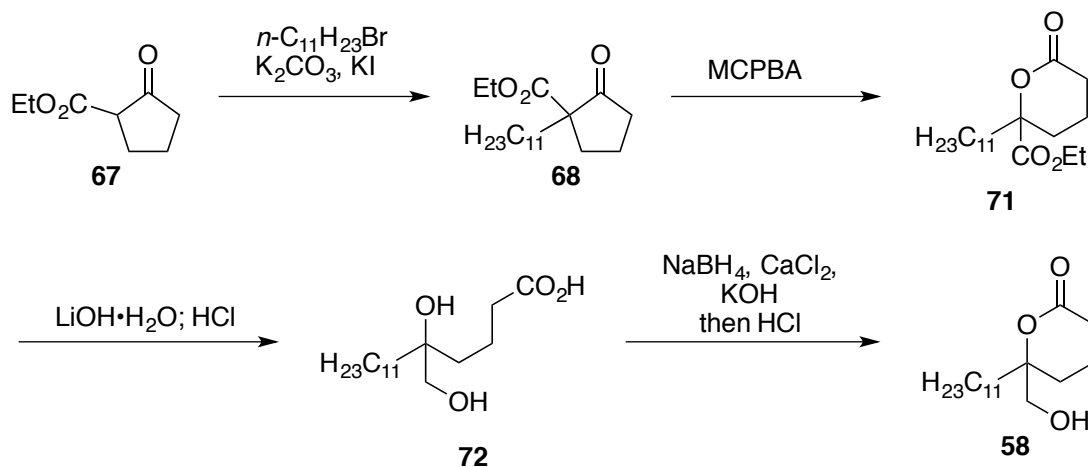
Scheme 16: Ogasawara Synthesis of Tanikolide

Among the previous syntheses of tanikolide, the shortest synthesis to date is the racemic synthesis of tanikolide by the Zhai group, which they achieved in four steps via two different routes.²¹ The first of these routes begins with the commercially available ethyl 2-oxocyclopentanecarboxylate **67**, which is used to add to undecylbromide via an enolate reaction to afford **68** (Scheme 17). The ethyl ester **68** is then hydrolyzed and decarboxylated to form ketone **69**. Subsequent enolate attack on formaldehyde formed alcohol **70**. Baeyer-Villiger oxidation of ketone **70** produced tanikolide (**58**) in four steps and 85% overall yield.



Scheme 17: Zhai Synthesis of Tanikolide

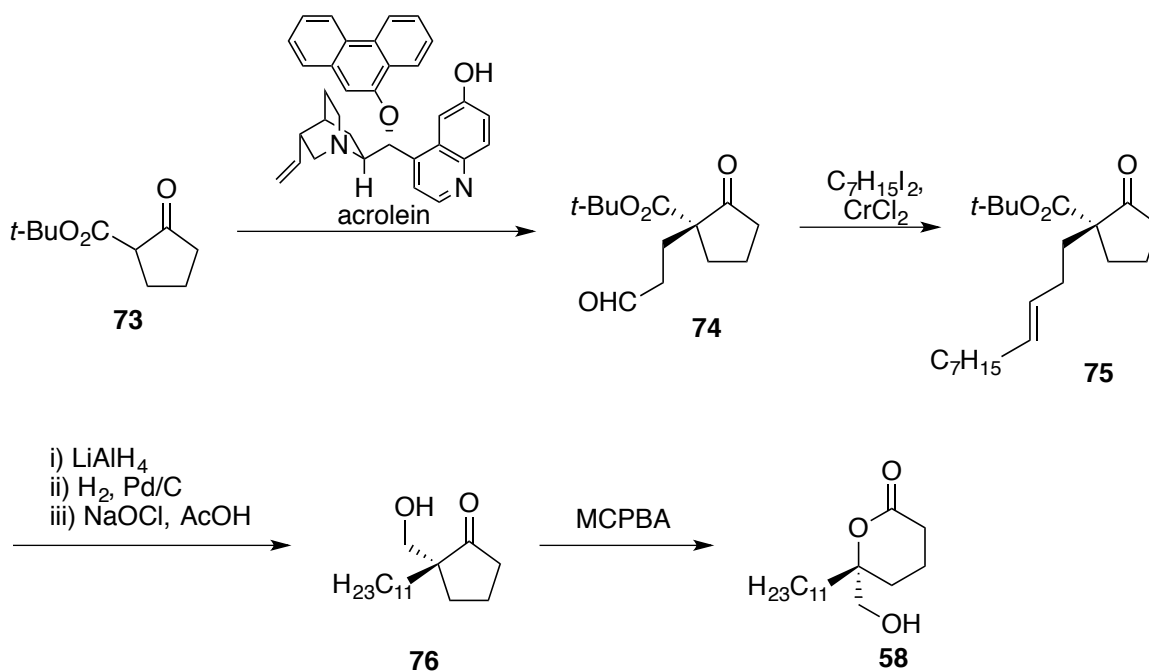
In addition, Zhai executed a different four-step route to tanikolide based around a similar enolate strategy (Scheme 18). Following the generation of **68**, Baeyer-Villiger oxidation of the ring and hydrolysis of the lactone results in carboxylic acid **72**. One-pot sodium borohydride reduction of the ester to the corresponding alcohol and dehydration-lactonization produced tanikolide (**58**) in four steps with an overall yield of 76%.



Scheme 18: Alternative Zhai Synthesis of Tanikolide

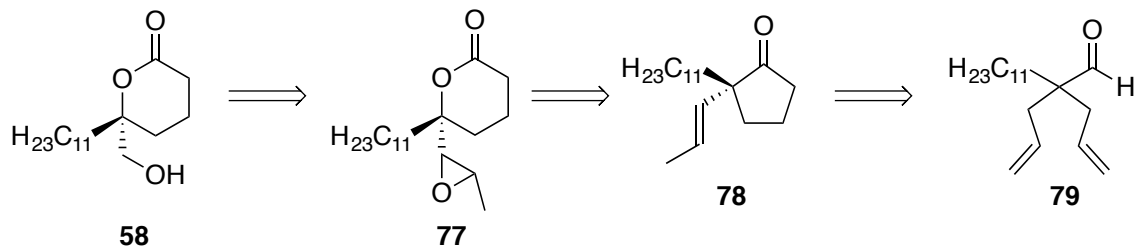
The Deng group achieved the shortest asymmetric synthesis of tanikolide in seven steps from commercially available starting material.²² This synthesis began with *t*-butyl 2-oxocyclopentanecarboxylate, **73**, generated from commercially available 2-oxo-cyclopentane carboxylic acid in one step. The key step of the Deng synthesis is the addition of this carboxylate

ester into acrolein to generate the quaternary center of tanikolide and produce aldehyde **74** >99% ee. Enantiopure aldehyde **74** was then olefinated to form undecene **75**. Reduction of the ester, hydrogenation of the olefin, and chemoselective Stevens oxidation of the secondary alcohol produced ketone **76**. Finally, the Deng group performed an acid-catalyzed Baeyer-Villiger oxidation to afford tanikolide (**58**) in a total of seven steps, longest linear sequence, and an overall yield of 40% (Scheme 19).



Scheme 19: Deng Synthesis of Tanikolide

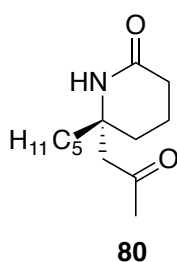
Our retrosynthetic plan for the synthesis of tanikolide began with the use of an oxidative cleavage and reduction to generate a primary alcohol from epoxide **77**. We envisioned a route to generate both the epoxide and the lactone simultaneously via Baeyer-Villiger oxidation and olefin epoxidation of cyclic ketone **78**. Using the enantioselective olefin desymmetrization-hydroacylation chemistry recently developed in our lab, we could generate cyclic ketone **78** from bis-allyl aldehyde **79** in one step (Scheme 20).¹⁶



Scheme 20: Retrosynthetic Analysis of Tanikolide

Total Synthesis of (-)-Adalinine

(-)-Adalinine is a piperidine alkaloid natural product isolated from the ladybird beetles *adalia bipunctata* and *adalia decempunctata* (Scheme 21). The Lognay group, which discovered the compound in 1995, detected adalinine at all stages of life in these insects, from the eggs through larval growth and into adulthood.²³ Adalinine is thought to be one of a number of compounds produced by the ladybird beetle as a deterrent against avian predation. When threatened, ladybird beetles secrete a potent mix of alkaloids, including adalinine, to ward off predators. Adalinine has not been tested further for biological activity, although similar piperidine alkaloids from ladybird beetles have been shown to be highly toxic to birds when ingested.²⁴



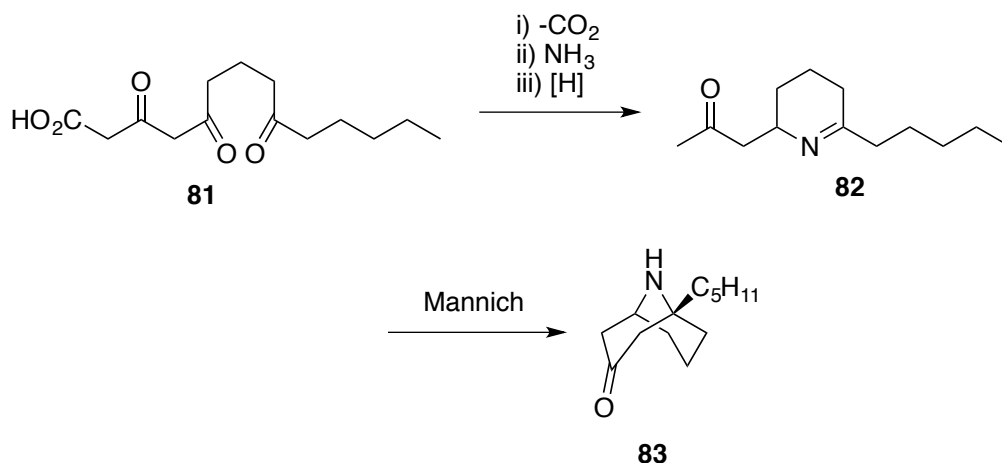
Scheme 21: Structure of (-)-Adalinine

The structure of (-)-adalinine, **80**, features a lactam core with *n*-pentyl and 2-propanone chains both attached at the C₁ position of the core. The Lognay group examined the structure of adalinine through a number of techniques, including high-resolution mass spectroscopy, ¹H-

NMR, ^{13}C -NMR, ^1H - ^1H COSY, and HMBC experiments.²³ However, the Lognay group did not determine the absolute configuration of the stereocenter in adalinine, choosing to focus instead on the biosynthesis of adalinine, which they hypothesized might come from adaline, a related natural product previously discovered in *a. bipunctata* and *a. decempunctata*.

The absolute configuration of (–)-adalinine was only determined after the racemic total synthesis of adalinine had been achieved. The Kibayashi synthesis, the first of two racemic syntheses of adalinine, allowed the Kibayashi group to determine the absolute configuration of adalinine.²⁵ In order to determine the stereochemistry of the C_1 position, the Kibayashi group generated adalinine derivatives for crystallization. These crystalline derivatives were tested via X-ray crystallography to find the absolute configuration of adalinine. Based on the X-ray crystal structure, the Kibayashi group determined that the stereogenic center in the natural product (–)-adalinine has an R configuration.

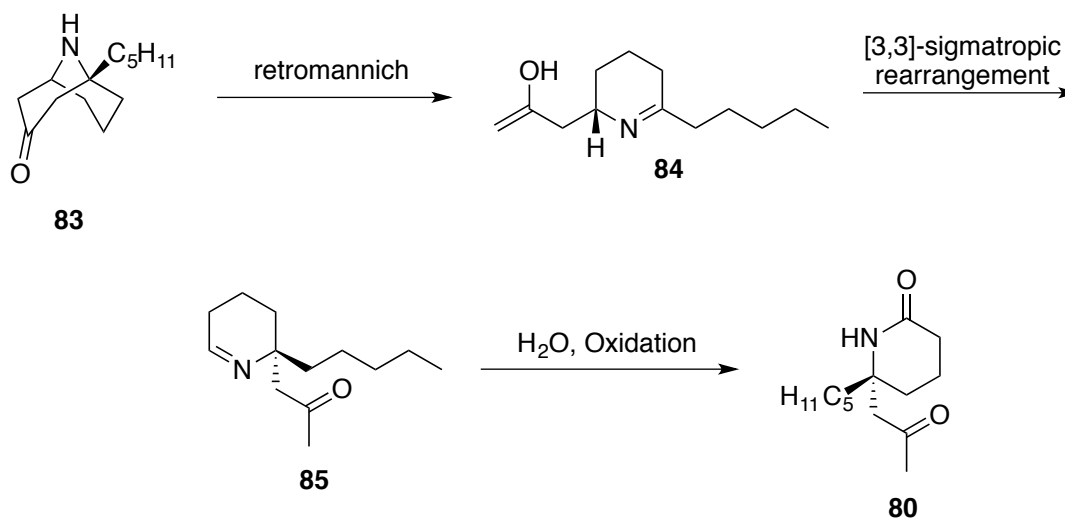
(–)-Adalinine is hypothesized to be biosynthetically derived from the related natural product (–)-adaline **83**.²³ Ultimately, adaline is sourced initially from the linear combination of seven acetate units via fatty synthases to afford a fourteen-carbon chain product **81**. Subsequent decarboxylation, amination, cyclization, and reduction of **81** produces **82**, which rapidly undergoes a Mannich reaction to produce the natural product (–)-adaline (**83**) (Scheme **22**).²⁶



Scheme 22: Biosynthesis of (-)-Adaline

The Daloz group tested this biosynthetic route by feeding *a. bipunctata* ^{14}C -labeled acetate sources and testing the resulting adaline.²⁶ The acetate experiment confirmed that (-)-adaline is generated biosynthetically from seven repeating acetate units.

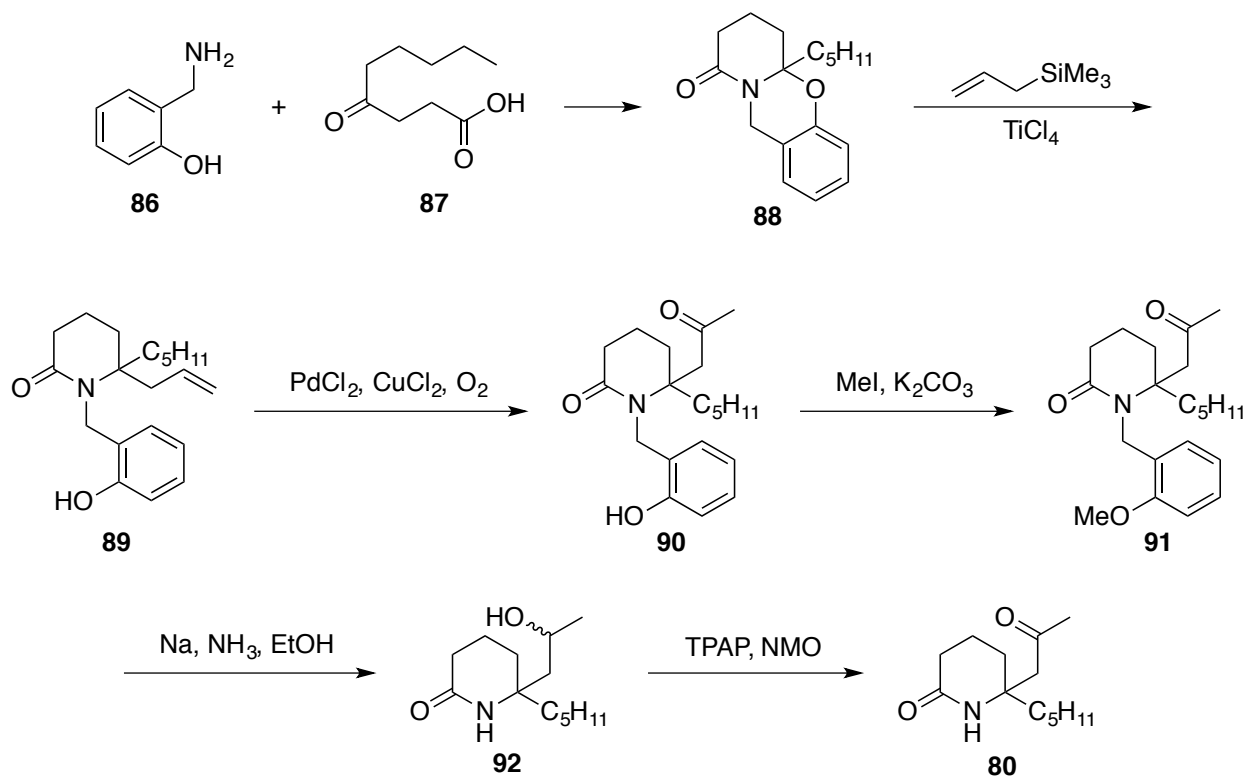
In the biosynthesis of (-)-adaline, (-)-adaline initially undergoes a retromannich reaction to afford imine **84**, which then undergoes a [3,3]-sigmatropic rearrangement to afford the rearranged imine **85**. Imine **85** is then hydrated and oxidized to form the lactam ring and afford (-)-adaline, **80** (Scheme 23).²⁶



Scheme 23: Biosynthesis of (-)-Adaline

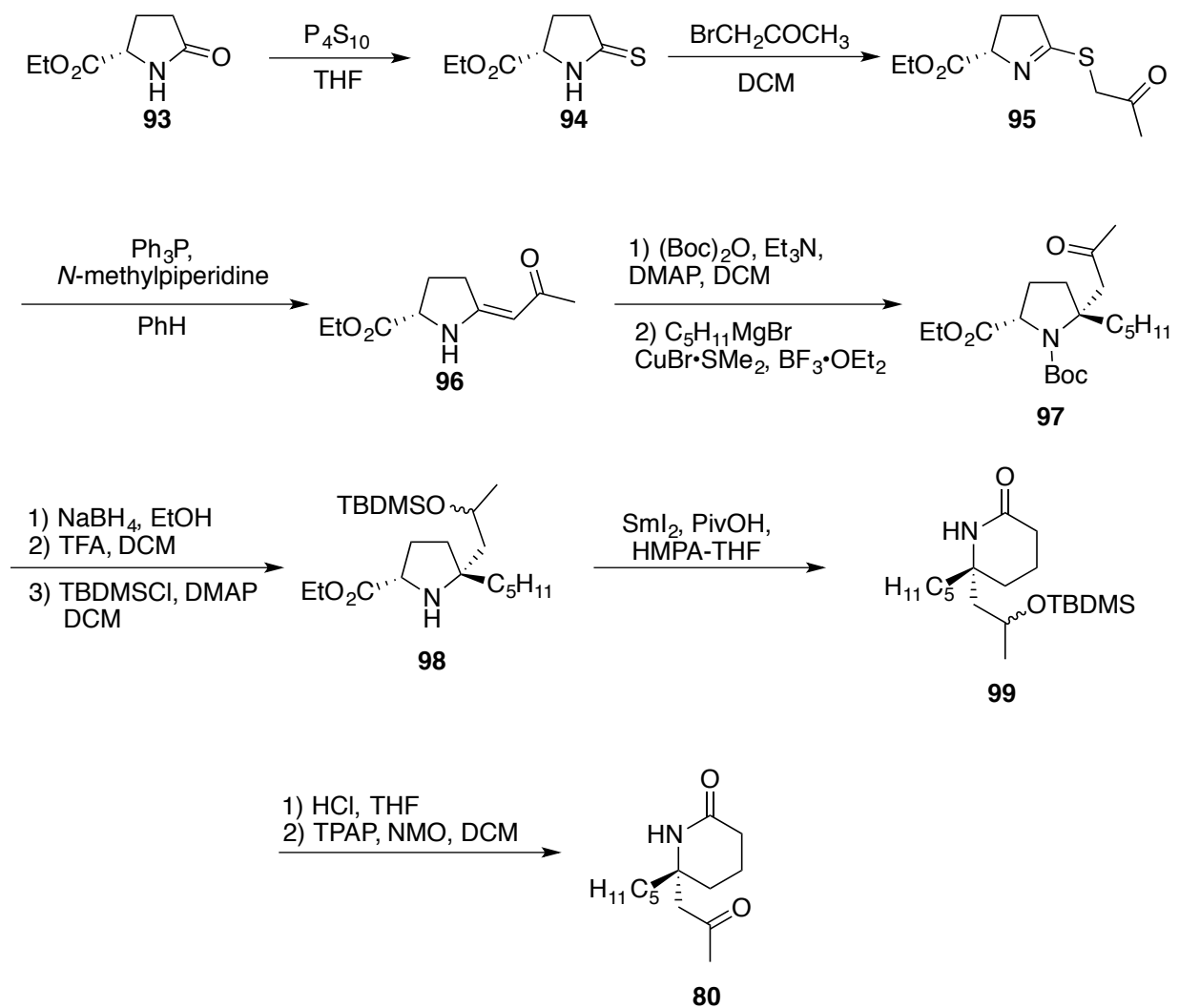
The Daloz group also tested this proposed biosynthetic route using deuterated synthetic adaline. Feeding this deuterated adaline to *a. bipunctata* and subsequent extraction of organic compounds from the subjected *adalia* adults produced deuterated (–)-adalinine in significant quantities, indicating that adalinine is indeed biosynthetically derived from adaline.¹⁴

In 1998, the Kibayashi group succeeded in the first total synthesis of racemic adalinine.²⁷ The Kibayashi synthesis relied on two key steps to generate adalinine rapidly in good yield. The first of these is a ring-closing condensation-amidation of **86** with **87** to generate the lactam ring **88**, followed by a Lewis-Acid-mediated ring-opening allylation, generating **89**. These two key steps generate the lactam ring and the quaternary center of adalinine, allowing for rapid increases in complexity during these steps in the synthesis. Subsequent Wacker oxidation of **89** to form ketone **87** followed by methylation to form **88** and hydrogenolysis afforded **89**. Alcohol **89** was then oxidized to generate the ketone, affording racemic adalinine. Overall, the Kibayashi synthesis produced racemic adalinine in six steps, longest linear sequence, from commercially available starting material, with 25% yield (Scheme 24).



Scheme 24: Kibayashi Synthesis of Adalinine

The Honda group has, thus far, achieved the only enantiospecific synthesis of adalinine via a samarium iodide-promoted fragmentation strategy. In the Honda synthesis, lactam **93** was treated with phosphorous pentasulfide to generate thiolactam **94**. Thiolactam **94** was then converted to thioether **95** and desulfurized to generate enaminone **96**. Amine protection and diastereoselective Michael addition of the C₅ side chain afforded **97** (Scheme 25).

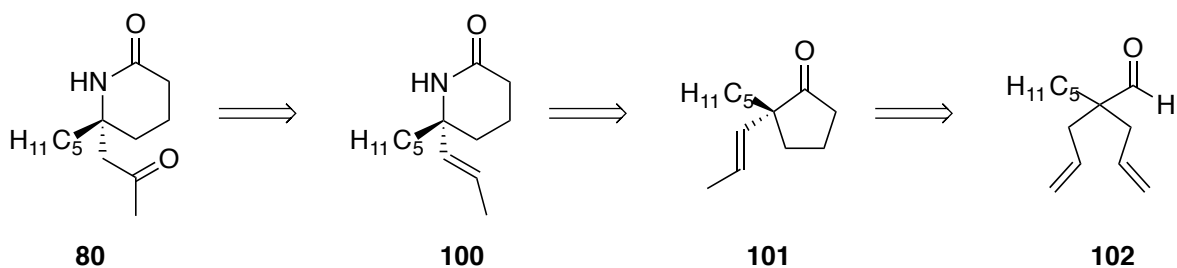


Scheme 25: Honda Synthesis of Adalinine

Ketone reduction, amine deprotection, and alcohol protection afforded silyl ether **98**. Subsequent samarium iodide-promoted amine cleavage and lactamization generated a ring expansion to form **99**. Deprotection under acidic conditions followed by oxidation afforded (–)-adalinine (**80**), completing the total synthesis in a total of 11 steps, longest linear sequence, with an overall yield of 27.6%.

While pursuing the synthesis of tanikolide, we noted that we could use the same type of desymmetrizing olefin hydroacylation strategy to synthesize (–)-adalinine. In our retrosynthetic analysis of adalinine, we envisioned the installation of the methyl ketone via a late state Wacker

oxidation from olefin **100**. Either a Schmidt reaction or a Beckmann rearrangement of cyclopentanone **101** could be used to generate the lactam ring of (-)-adalinine. Our desymmetrizing hydroacylation reaction could be used to generate the cyclopentanone from aldehyde **102** (Scheme 26).

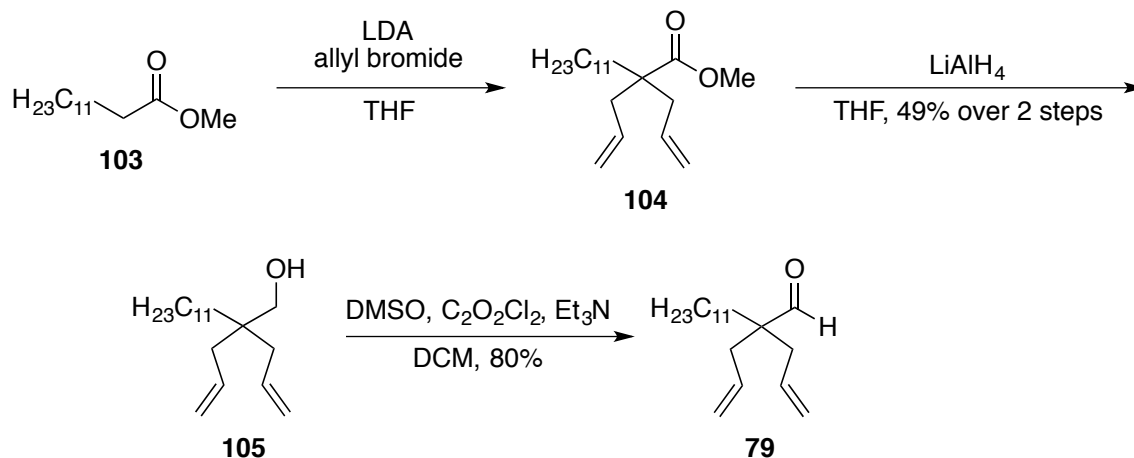


Scheme 26: Retrosynthesis of Adalinine

1.2: Results and Discussion

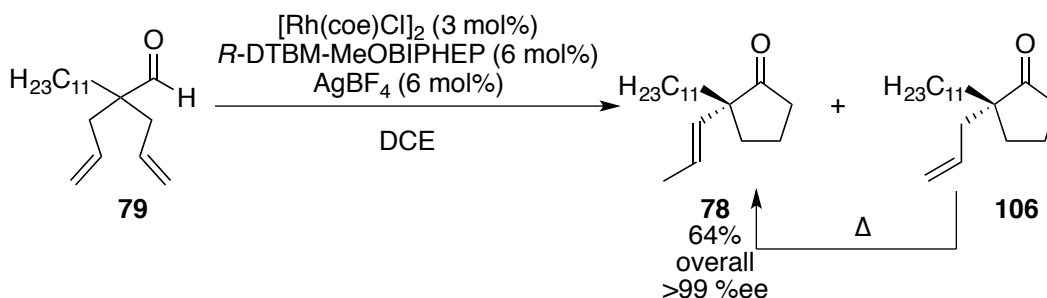
Efforts Towards the Total Synthesis of (+)-Tanikolide

Dr. Jung-Woo Park and I successfully generated the desired aldehyde, **79**, in 3 steps from the commercially available methyl ester **103**. Alkylation of the methyl ester afforded **104**. I tested the DIBAL-H reduction of **104**, which would have shortened the synthetic route by one step. However, my attempts to achieve this reduction gave a 2:3 mixture of the aldehyde and over-reduced alcohol, with significant quantities of unreacted starting material also being present, leading us to use the longer but more reliable route of over-reduction via LiAlH_4 to form alcohol **105**. Swern oxidation of alcohol **105** gave the desired *bis*-allyl aldehyde **79** (Scheme 27).



Scheme 27: Synthesis of Aldehyde **79**

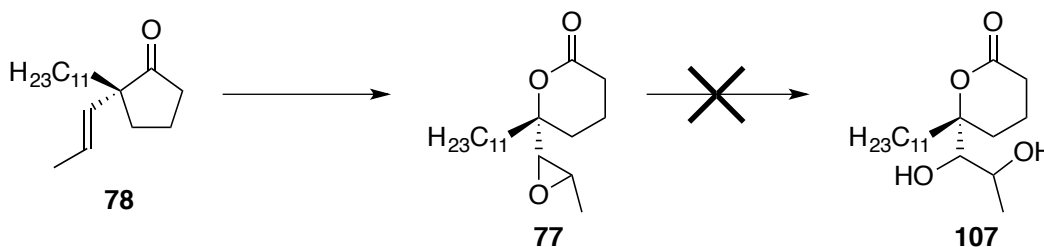
Hydroacylation of **79** afforded a mixture of olefins **78** and **106**, as had been noted previously in our hydroacylation work (see section on hydroacylation) (Scheme 28).



Scheme 28: Hydroacylation of **79**

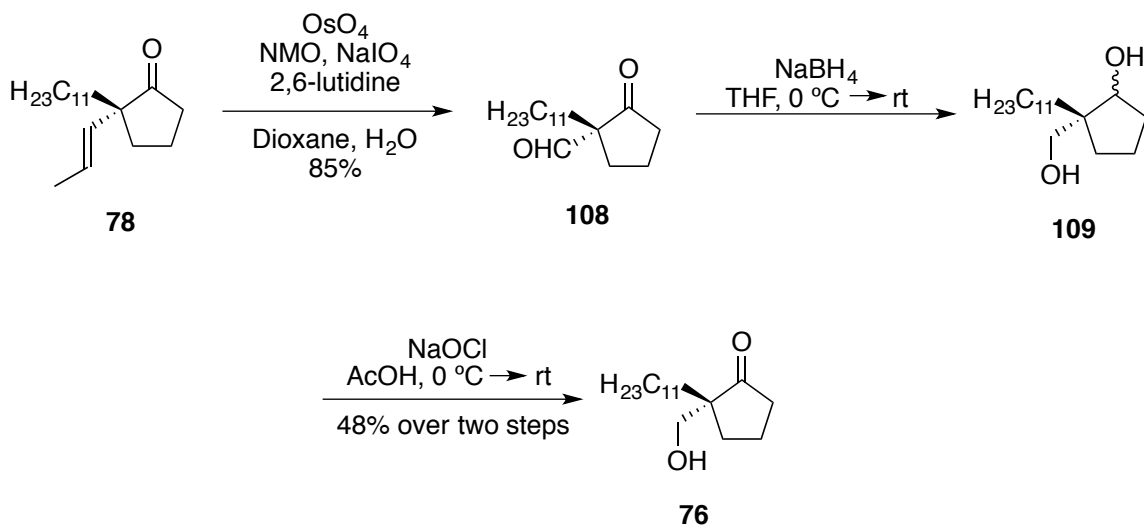
However, heating the reaction mixture following completion of the initial hydroacylation allowed for the rhodium-catalyzed isomerization of primary olefins to secondary olefins, affording only the fully isomerized **78** in 64% yield with 99% ee.

The simultaneous Baeyer-Villiger oxidation and olefin epoxidation of **78** gave the desired lactone **77**. However, Dr. Park's efforts towards the hydrolysis of the epoxide were unsuccessful, preventing the generation of diol **107** (Scheme 29).



Scheme 29: Initial Synthetic Approach to Tanikolide

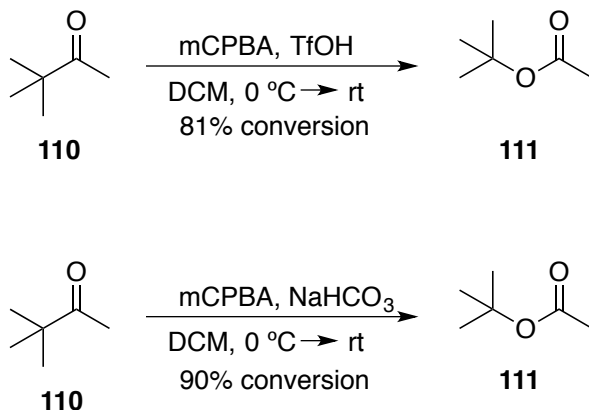
As such, the synthetic strategy was adapted to begin with the oxidative cleavage of the olefin before lactonization, allowing us to merge synthetic routes with the Deng synthesis of tanikolide (Scheme 30).²² At this point in the project, I took over efforts to the synthesis, performing all aspects of the efforts towards the synthesis of tanikolide.



Scheme 30: Revised Synthetic Strategy towards Tanikolide

Oxidative cleavage of olefin **78** using osmium tetroxide, NMO, and sodium periodate afforded aldehyde **108** with 85% yield. Subsequent reduction of both the aldehyde and the ketone afforded diol **109**, which was not isolated due to the mixture of diastereomers. At this point in the synthesis, our route intersected with the Deng route to tanikolide, providing a formal synthesis of tanikolide. Subsequent Stevens' oxidation of the secondary alcohol gave ketone **76** with 48% yield over two steps.

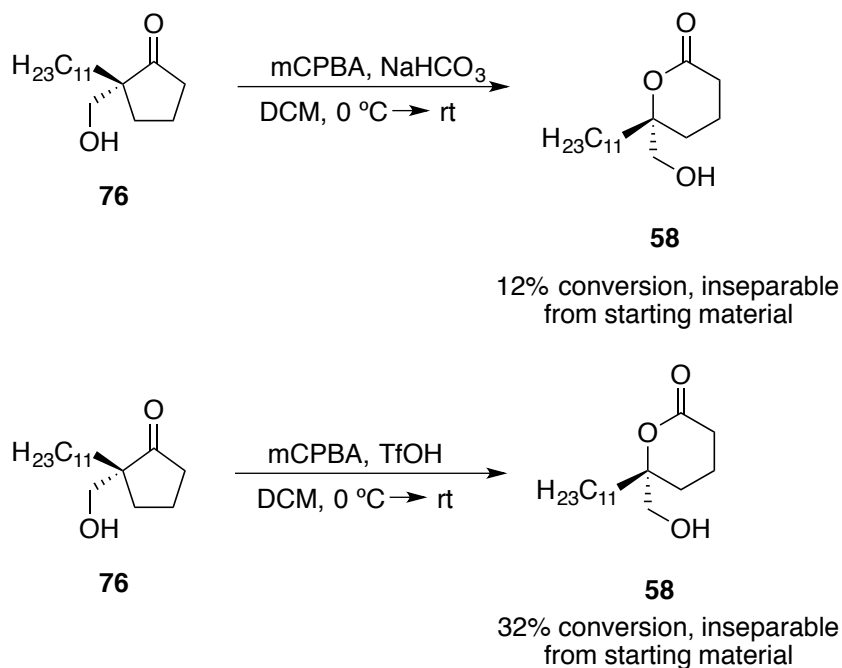
Due to low conversions (below 10%) for initial attempts towards the Baeyer-Villiger oxidation of **76**, I decided to use pinacolone (**110**) as a model system for cyclopentanone **76** in order to optimize the reaction conditions (Scheme **31**). Pinacolone was tested for Baeyer-Villiger conditions under acidic conditions and basic conditions.



Scheme 31: Baeyer-Villiger Oxidation of Pinacolone Model System

The conversions of 81% and 90% and selectivity (no methyl ester was observed under either set of conditions) of the Baeyer-Villiger reaction of pinacolone under both acidic and basic conditions led me to believe that both sets of conditions could afford the desired lactone ring. Thus, I decided to try both sets of conditions in our Baeyer-Villiger oxidation.

Testing the Baeyer-Villiger reaction with ketone **76** with basic conditions gave conversions of 12%, while acidic conditions gave conversions of up to 32% (Scheme **32**).

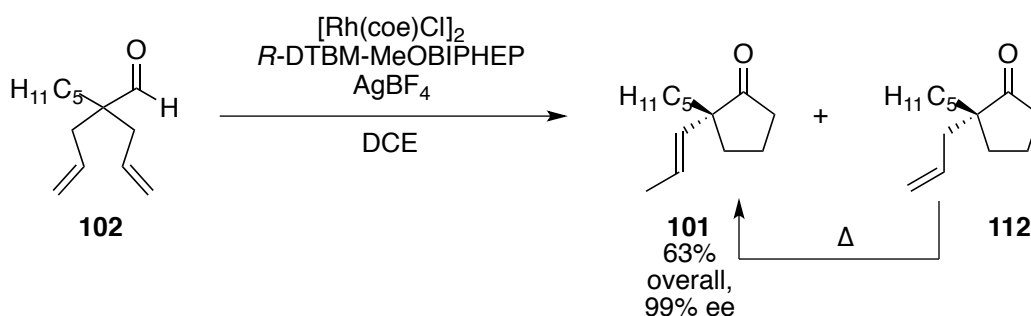


Scheme 32: Attempted Baeyer-Villiger Oxidation of Ketone **76**

However, due to a combination of low conversion and difficulty isolating the natural product from the starting material, these conditions were not found to be suitable to complete the total synthesis. The Baeyer-Villiger oxidation conditions do need further optimization. However, I believe that this transformation can be further optimized to afford (+)-tanikolide from **105**.

Efforts Towards the Total Synthesis of (-)-Adalinine

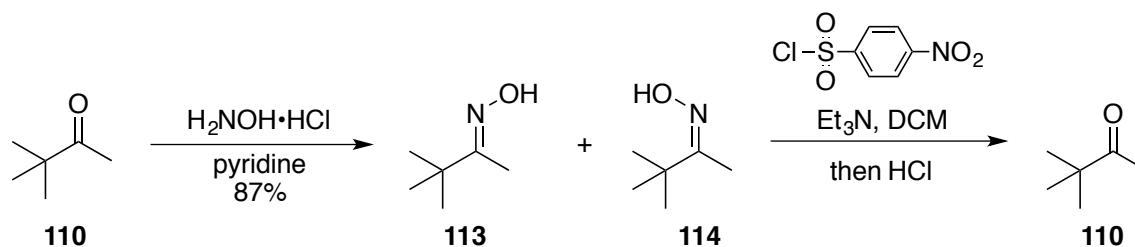
Following our previous procedure, Dr. Park generated aldehyde **102** in three steps from commercially available methyl heptanoate. Desymmetrizing hydroacylation followed by heating to promote full isomerization of the olefin gave cyclopentanone **101** in 63% yield and 99% ee (Scheme 33).



Scheme 33: Hydroacylation of Aldehyde **102**

Before proceeding with the total synthesis, we decided to use a model system to evaluate possible methods for generating the lactam ring from the ketone, either via a Schmidt reaction or by a Beckmann rearrangement. Initial testing of the Schmidt reaction by Dr. Park only resulted in the recovery of starting material. Before attempting the Beckmann rearrangement using our actual system, we used pinacolone as a model system to test the reactivity and selectivity of a variety of methods for achieving the desired transformation. Initially, we decided to use a two-step procedure for the Beckmann rearrangement, beginning with condensation of hydroxylamine

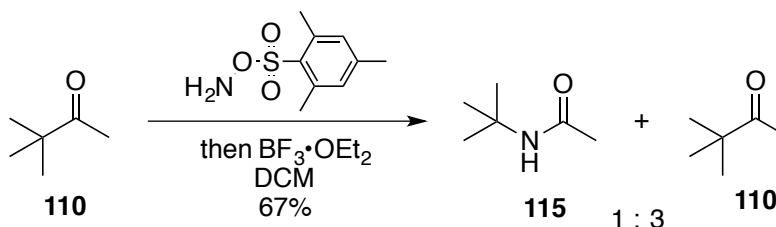
into the pinacolone (**110**), followed by installation of a sulfonyl leaving group and treatment with acid to generate the desired transformation (Scheme 34).²⁸



Scheme 34: Attempted Beckmann Rearrangement of Pinacolone Model System

The initial condensation occurred afforded both the desired oxime **113** and the undesired oxime **114** in 87% yield and only a moderate *cis/trans* selectivity of 2:1. Despite this, I proceeded with **113** to test the viability of these conditions for the Beckmann rearrangement. However, upon sequential treatment of the two oximes with the *p*-nosyl chloride and aqueous hydrochloric acid, the only result was oxime hydrolysis to regenerate **110**, rather than the desired *t*-butyl acetamide.

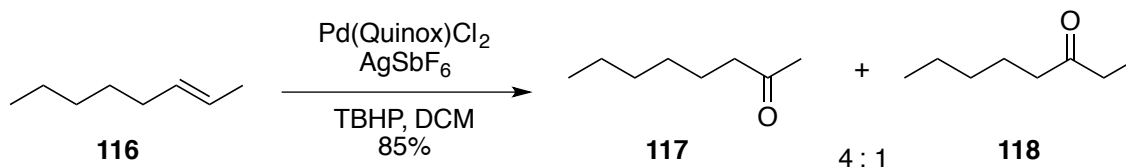
Based on the combination of the *cis/trans* selectivity issues and the hydrolysis of the oxime, I decided to attempt the rearrangement via a one-pot condensation-Beckmann rearrangement using MSH and borontrifluoride etherate.²⁹ Given the increase in steric bulk of the MSH compared to a free hydroxyl, I envisioned high *cis/trans* selectivity for this transformation. Further, since the leaving group was pre-installed in the reagent, this method would reduce the number of steps required in our synthetic plan (Scheme 35).



Scheme 35: Beckmann Rearrangement of Pinacolone Model System

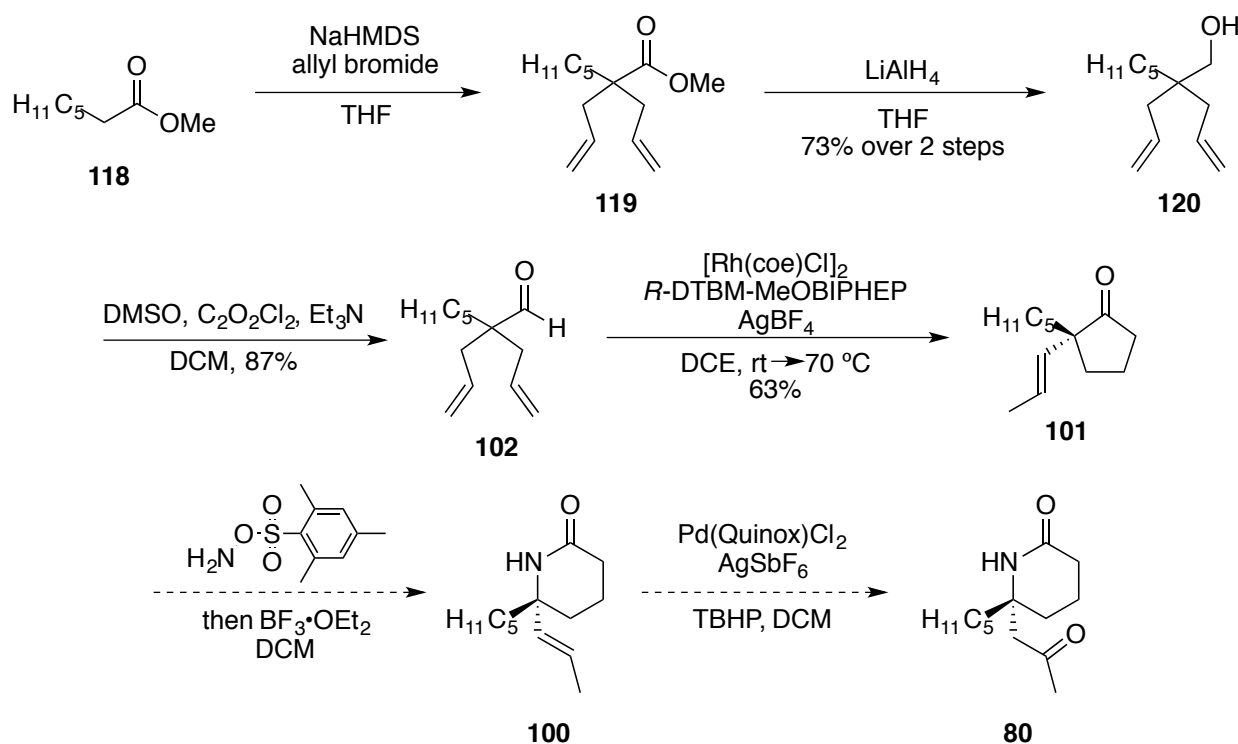
Following the generation of MSH according to literature precedent, I treated **110** with the MSH to afford a 1:3 mixture of the desired amide **115** and the unreacted **110**, with no methyl amide observed in the crude reaction mixture. This set of conditions is promising, given the high selectivity for the quaternary carbon over the primary carbon. While the conversion was not as high as could be desired, treatment with a larger excess of MSH and allowing a longer time for the condensation before addition of the acid should allow us to overcome the low conversion for this substrate. As such, I believe that this set of conditions will allow us to achieve the Beckmann rearrangement of ketone **101** to generate lactam **100**.

Following the use of the pinacolone model system to develop a reliable method for the Beckmann rearrangement, I decided to find a suitable method for the Wacker oxidation of olefin **100** to generate the methyl ketone with high selectivity over the undesired ethyl ketone. The Sigman group has published a modification of Wacker oxidation conditions that oxidize olefins to afford ketones with high regioselectivity and functional group tolerance.³⁰ This method provides a relatively mild set of conditions to preferentially oxidize secondary positions that are electronically rich and lack steric hindrance. Based on the structure of olefin **100**, I believed that this methodology should favor the formation of the desired methyl ketone both sterically and electronically, since this position is both less sterically hindered and has greater electron density than the internal position of the olefin. In order to test the viability of this strategy, I decided to test the steric factors using an internal olefin model system. Although 2-octene is not sterically similar to our olefin system, changing the α -position from a secondary carbon to a quaternary center should only magnify any steric factors on the oxidation that we observe, making it a valid comparison (Scheme **36**).



Scheme 36: Wacker Oxidation of 2-Octene Model System

Since I saw a 4:1 selectivity between methyl ketone **116** and ethyl ketone **117**, based on simple steric influences, I should expect the selectivity to increase in the case of our substrate. Based on this selectivity, I believe that this set of conditions will afford methyl ketone **99** via the Wacker oxidation (Scheme 37).



Scheme 37: Projected Synthesis of Adaline

Based on the results of our model testing, our current synthetic route to (–)-adalinine relies on the generation of cyclopentanone **101** via hydroacylation, followed by the Beckmann rearrangement using the MSH conditions after further optimization. I then plan to use the

Sigman modification of the Wacker oxidation to oxidize olefin **101** to generate the natural product (-)-adalinine (**80**).

1.3: Conclusions:

We have faced some difficulties in the completion of the total synthesis of tanikolide: particularly Baeyer-Villiger oxidation. However, given our progress towards the total synthesis of (+)-tanikolide, in addition to developing a formal synthesis, we believe that we will be able to complete the total synthesis of tanikolide in the future. Efforts towards the completion of this total synthesis are of ongoing study in our lab.

Based on our successful model studies, our current synthetic route to (-)-adalinine is promising. The success of the Wacker oxidation using our model system and the high selectivity of the Beckmann rearrangement via MSH both are promising results that indicate the likely viability of these two reactions in the synthesis. Using this synthetic strategy, we believe that we will be able to complete the shortest total synthesis of (-)-adalinine yet. Efforts towards the completion of this natural product are being continued in our group.

1.4 Supporting Information

General Experimental Information

Commercial reagents were purchased from Sigma Aldrich, Alfa Aesar, Strem, or Combi Blocks and used without further purification. Reactions were monitored using thin-layer chromatography (TLC) on EMD Silica Gel 60 F254 plates. Visualization of the developed plates was performed under UV light (254 nm) or KMnO₄ stain. Organic solutions were concentrated under reduced pressure on a Büchi rotary evaporator. ¹H and ¹³C NMR were taken using ¹H and ¹³C NMR spectra were recorded on any of six instruments: Bruker AV600, Bruker GN500, Bruker CRYO500, or Bruker DRX400 NMR. ¹H NMR spectra were internally referenced to the residual solvent signal or TMS, while ¹³C NMR spectra were internally referenced to the residual solvent signal. Data for ¹H NMR are reported as follows: chemical shift (δ ppm), multiplicity (s = singlet, d = doublet, t = triplet, q = quartet, m = multiplet, b = broad), coupling constant (Hz), integration. Data for ¹³C NMR are reported in terms of chemical shift (δ ppm). Column chromatography was performed with Silicycle Silica-P Flash Silica Gel, using either glass columns or a Biotage SP-1 system. Preparative thin-layer chromatography was performed using EMD Silica Gel 60 F254 plates. Solvents used in hydroacylations and dehydroformylations were degassed by three freeze-pump-thaw cycles. Chiral ligands were purchased from Strem. All reactions were carried out in flame-dried glassware under nitrogen atmosphere unless otherwise noted. Please note that number of different spectra are missing or impure due to being unable to return to the lab to analyze purified samples or take new spectra of saved samples. These spectra will be acquired by Dr. Jung-Woo Park as he continues the project.

General Procedures

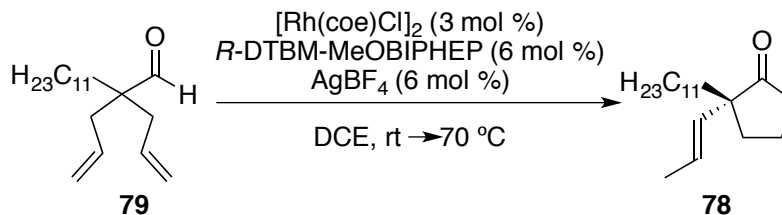
General Procedure for the Desymmetrizing Hydroacylation of bis-allyl aldehydes

Chlorobis(cyclooctene) rhodium(I) dimer (6 mol %) was combined with (R)-DTBM-MeOBIPHEP (12 mol %) and dissolved in DCE (0.1 M), then stirred for 40 minutes. AgBF₄ (12 mol %) was added to the reaction mixture and stirred for 15 minutes longer. Aldehyde substrate (1.00 equiv.) was then added to the mixture, and was allowed to stir at room temperature for 2 h. Following completion of the hydroacylation, as judged by ¹H NMR analysis, the reaction was heated to 70 °C and stirred for 18 h. Upon completion of the olefin isomerization, as judged by NMR analysis, the reaction was cooled to room temperature and opened to atmosphere to halt reaction progress. Purification via preparative TLC (5% EtOAc/ 95% hexanes) afforded the cyclopentanone product.

Synthesis of Tanikolide Substrates

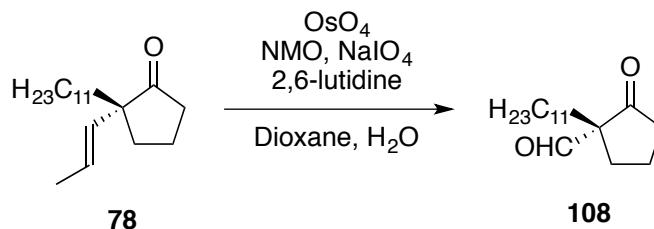
Aldehyde **79** was obtained from Dr. Jung-Woo Park for use in hydroacylation

Synthesis of Cyclopentanone **78**



The general procedure for desymmetrizing hydroacylation was followed as written for aldehyde **79** (27.8 mg, 0.1 mmol). The product, olefin **78**, was afforded as a colorless oil (17.7 mg, 0.064 mmol, 64% yield). ^1H NMR (400 MHz, CDCl_3) δ 5.50 (dq, $J = 15.7, 6.3$ Hz, 1H), 5.36–5.32 (m, 1H), 2.36–2.29 (m, 1H), 2.24–2.19 (m, 1H), 2.18–2.12 (m, 1H), 1.9–1.83 (m, 3H), 1.71 (dd, $J = 6.3, 1.5$ Hz, 3H), 1.31–1.28 (m, 18H), 0.92 (t, $J = 6.9$ Hz, 3H). For information regarding enantioselectivity, see literature precedent.¹⁶

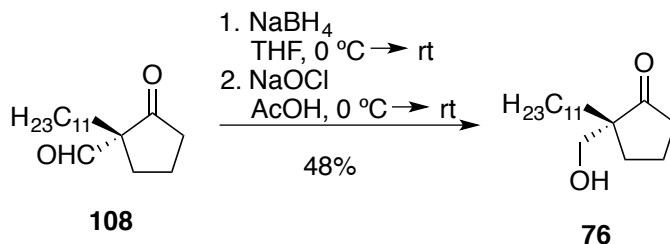
Synthesis of Aldehyde **108**



Olefin **108** (37.1 mg, 0.13 mmol) was dissolved in dioxane (975 μL) and water (325 μL). Osmium tetroxide (4% in H_2O) (42.4 mg, 0.007 mmol, 5 mol %) was added to the reaction mixture, followed by the addition of NMO (31.2 mg, 0.27 mmol, 2.00 equiv.), NaIO_4 (57.0 mg,

0.27 mmol, 2.00 equiv.), and 2,6-lutidine (30 μ L, 0.27 mmol, 2.00 equiv.). The reaction was allowed to stir for 12 h at room temperature. Upon completion of the reaction, as judged by TLC analysis, the reaction was extracted with DCM (3 x 3 mL). The organic layers were combined, dried over MgSO_4 , filtered, and evaporated under reduced pressure. Purification via preparative TLC (10% EtOAc/ 90% hexanes) afforded aldehyde **108** (29.7 mg, 0.28 mmol, 85% yield) as a colorless oil. ^1H NMR (400 MHz, CDCl_3) δ 9.34 (s, 1H), 2.51–2.46 (m, 1H), 2.23–2.17 (m, 1H), 1.92–1.84 (m, 1H), 1.76–1.75 (m, 1H), 1.74–1.68 (m, 1H), 1.18 (br, 20H), 0.81 (t, $J = 7.2$ Hz); ^{13}C NMR (100 MHz, CDCl_3) δ 215.4, 199.1, 67.7, 49.2, 38.7, 33.1, 31.9, 29.8, 29.6, 29.6, 29.5, 29.4, 29.3, 27.8, 24.6, 22.7, 19.4.

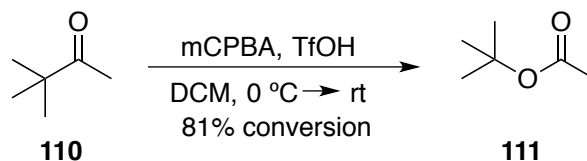
Synthesis of ketone **76**



Aldehyde **108** (7.6 mg, 0.03 mmol) was dissolved in THF (30 μ L) and cooled to 0 $^\circ\text{C}$ in an ice bath. NaBH_4 (38.6 mg, 0.06 mmol, 2.00 equiv.) was then added to the reaction mixture and the reaction was allowed to warm to room temperature over the course of 12 h. Following completion of the reaction, as judged by TLC, the reaction was quenched via addition of HCl (1 M, 2 mL) and extracted with DCM (3 x 5 mL). The organic layers were combined, dried over MgSO_4 , filtered, and concentrated under reduced pressure. The resulting diol was carried on without further purification.

The diol was dissolved in acetic acid (350 μ L) and cooled to 0 $^{\circ}$ C. Aqueous sodium hypochlorite (13% in H₂O, 38.6 mg, 0.06 mmol (2.00 equiv.) was then added to the reaction mixture. The reaction was allowed to react for 2 h until it was judged to be complete based on TLC analysis. The reaction mixture was then diluted with 2 mL H₂O extracted with DCM (3X5 mL). The organic layers were combined, dried over MgSO₄, filtered, and dried under reduced pressure. The resulting oil was purified via preparative TLC (5% EtOAc/Hex) to afford the desired ketone **76** as a colorless oil (3.7 mg, 0.014 mmol, 48% over two steps). ¹H NMR (400 MHz, CDCl₃) δ 3.67 (d, J = 10.8 Hz, 1H), 3.54 (d, J = 10.8 Hz, 1H), 2.36–2.31 (m, 2H), 1.98–1.94 (m, 3H), 1.54–1.46 (m, 3H), 1.30 (br, 20H), 0.931 (t, J = 6.8 Hz, 3H).

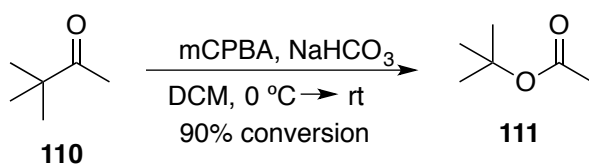
Acid-catalyzed Baeyer-Villiger oxidation of pinacolone



Pinacolone (**110**) (51.7 mg, 0.52 mmol) was dissolved in DCM (5 mL) and cooled to 0 $^{\circ}$ C. *m*-Chloroperoxybenzoic acid (492 mg, 2.0 mmol, 3.80 equiv.) was added to the reaction mixture, followed by triflic acid (0.1 mL, 0.05 mmol, 10 mol %), which was added dropwise. The reaction was allowed to warm to room temperature and stirred for 8 h. Upon completion of the reaction, as judged by TLC, the reaction was quenched via addition of H₂O (2 mL). The reaction was then extracted with DCM (3 x 4 mL). The organic layers were combined, dried over MgSO₄, filtered, passed through a layer of silica, and concentrated under reduced pressure. The resulting oil was left crude and tested by NMR spectroscopy to determine the conversion to **111** (81% yield). The NMR spectrum matched previously reported values. For **111** ¹H NMR (400

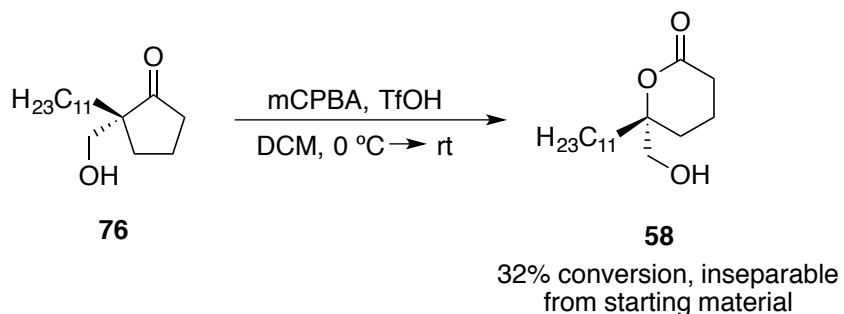
MHz, CDCl₃) δ 2.04 (s, 3H), 1.52 (s, 9H); for **110** ¹H NMR (400 MHz, CDCl₃) δ 2.33 (s, 3H), 1.00 (s, 1H).

Base-catalyzed Baeyer-Villiger oxidation of pinacolone



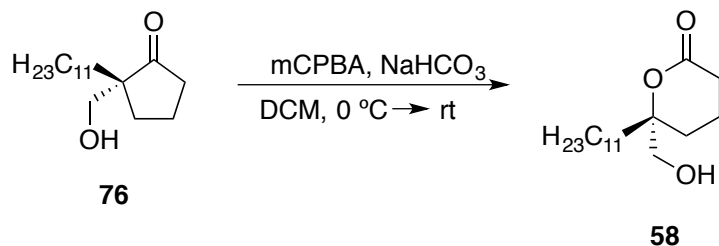
Pinacolone (**110**) (54.1 mg, 0.54 mmol) was dissolved in DCM (5 mL) and cooled to 0 °C. *m*-Chloroperoxybenzoic acid (502 mg, 2.0 mmol, 3.70 equiv.) was added, followed by sodium bicarbonate (168 mg, 2.0 mmol, 3.70 equiv.). The reaction was allowed to warm to room temperature and stirred for 14 h. Upon completion of the reaction, as judged by TLC, the reaction was quenched via addition of H₂O (2 mL). The reaction was then extracted with DCM (3 x 5 mL). The organic layers were combined, dried over MgSO₄, filtered, passed through a layer of silica, and concentrated under reduced pressure. The resulting oil was left crude and tested by NMR spectroscopy to determine the conversion to **111** (90% conversion from pinacolone). The NMR spectrum matched previously reported values. For **111** ¹H NMR (400 MHz, CDCl₃) δ 2.01 (s, 3H), 1.50 (s, 9H); for **110** ¹H NMR (400 MHz, CDCl₃) δ 2.33 (s, 3H), 1.00 (s, 1H).

Acid-catalyzed Baeyer-Villiger oxidation of ketone **76**



Ketone **76** (2.6 mg, 0.0096 mmol) was dissolved in DCM (0.50 mL) and cooled to 0 °C. *m*-Chloroperoxybenzoic acid (9.6 mg, 0.39 mmol, 4.0 equiv.) was added to the reaction mixture, followed by triflic acid (0.08 mL, 0.00096 mmol, 10 mol %), which was added dropwise. The reaction was allowed to warm to room temperature and stirred for 14 h. Upon completion of the reaction, as judged by TLC, the reaction was quenched via addition of H₂O (2 mL). The reaction was then extracted with DCM (3 x 4 mL). The organic layers were combined, dried over MgSO₄, filtered, passed through a layer of silica, and concentrated under reduced pressure. The resulting oil was left crude and tested by NMR spectroscopy to determine the conversion to **58** (32% yield). The NMR spectrum matched previously reported values. For **58** ¹H NMR (400 MHz, CDCl₃) δ 3.67 (d, *J* = 1.0 Hz, 2H), 2.52–2.48 (m, 2H), 2.26–2.21 (m, 2H), 1.56–1.50 (m, 2H), 1.20–1.17 (m, 19H) 0.931 (t, *J* = 6.8 Hz, 3H).

Base-catalyzed Baeyer-Villiger oxidation of **76**

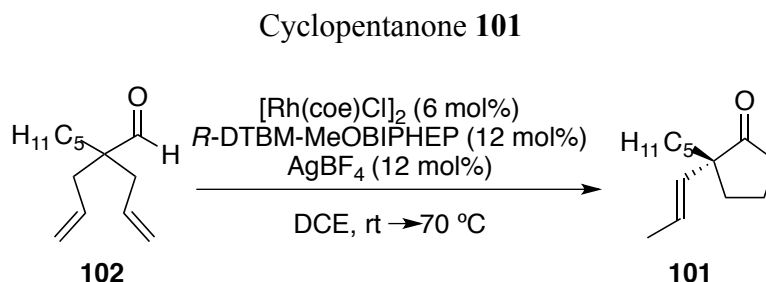


12% conversion, inseparable
from starting material

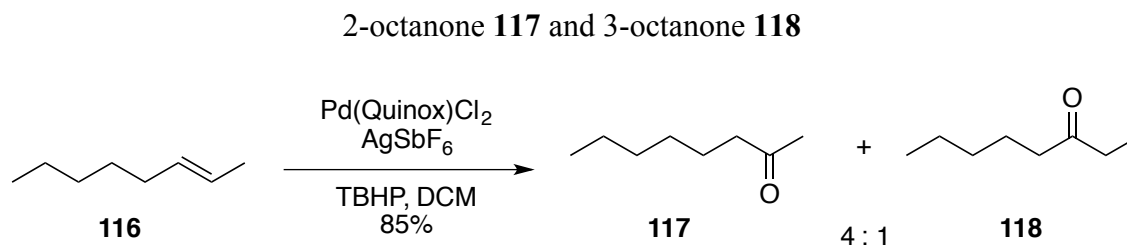
Ketone **76** (1.6 mg, 0.0060 mmol) was dissolved in DCM (5 mL) and cooled to 0 °C. *m*-Chloroperoxybenzoic acid (6.0 mg, 0.024 mmol, 4.0 equiv.) was added, followed by sodium bicarbonate (3.0 mg, 0.036 mmol, 6.0 equiv.). The reaction was allowed to warm to room temperature and stirred for 14 h. Upon completion of the reaction, as judged by TLC, the reaction was quenched via addition of H₂O (2 mL). The reaction was then extracted with DCM (3 x 5 mL). The organic layers were combined, dried over MgSO₄, filtered, passed through a layer of silica, and concentrated under reduced pressure. The resulting oil was left crude and tested by NMR spectroscopy to determine the conversion to **58** (12% conversion to **58**). The NMR spectrum matched previously reported values. For **58** ¹H NMR (400 MHz, CDCl₃) δ 3.42 (s, 2H), 2.44–2.41 (m, 2H), 2.10–1.98 (m, 2H), 1.84–1.80 (m, 1H), 1.56–1.50 (m, 1H), 1.20–1.17 (m, 19H) 0.931 (t, J = 6.8 Hz, 3H).

Synthesis of Adalinine Substrates

Aldehyde **102** was obtained from Dr. Jung-Woo Park for use in hydroacylation.

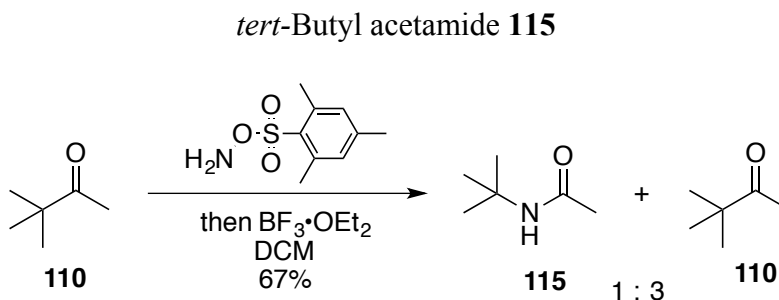


Aldehyde **102** (19.4 mg, 0.1 mmol) was subjected to the standard desymmetrizing hydroacylation conditions with the only modification being the catalyst loading being doubled to 12 mol %, as noted in the scheme above. The product, olefin **101**, was afforded as a colorless oil (12.2 mg, 0.063 mmol, 63% yield, 99 % ee). ¹H NMR (400 MHz, CDCl₃) δ 5.53–5.46 (m, 1H), 5.36–5.32 (m, 1H), 2.37–2.30 (m, 1H), 2.23–2.13 (m, 1H), 2.08–2.05 (m, 1H), 1.94–1.84 (m, 3H), 1.71 (dd, J = 6, 2.4 Hz, 3H), 1.32–1.28 (br, 8H), 0.91 (t, J = 6.8 Hz, 3H). For information regarding enantioselectivity, see literature precedent.¹⁶



Palladium dichloride (0.9 mg, 0.005 mmol, 5 mol %) was combined with Quinox (1.0 mg, 0.005 mmol, 5 mol %) and stirred in DCE (0.3 mL) for 2 h. Silver hexafluoroantimonate (4.5 mg, 0.012 mmol, 12 mol %) was then added to the reaction mixture and allowed to stir for

another 1 h. TBHP (0.2 mL, 1.2 mmol, 10.0 equiv.) was added and stirred for a further 10 minutes before an additional portion of DCE (0.58 mL). **116** (11.2 mg, 0.1 mmol) was added to the reaction mixture immediately following the dilution with DCE. The reaction was set to stir for 24 h. Upon completion of the reaction, as judged by NMR analysis, the reaction was flushed through a silica plug in DCM, evaporated under reduced pressure, and tested by NMR spectroscopy to assess the mixture of the two ketone products. The NMR spectrum matched previously reported values. ^1H NMR (400 MHz, CDCl_3) for **117** ^1H NMR (400 MHz, CDCl_3) δ 2.36 (t, $J = 7.2$ Hz, 2H), 2.07 (s, 3H), 1.21–1.15 (m, 8H), 0.87–0.80 (m, 3H); ^1H NMR (400 MHz, CDCl_3) for **117** δ 2.35 (t, $J = 7.6$ Hz, 4H), 1.21–1.15 (m, 9H), 0.87–0.80 (m, 3H).



Pinacolone (**110**) (49.7 mg, 0.50 mmol) was dissolved in DCM (1.0 mL). MSH (139.9 mg, 0.65 mmol, 1.25 equiv.) was dissolved in DCM (0.65 mL) and added to the reaction mixture and set to stir for 2 h. The reaction was then cooled to 0 °C for the addition of $\text{BF}_3 \cdot \text{OEt}_2$ (0.18 mL, 1.5 mmol, 3.00 equiv.), after which it was warmed back to room temperature for 3 h. Upon completion of the reaction, as judged by TLC, the reaction mixture was quenched via addition of H_2O (2 mL). The layers were separated, and the aqueous layer was extracted with DCM (3 x 5 mL). The organic layers were combined, dried over MgSO_4 , filtered, and concentrated under reduced pressure. The crude reaction mixture was tested via NMR analysis without further purification. The NMR values reported match those previously reported for *t*-butyl acetamide.

For **115** ^1H NMR (400 MHz, CDCl_3) δ 1.91 (s, 3H), 1.00 (s, 9H); for **110** ^1H NMR (400 MHz, CDCl_3) δ 2.33 (s, 3H), 1.00 (s, 1H).

1.5 References

1. Gutekunst, W. R.; Baran, P. S., C–H functionalization logic in total synthesis. *Chemical Society Reviews* **2011**, *40* (4), 1976-1991.
2. (a) Hofmann, A. W., Ueber die Einwirkung des Broms in alkalischer Lösung auf die Amine. *Berichte der deutschen chemischen Gesellschaft* **1883**, *16* (1), 558-560; (b) Löffler, K.; Kober, S., Über die Bildung des i-Nicotins aus N-Methyl-p-pyridyl-butylamin (Dihydrometanicotin). *Berichte der deutschen chemischen Gesellschaft* **1909**, *42* (3), 3431-3438.
3. (a) Trost, B. M.; Godleski, S. A.; Genet, J. P., A total synthesis of racemic and optically active ibogamine. Utilization and mechanism of a new silver ion assisted palladium catalyzed cyclization. *Journal of the American Chemical Society* **1978**, *100* (12), 3930-3931; (b) Taber, D. F.; Schuchardt, J. L., Intramolecular carbon-hydrogen insertion: synthesis of (+-)-pentalenolactone E methyl ester. *Journal of the American Chemical Society* **1985**, *107* (18), 5289-5290; (c) Taber, D. F.; Petty, E. H.; Raman, K., Enantioselective ring construction: synthesis of (+)-.alpha.-cuparenone. *Journal of the American Chemical Society* **1985**, *107* (1), 196-199.
4. Schultz, D. M.; Wolfe, J. P., Recent Developments in Palladium-Catalyzed Alkene Aminoarylation Reactions for the Synthesis of Nitrogen Heterocycles. *Synthesis* **2012**, *44* (03), 351-361.
5. Srikrishna, A.; Sheth, V. M.; Nagaraju, G., Rhodium Carbenoid Mediated C–H Activation of a Tertiary Methyl Group: An Enantiospecific Approach to the Angular Triquinanes Norsilphiperfolane and Norcameroonanes. *Synlett* **2011**, *2011* (16), 2343-2346.
6. (a) Rasik, C. M.; Brown, M. K., Total Synthesis of Gracilioether F: Development and Application of Lewis Acid Promoted Ketene–Alkene [2+2] Cycloadditions and Late-Stage C–H Oxidation. *Angewandte Chemie International Edition* **2014**, *53* (52), 14522-14526; (b) Li, Y.; Ding, Y.-J.; Wang, J.-Y.; Su, Y.-M.; Wang, X.-S., Pd-Catalyzed C–H Lactonization for Expedient Synthesis of Biaryl Lactones and Total Synthesis of Cannabinol. *Organic Letters* **2013**, *15* (11), 2574-2577.
7. Dhara, S.; Singha, R.; Ahmed, A.; Mandal, H.; Ghosh, M.; Nuree, Y.; Ray, J. K., Synthesis of α , β and γ -carbolines via Pd-mediated Csp²-H/N-H activation. *RSC Advances* **2014**, *4* (85), 45163-45167.
8. Huang, P.-C.; Parthasarathy, K.; Cheng, C.-H., Copper-Catalyzed Intramolecular Oxidative C–H Functionalization and C–N Formation of 2-Aminobenzophenones: Unusual Pseudo-1,2-Shift of the Substituent on the Aryl Ring. *Chemistry – A European Journal* **2013**, *19* (2), 460-464.
9. Pitts, A. K.; O'Hara, F.; Snell, R. H.; Gaunt, M. J., A Concise and Scalable Strategy for the Total Synthesis of Dictyodendrin B Based on Sequential C–H Functionalization. *Angewandte Chemie International Edition* **2015**, *54* (18), 5451-5455.
10. (a) Julich-Gruner, K. K.; Kataeva, O.; Schmidt, A. W.; Knölker, H.-J., Total Synthesis of 7- and 8-Oxygenated Pyrano[3,2-a]carbazole and Pyrano[2,3-a]carbazole Alkaloids via Boronic Acid-Catalyzed Annulation of the Pyran Ring. *Chemistry – A European Journal* **2014**, *20* (28), 8536-8540; (b) Kumar, V. P.; Gruner, K. K.; Kataeva, O.; Knölker, H.-J., Total Synthesis of the Biscarbazole Alkaloids Murrafoline A–D by a Domino Sonogashira Coupling/Claisen Rearrangement/Electrocyclization Reaction. *Angewandte Chemie International Edition* **2013**, *52*

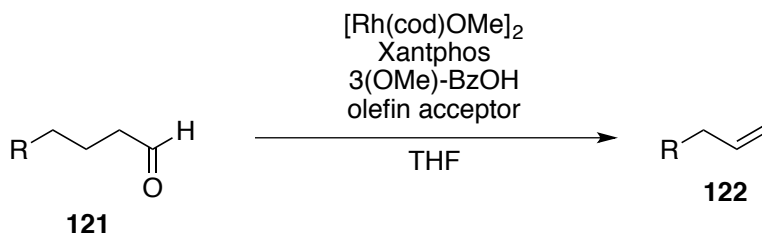
- (42), 11073-11077; (c) Hesse, R.; Kataeva, O.; Schmidt, A. W.; Knölker, H.-J., Synthesis of Prenyl- and Geranyl-Substituted Carbazole Alkaloids by DIBAL-H Promoted Reductive Pyran Ring Opening of Dialkylpyrano[3,2-a]carbazoles. *Chemistry – A European Journal* **2014**, *20* (31), 9504-9509; (d) Hesse, R.; Krahl, M. P.; Jäger, A.; Kataeva, O.; Schmidt, A. W.; Knölker, H.-J., Palladium(II)-Catalyzed Synthesis of the Formylcarbazole Alkaloids Murrayaline A–C, 7-Methoxymukonal, and 7-Methoxy-O-methylmukonal. *European Journal of Organic Chemistry* **2014**, *2014* (19), 4014-4028.
11. Bartholomäus, R.; Dommershausen, F.; Thiele, M.; Karanjule, N. S.; Harms, K.; Koert, U., Total Synthesis of the Postulated Structure of Fulcineroside. *Chemistry – A European Journal* **2013**, *19* (23), 7423-7436.
12. Mikula, H.; Skrinjar, P.; Sohr, B.; Ellmer, D.; Hametner, C.; Fröhlich, J., Total synthesis of masked *Alternaria* mycotoxins—sulfates and glucosides of alternariol (AOH) and alternariol-9-methyl ether (AME). *Tetrahedron* **2013**, *69* (48), 10322-10330.
13. Zhou, B.; Du, J.; Yang, Y.; Li, Y., Rhodium(III)-Catalyzed Intramolecular Redox-Neutral Annulation of Tethered Alkynes: Formal Total Synthesis of (±)-Goniomitine. *Chemistry – A European Journal* **2014**, *20* (40), 12768-12772.
14. (a) Chu, H.; Sun, S.; Yu, J.-T.; Cheng, J., Rh-catalyzed sequential oxidative C–H activation/annulation with geminal-substituted vinyl acetates to access isoquinolines. *Chemical Communications* **2015**, *51* (68), 13327-13329; (b) Jayakumar, J.; Parthasarathy, K.; Cheng, C.-H., One-Pot Synthesis of Isoquinolinium Salts by Rhodium-Catalyzed C–H Bond Activation: Application to the Total Synthesis of Oxychelerythrine. *Angewandte Chemie International Edition* **2012**, *51* (1), 197-200.
15. Dailler, D.; Danoun, G.; Ourri, B.; Baudoin, O., Divergent Synthesis of Aeruginosins Based on a C(sp³)-H Activation Strategy. *Chemistry – A European Journal* **2015**, *21* (26), 9370-9379.
16. Park, J.-W.; Kou, K. G. M.; Kim, D. K.; Dong, V. M., Rh-catalyzed desymmetrization of α-quaternary centers by isomerization-hydroacylation. *Chemical Science* **2015**, *6* (8), 4479-4483.
17. Singh, I. P.; Milligan, K. E.; Gerwick, W. H., Tanikolide, a Toxic and Antifungal Lactone from the Marine Cyanobacterium *Lyngbya majuscula*. *Journal of Natural Products* **1999**, *62* (9), 1333-1335.
18. Gutiérrez, M.; Andrianasolo, E. H.; Shin, W. K.; Goeger, D. E.; Yokochi, A.; Schemies, J.; Jung, M.; France, D.; Cornell-Kennon, S.; Lee, E.; Gerwick, W. H., Structural and Synthetic Investigations of Tanikolide Dimer, a SIRT2 Selective Inhibitor, and Tanikolide seco-Acid from the Madagascar Marine Cyanobacterium *Lyngbya majuscula*. *The Journal of Organic Chemistry* **2009**, *74* (15), 5267-5275.
19. (a) Mahajan, S. S.; Scian, M.; Sripathy, S.; Posakony, J.; Lao, U.; Loe, T. K.; Leko, V.; Thalhofer, A.; Schuler, A. D.; Bedalov, A.; Simon, J. A., Development of Pyrazolone and Isoxazol-5-one Cambinol Analogues as Sirtuin Inhibitors. *Journal of Medicinal Chemistry* **2014**, *57* (8), 3283-3294; (b) Heltweg, B.; Gathbonton, T.; Schuler, A. D.; Posakony, J.; Li, H.; Goehle, S.; Kollipara, R.; DePinho, R. A.; Gu, Y.; Simon, J. A.; Bedalov, A., Antitumor Activity of a Small-Molecule Inhibitor of Human Silent Information Regulator 2 Enzymes. *Cancer Research* **2006**, *66* (8), 4368-4377.
20. Kanada, R. M. T., T.; Ogasawara, K., The First Synthesis of (+)-Tanikolide, a Toxic and Antifungal Lactone from the Marine Cyanobacterium *Lyngbya Majuscula*. *Synlett* **2000**, *7*, 1019-1021.

21. Chen, Q. D., Haibing; Zhao, Jingrui; Lu, Yong; He, Mingyuan; Zhai, Hongbin, Two Efficient Four-Step Routes to Marine Toxin Tanikolide. *Tetrahedron* **2005**, *61*, 8390-8393.
22. Wu, F.; Hong, R.; Khan, J.; Liu, X.; Deng, L., Asymmetric Synthesis of Chiral Aldehydes by Conjugate Additions with Bifunctional Organocatalysis by Cinchona Alkaloids. *Angewandte Chemie International Edition* **2006**, *45* (26), 4301-4305.
23. Lognay, G.; Hemptinne, J. L.; Chan, F. Y.; Gaspar, C. H.; Marlier, M.; Braekman, J. C.; Dalozé, D.; Pasteels, J. M., Adalinine, a New Piperidine Alkaloid from the Ladybird Beetles *Adalia bipunctata* and *Adalia decempunctata*. *Journal of Natural Products* **1996**, *59* (5), 510-511.
24. Marples, N. M. B., P. M.; Cowie, R. J., Differences Between the 7-Spot and 2-Spot Ladybird Beetles (Coccinellidae) in Their Toxic Effects on a Bird Predator. *Ecological Entomology* **1989**, *14*, 79-84.
25. Yamazaki, N.; Ito, T.; Kibayashi, C., Total synthesis of the coccinellid alkaloid (-)-adalinine and the assignment of its absolute configuration. *Tetrahedron Letters* **1999**, *40* (4), 739-742.
26. Laurent, P.; Lebrun, B.; Braekman, J.-C.; Dalozé, D.; Pasteels, J. M., Biosynthetic studies on adaline and adalinine, two alkaloids from ladybird beetles (Coleoptera: Coccinellidae). *Tetrahedron* **2001**, *57* (16), 3403-3412.
27. Naoki Yamazaki, T. I., Chihiro Kibayashi, Facile Total Synthesis of (±)-Adalinine. *Synlett* **1998**, *1*, 37-40.
28. Shi, J.; Qiu, D.; Wang, J.; Xu, H.; Li, Y., Domino Aryne Precursor: Efficient Construction of 2,4-Disubstituted Benzothiazoles. *Journal of the American Chemical Society* **2015**, *137* (17), 5670-5673.
29. Elliott, C. E.; Miller, D. O.; Burnell, D. J., Synthesis of 6-alkyl analogues of the 1-azabicyclo[4.3.0]nonan-2-one system by a strategy of geminal acylation and Beckmann rearrangement. *Journal of the Chemical Society, Perkin Transactions 1* **2002**, (2), 217-226.
30. Michel, B. W.; Camelio, A. M.; Cornell, C. N.; Sigman, M. S., A General and Efficient Catalyst System for a Wacker-Type Oxidation Using TBHP as the Terminal Oxidant: Application to Classically Challenging Substrates. *Journal of the American Chemical Society* **2009**, *131* (17), 6076-6077.

Chapter 2: Tandem Oxidation-Dehydroformylation of Alcohols

2.1 Introduction

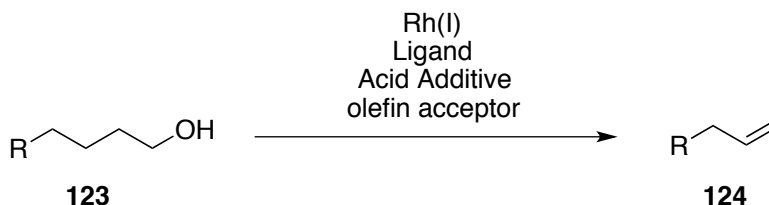
Historically, C–H activation of aldehydes via rhodium has been of significant interest to the scientific community. However, these acyl-rhodium-hydrides have generally been used for hydroacylation and decarbonylation.³¹ A far less common transformation is the dehydroformylation of the aldehyde to produce an olefin. A synthetic dehydroformylation can be used to mimic lanosterol demethylase, a cytochrome P450 enzyme that produces sterols in a wide variety of organisms.³² In addition, dehydroformylation allows for the modification of natural products and drugs for derivatization. The Dong group recently developed the first catalytic synthetic dehydroformylation of aldehydes to produce olefins using a rhodium catalyst (Scheme 38).³³ This reaction relies on the use of a carboxylate additive to prevent decarbonylation by acting as a proton shuttle to remove the hydride ligand from the acyl-rhodium (III)-hydride species and reduce the rhodium, forming an acyl-rhodium(I) species. As such, this methodology is able to transfer the aldehyde to a strained olefin acceptor at low catalyst loadings and under mild conditions.



Scheme 38: Rh-Catalyzed dehydroformylation of aliphatic aldehydes

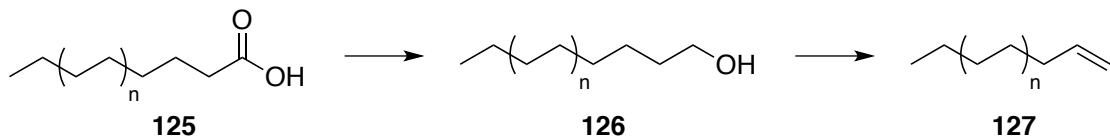
Although the new dehydroformylation protocol developed by our group is broadly applicable, aldehyde substrates are limited in their versatility. Thermal and photolytic

decomposition of aldehydes has been documented extensively.³⁴ These types of decomposition make them difficult substrates to generate and work with on a large scale. In addition, aldehydes are frequently incompatible with other common functional groups and generally require additional steps to generate them from other functional groups before dehydroformylation. In light of the disadvantages of aldehyde substrates, we decided to examine the possibility of using other starting materials for our dehydroformylation procedure. Since rhodium-catalyzed Oppenauer-type oxidations are precedented, we decided to investigate whether we could use primary alcohol substrates, which we could first oxidize, then dehydroformylate to afford the olefin in one reaction mixture.³⁵ Given the possibility of both performing the oxidation and the dehydroformylation with rhodium (I) catalysts, we decided to examine the possibility of a tandem oxidation-dehydroformylation (Scheme 39).



Scheme 39: Oxidation-Dehydroformylation of Alcohols

In addition to providing a useful method to avoid the need for aldehydes in dehydroformylation, a tandem oxidation-dehydroformylation reaction would provide a rapid, catalytic reaction to access odd-numbered olefins from the corresponding even numbered alcohols. Naturally abundant, affordable even-numbered fatty acids and esters can be reduced to the corresponding alcohols at low cost, making these alcohols an inexpensive feedstock. Odd-numbered olefins, however, are quite expensive, usually costing between 2 and 3 orders of magnitude more than the even-numbered alcohols and acids (Scheme 40).³⁶



Scheme 40: Generation of Odd-Numbered Olefins from Even-Numbered Acids

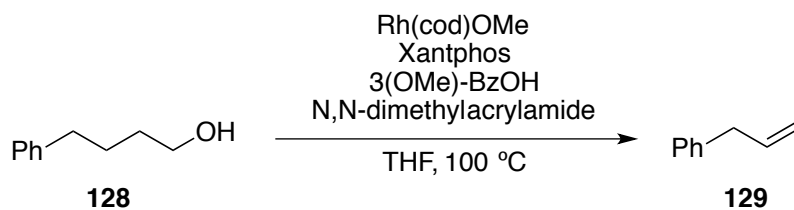
Dehydrogenation of alcohols has been known since the development of the original Oppenauer oxidation, discovered in the 1930's.^{35b} However, over the past several decades, the transition-metal catalyzed dehydrogenation of alcohols has gained significant interest. This transformation offers a catalytic method to activate sp^3 -hybridized carbons and generate olefins through the cleavage of a carbon-carbon bond.

We saw several potential difficulties in the development of this methodology. Metal-catalyzed oxidation of alcohols via dehydrogenation is widely preceded.^{35b} However, rhodium-catalyzed oxidation of primary alcohols usually requires harsh conditions, such as elevated temperature, to afford aldehydes in significant yield.³⁷ In addition, the basic conditions required for these oxidations led us to believe that we would likely need to adjust the buffer system for our reaction from the original dehydroformylation conditions in order to effect the tandem oxidation-dehydroformylation. In order to develop the tandem oxidation-dehydroformylation, we decided to screen a wide variety of conditions in order to find trends that might help in the optimization of both catalytic cycles simultaneously.

2.2 Results and Discussion:

Initially, Faben Cruz attempted to use our conditions from the group's previous transfer dehydroformylation for the tandem process.³³ However, Faben soon found that our original olefin acceptors and conditions resulted in low conversion, even when heated to improve conversion.

Both Faben and I screened a wide variety of olefin acceptors in our initial attempts to develop this reaction. The only acceptor that showed conversions over 50% was *N,N*-dimethyl acrylamide (initial conditions shown in Scheme 41). Even when combined as part of a mixed acceptor system, I saw no effect on the yield of the reaction compared to the same equivalents of acrylamide acceptor. In order to optimize our reaction conditions, I tested a number of parameters, including the solvent, ligand, and acid additive. Selected results of these screens are shown below in table 1.



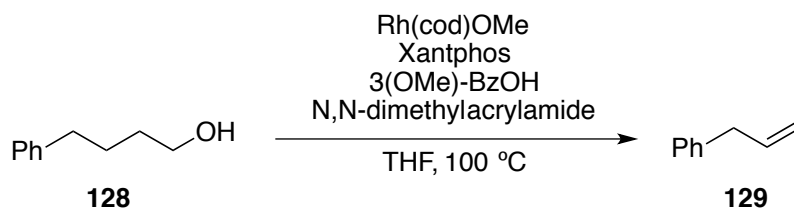
Scheme 41: Standard Conditions in Initial Screening

Table 1: Initial Parameter Screening for Reaction Optimization

Solvent	Ligand	Acid	Yield
THF	Xantphos	3(OMe)BzOH	85%
Dioxane	Xantphos	3(OMe)BzOH	59%
Toluene	Xantphos	3(OMe)BzOH	66%
DCE	Xantphos	3(OMe)BzOH	35%
MeCN	Xantphos	3(OMe)BzOH	15%
Acetone	Xantphos	3(OMe)BzOH	17%
EtOAc	Xantphos	3(OMe)BzOH	23%
2MeTHF	Xantphos	3(OMe)BzOH	66%
THF	DPEPhos	3(OMe)BzOH	27%
THF	BINAP	3(OMe)BzOH	0%
THF	PPh ₃	3(OMe)BzOH	7%
THF	Nixantphos	3(OMe)BzOH	42%
THF	dppp	3(OMe)BzOH	5%
THF	<i>t</i> Bu-Xantphos	3(OMe)BzOH	0%
THF	Walphos	3(OMe)BzOH	13%
THF	MeOBIPHEP	3(OMe)BzOH	0%
THF	Xantphos	4(OMe)BzOH	84%
THF	Xantphos	2(OMe)BzOH	80%
THF	Xantphos	BzOH	33%
THF	Xantphos	TFA	3%
THF	Xantphos	Tartaric Acid	6%
THF	Xantphos	Cinnamic Acid	72%
THF	Xantphos	4-F-BzOH	74%
THF	Xantphos	PivOH	76%

The results of this screening revealed that using *N,N*-dimethyl acrylamide as an acceptor resulted in higher conversion than any other strained olefin acceptor we tested. In addition, I found that THF was the best solvent for the reaction and that Xantphos outperformed the other ligands screened for this transformation, which is consistent with the group's previous dehydroformylation protocol.³³ 3-Methoxybenzoic acid and 4-methoxybenzoic acid were

comparable in their yields. As such, we decided to continue using 3-methoxybenzoic acid as our carboxylate additive (Scheme 42).



Scheme 42: Conditions for Tandem Oxidation-Dehydroformylation Following Initial Screening

However, since conversions remained at 85% even when heated to 100 °C for 24 h, I continued optimizing conditions for the reaction.

Interestingly, I only observed the hydrogenated olefin acceptors in all cases, seeing no evidence of the transfer of the carbonyl to any acceptor for our tandem oxidation-dehydroformylation. The hydroformylated acceptor was not observed in any of our reactions, unlike the group's previous dehydroformylation method.³³ I do not believe that this lack of transfer-hydroformylation is due to a decarbonylation of the hydroformylated acceptor, since I have found no evidence of the decarbonylation product of **128** as long as the acid proton shuttle is present in the reaction. Instead, I assessed that the rhodium catalyst dissociates from the carbonyl ligand at some point before the transfer hydroformylation can occur, releasing carbon monoxide gas into the headspace of the vial.

In order to assess which catalytic cycle was limiting the rate of the reaction, I monitored the reaction via NMR spectroscopy at a number of time points. This revealed that there was no observable buildup of aldehyde during the course of the reaction. As such, I believe that the dehydroformylation catalytic cycle takes place much faster than the transfer dehydrogenation.

Based on these results and the previous dehydroformylation project, our proposed catalytic cycle relies on two tandem catalytic cycles. One is based on the classic metal-catalyzed,

Oppenauer-type transfer dehydrogenation mechanistic cycle, as shown in figure 3. The resulting aldehyde intermediate is rapidly consumed in the second catalytic cycle, undergoing C–H activation through oxidative addition and dehydroformylation via insertion and β -hydride elimination from the aldehyde donor to form the desired olefin product.

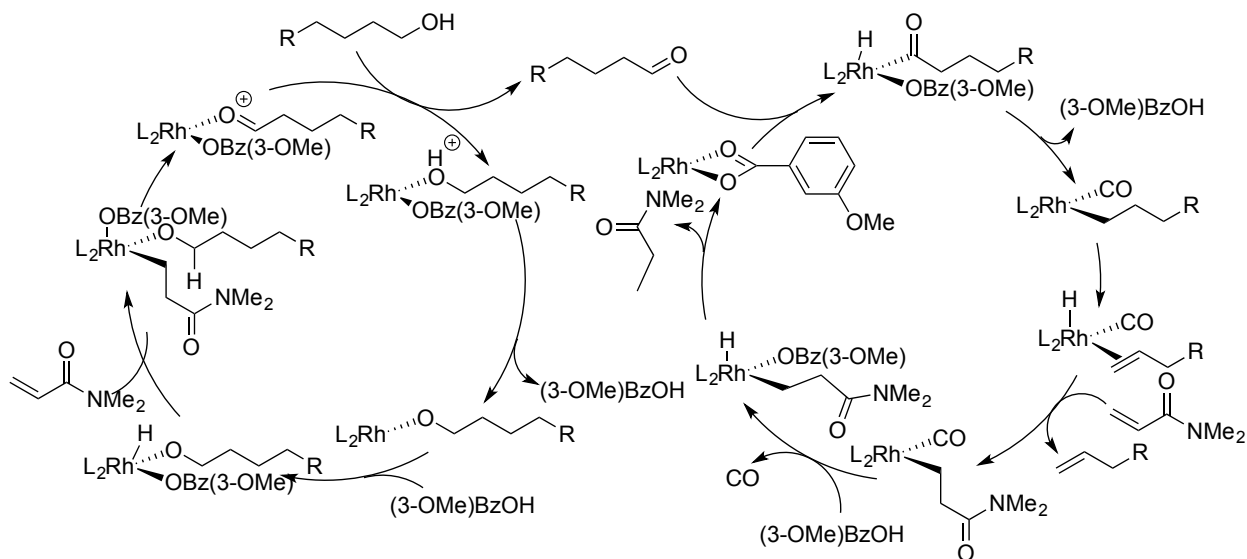


Figure 3: Proposed Mechanism for the Tandem Oxidation-Dehydroformylation

The removal of the hydride via reductive elimination with the carboxylate proton shuttle allows for the β -hydride elimination to take place without the competing decarbonylation.³³ However, following the dehydroformylation, the carbonyl ligand dissociates from the rhodium catalyst before binding to the olefin acceptor, generating another equivalent of the hydrogenated *N,N*-propylamide acceptor and carbon monoxide.

In order to enhance the rate of the alcohol oxidation cycle, I examined previous metal-catalyzed Oppenauer-type oxidations. Since most of these reactions require catalytic quantities of base, we realized that the acid required for the dehydroformylation might be inhibiting the oxidation cycle. As such, I worked to find a buffer system that would enhance the rate of the oxidation while allowing the dehydroformylation to take place. Since the majority of rhodium-catalyzed Oppenauer oxidations take place at high temperatures, I also investigated the optimal

temperature for the reaction.^{35b} The results of the temperature and base buffer screens are shown below in table 2.

Table 2: Base and Temperature Screening

Additional Base	Temperature	Yield
None	25 °C	0%
None	40 °C	0%
None	50 °C	2%
None	70 °C	5%
None	80 °C	32%
None	90 °C	45%
None	100 °C	83%
None	110 °C	95%
None	120 °C	52%
None	130 °C	41%
K ₂ CO ₃ (5 mol%)	100 °C	25%
NaHCO ₃ (5 mol%)	100 °C	72%
KOtBu (5 mol%)	100 °C	30%
DBU (5 mol%)	100 °C	67%
Et ₃ N (5 mol%)	100 °C	71%
<i>i</i> PrNEt ₂ (2 mol%)	100 °C	80%
<i>i</i> PrNEt ₂ (5 mol%)	100 °C	93%
<i>i</i> PrNEt ₂ (8 mol%)	100 °C	56%

Interestingly, I observed an increase in conversion with heating until a temperature of 110 °C. Although an increase in temperature should result in the acceleration of the reaction, the reaction did not progress beyond 24 h, indicating that this increase in conversion was likely due to degradation of the catalyst since starting material was still observed in the reaction. Since our reaction results in the buildup of carbon monoxide, I believe that this is the result of carbon monoxide binding to the rhodium and poisoning the catalyst. The observed temperature effect is due to the shift in equilibrium for carbon monoxide binding to rhodium, which favors the free catalyst and release of the carbonyl as a gas at high temperatures. When reactions over 110 °C were observed, very little solvent remained in the liquid phase in the vial, effectively increasing the concentration of the reaction, which is the likely cause for the decrease in yield at

temperatures above 110 °C. In addition to the observed temperature effect, the addition of Hünig's base appeared to generate a buffer system in the reaction that was more favorable for the oxidation of the alcohol substrate to the aldehyde than just the carboxylate formed from deprotonation of the benzoic acid additive. Following the screening of these conditions, I decided to use the combination of these conditions as our newly improved set of conditions for our reaction system, which resulted in yields of 95%.

Examining this theory of carbon monoxide poisoning the catalyst, I decided to attempt to use additives to remove the carbonyl ligand and re-activate the catalyst and increase the rate of the reaction. Based on earlier methods to remove carbonyls from metal centers, we decided to test amine-oxides to remove the carbonyl ligand from the metal.³⁸ However, the addition of trimethylamine N-oxide to the reaction, even in a quantity as low as 10 mol %, lowered the yield of the reaction to 10%. This may be due to binding of the amine-oxide to the metal center as another ligand, or due to oxidation of phosphine ligands by the amine-oxide at high temperatures.

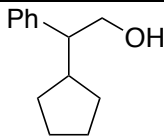
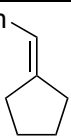
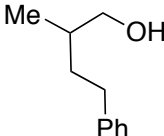
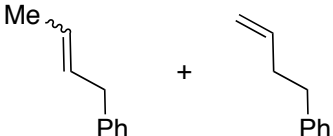
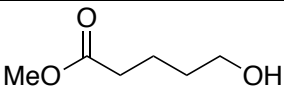
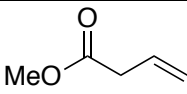
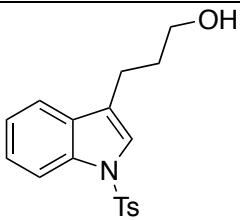
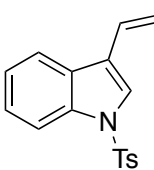
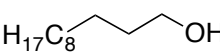
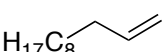
I also attempted to use trifuryl phosphine as a ligand in order to force the dissociation of the carbonyl from the catalyst via steric crowding of the rhodium catalyst.³⁹ Based on previous methods using this additional ligand to remove carbonyls from metal centers, we believed that these conditions might increase the rate of the reaction. However, upon addition of the trifuryl phosphine under the standard reaction conditions, the reaction yield decreased from 83% to 73%. As such, we believe that the trifuryl phosphine slows the reaction by binding to the rhodium catalyst in a reversible fashion, making the catalyst less accessible to the alcohol substrate. Based on these results, we decided to abandon attempts to use additives or additional ligands to prevent

carbonyl binding to the rhodium catalyst and to use the increased temperature conditions to favor the free catalyst.

Based on the success of our newly optimized standard conditions, and the failure of the efforts to remove the carbonyl ligand from the rhodium catalyst at lower temperatures, I decided to proceed with the current conditions for the oxidation-dehydroformylation reaction at the elevated temperature but without the Hünig's base. We decided that the use of Hünig's base was unnecessary, since the conversion was relatively high with just elevated temperature, and the base did not appear to significantly shorten the time of the reaction or lower catalyst loadings.

In order to test the functional group tolerance of the tandem oxidation-dehydroformylation, I synthesized a number of different substrates containing primary alcohols and subjected them to our original conditions while optimizing the reaction. The results of this preliminary substrate scope testing are shown below in table 3. Substrates were tested for conversion, but were not isolated and fully characterized since we were still optimizing the conditions at the time of the initial substrate scope.

Table 3: Preliminary Substrate Scope (only crude conversions and crude NMR spectra were taken as the project was put on hold before a formal substrate scope could be performed)

Substrate	Product	Yield
 <p>130</p>	 <p>131</p>	27%
 <p>132</p>	 <p>133 134</p>	58% 62 : 38 133 : 134
 <p>135</p>	 <p>136</p>	7%
 <p>137</p>	 <p>138</p>	6%
 <p>139</p>	 <p>140</p>	66%

Based on the results of the initial substrate scope, we observed that our tandem oxidation-dehydroformylation favors the formation of disubstituted olefins over monosubstituted olefins in a ratio of 62:38, despite the additional hydrogen atom present on the terminal position compared to the internal position. In addition, our tandem oxidation-dehydroformylation is able to generate trisubstituted olefins in addition to mono- and di-substituted olefins. In addition, I demonstrated that our methodology could be used to generate odd-numbered olefins from even-numbered alcohols, which are accessible via reduction of fatty acids. However, I found that our method does not provide high conversions for tosyl-protected indoles or methyl esters, resulting in a

large amount of starting material, possibly due to rhodium binding to these groups rather than performing the desired reaction.

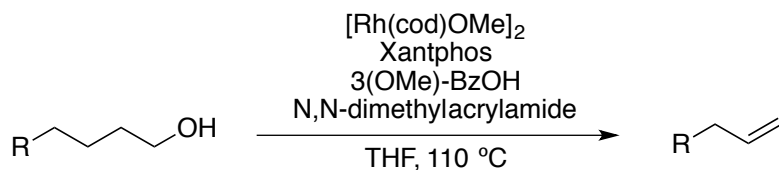
2.3 Conclusions:

Our efforts to generate a tandem oxidation-dehydroformylation reaction have been successful. In order to increase the rate and conversion of the reaction, we increased the temperature of the reaction and used Hünig's base as an extra additive. Initial substrate scope was then performed, showing that the reaction favors the formation of internal olefins over external olefins and is able to form mono-, di-, and trisubstituted olefins via the dehydroformylation reaction. In addition, we found that this method could be used in a two-step process to generate odd-numbered olefins from naturally abundant even-numbered carboxylic acids. This tandem oxidation-dehydroformylation is a subject of ongoing study in our lab.

2.4 Supporting Information

General Procedures

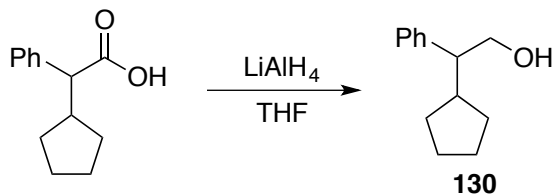
General Procedure for the tandem oxidation-dehydroformylation of primary alcohols



Methoxybis(cyclooctene) rhodium(I) dimer (2.5 mol %) was combined with Xantphos (5.5 mol %) and 3-(methoxy)benzoic acid (8 mol %), followed by THF (1.0 M). Alcohol substrate (1.00 equiv.) was then added to the reaction mixture, followed by *N,N*-dimethyl acrylamide (4.00 equiv.). The reaction mixture was then heated to 110 °C for 24 h, at which time it was cooled back to room temperature and opened to atmosphere to halt reaction progress.

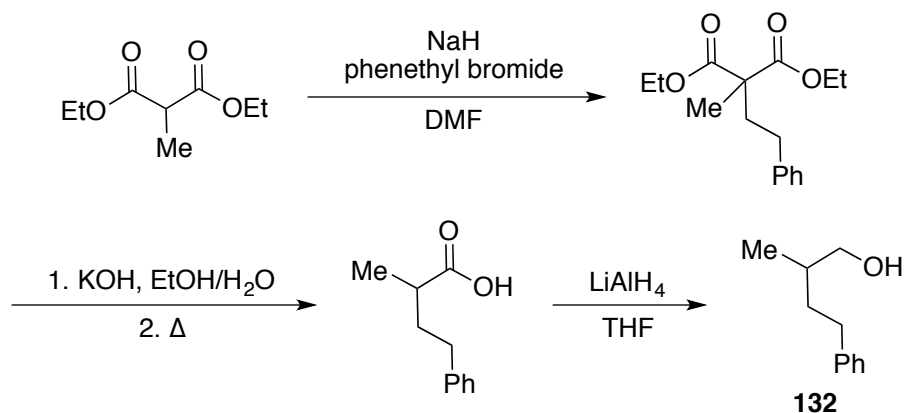
Synthesis of Substrates:

Synthesis of alcohol **130**



α -Phenyl cyclopentyl acetic acid (2.04 g, 10.0 mmol, 1.00 equiv.) was dissolved in THF (20 mL) and cooled to 0 °C. LiAlH_4 (0.950 g, 25.0 mmol, 2.50 equiv.) was added in portions and the reaction was stirred for 3 h. Upon completion of the reaction, as judged by TLC analysis, the reaction was quenched using the Fieser method and filtered through a pad of celite. Purification via a silica plug (25% EtOAc/75% Hex) afforded alcohol **130** (1.37 g, 7.20 mmol, 72% yield). ^1H NMR (400 MHz, CDCl_3) δ 7.40–7.36 (m, 2H), 7.31–7.27 (m, 3H), 3.95 (dd, $J = 10.8, 4.4$ Hz, 1H), 3.82 (dd, $J = 10.8, 5.2$ Hz, 1H), 3.97–3.80 (m, 1H), 2.64–2.58 (m, 1H), 2.12–2.08 (m, 1H), 1.98–1.95 (m, 1H), 1.74–1.70 (m, 1H), 1.62–1.56 (m, 2H), 1.49–1.46 (m, 2H), 1.34–1.29 (m, 1H), 1.09–1.04 (m, 1H).

Synthesis of alcohol **132**



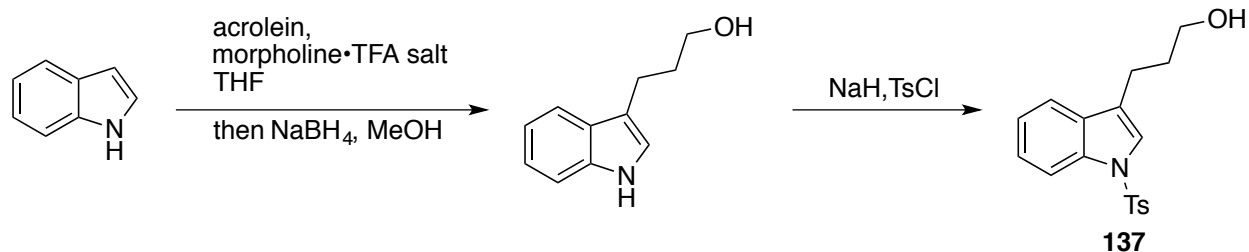
Sodium hydride (70% suspension in mineral oil, 600 mg, 17.5 mmol, 1.75 equiv.) was combined with DMF (20 mL) and cooled to 0 °C. Methyl diethyl malonate (1.74 mL, 10.0 mmol) was added to the reaction mixture dropwise. The reaction was allowed to stir for 10 minutes. Phenethyl bromide (1.64 mL, 12.0 mmol, 1.20 equiv.) was added to the reaction mixture dropwise, and the reaction was allowed to warm to room temperature while stirring for 4 h. Following completion of the reaction, as judged by TLC analysis, the reaction was quenched via dropwise addition of saturated NH₄Cl solution (10 mL) at 0 °C and diluted with ethyl acetate (30 mL). The organic and aqueous layers were separated, and the organic layer was washed with H₂O (3 x 10 mL). The organic layer was dried over MgSO₄, filtered, and concentrated under reduced pressure. Purification via column chromatography afforded the malonate as a colorless oil (1.73 g, 6.22 mmol, 62% yield). ¹H NMR: (400 MHz, CDCl₃): δ 7.38–7.28 (m, 2H), 7.26–7.23 (m, 3H), 4.24 (q, J = 7.2 Hz, 4H), 2.65–2.61 (m, 2H), 2.24–2.20 (m, 2H), 1.55 (s, 3H), 1.31 (t, J = 7.2 Hz, 6H).

Malonate (1.73 g, 6.22 mmol) was dissolved in EtOH (15 mL). 2M KOH (3.50 g, 62.3 mmol, 10.0 equiv.) in H₂O was added to the reaction mixture and heated to 80 °C for 14 h. Upon

completion of the reaction, as judged by TLC analysis, the reaction was cooled to room temperature and quenched with addition of excess 2 M HCl. Extraction with ethyl acetate (3 x 40 mL) was then performed. The organic layers were combined, dried over MgSO₄, filtered, and concentrated under reduced pressure. The crude malonic acid was then heated to 155 °C for 3 h. The resulting brown oil was purified via column chromatography to obtain the desired acid as a yellow oil (0.164 g, 0.921 mmol, 15% yield). ¹H NMR (400 MHz, CDCl₃): δ 7.35–7.31 (m, 2H), 7.25–7.24 (m, 3H), 2.74–2.70 (m, 2H), 2.57 (sextet, J = 7.2 Hz, 1H), 2.13–2.05 (m, 1H), 1.85–1.76 (m, 2H), 1.28 (d, J = 7.0 Hz, 6H).

The carboxylic acid (0.164 g, 0.921 mmol) was dissolved in THF (5 mL) and cooled to 0 °C. LiAlH₄ (87.0 mg, 2.30 mmol, 2.50 equiv.) was added in portions, and the reaction was allowed to warm to room temperature for 2 h. Upon completion of the reaction, as judged by TLC analysis, the reaction was quenched using the Fieser method and filtered through a celite plug in DCM. Purification via a silica plug (20% EtOAc/80% Hex) afforded alcohol **132** as a colorless oil (106 mg, 0.64 mmol, 70% yield). ¹H NMR (400 MHz, CDCl₃): δ 7.35–7.33 (m, 2H), 7.25–7.23 (m, 3H), 3.60 (dd, J = 10.4, 5.6 Hz, 1H), 3.53 (dd, J = 10.4, 6.4 Hz, 1H), 2.80–2.73 (m, 1H), 2.69–2.62 (m, 1H), 1.86–1.78 (m, 1H), 1.76–1.70 (m, 1H), 1.56–1.49 (m, 1H), 1.04 (d, J = 5.2 Hz, 3H).

Synthesis of alcohol **137**

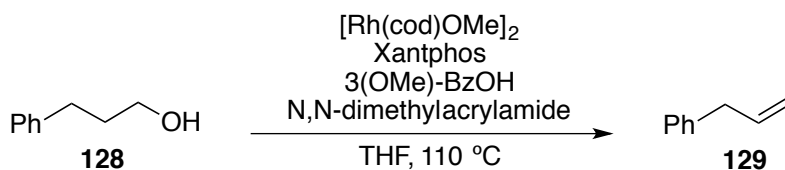


Acrolein (5.0 mL, 75 mmol, 3.00 equiv.) was dissolved in THF (100 mL). Morpholine·TFA salt (1.26 g, 6.35 mmol, 25 mol %) was added, followed by indole (2.86 g, 25.0 mmol, 1.00 equiv.). The reaction was warmed to 30 °C and stirred for 3.5 h. Following completion of the reaction, as judged by TLC, the reaction was concentrated under reduced pressure. The crude mixture was then dissolved in MeOH (100 mL) and cooled to 0 °C. NaBH₄ (1.89 g, 50.0 mmol, 2.00 equiv.) was added in portions, and the reaction mixture was warmed to ambient temperature, then stirred for 3 h. Upon completion of the reaction, as judged by TLC analysis, the reaction was quenched via addition of 1 M HCl (10 mL). The reaction mixture was diluted with 20 mL H₂O and concentrated under reduced pressure to remove methanol. The reaction mixture was then diluted with EtOAc (100 mL) and washed with H₂O (100 mL) and brine (100 mL). The organic layer was then dried over MgSO₄, filtered, and concentrated under reduced pressure. Purification via column chromatography (40% EtOAc/60% Hex) afforded 3-(3-hydroxypropyl)-1H-indole (3.0 g, 17 mmol, 68% yield). ¹H NMR (400 MHz; CDCl₃): δ 7.68 (dd, J = 7.9, 0.7 Hz, 1H), 7.41 (dd, J = 8.1, 0.7 Hz, 1H), 7.25 (td, J = 7.6, 0.9 Hz, 1H), 7.19 (td, J = 7.4, 1.0 Hz, 1H), 7.06 (s, 1H), 3.79 (t, J = 6.4 Hz, 2H), 2.92 (t, J = 7.5 Hz, 2H), 2.09–2.02 (m, 2H).

3-(3-Hydroxypropyl)-1H-indole (2.00 g, 11.4 mmol, 1.00 equiv.) was dissolved in DMF (57 mL) and cooled to 0 °C. NaH (0.500 g, 12.6 mmol, 1.10 equiv.) was added to the mixture and was stirred for 1 h. DMAP (140 mg, 1.14 mmol, 10 mol %) and TsCl (2.39 g, 12.6 mmol, 1.10 equiv.) were then added, and the reaction was warmed to 60 °C for 24 h. Upon completion of the reaction, as judged by TLC analysis, the reaction was quenched via addition of sat. aq. NH₄Cl (20 mL). The reaction mixture was then extracted with EtOAc (3 x 125 mL). The organic layers were combined, dried over MgSO₄, filtered, and concentrated under reduced pressure. Purification via column chromatography afforded alcohol **138** as a yellow oil (1.01 g, 28% yield). ¹H NMR (400 MHz; CDCl₃): δ 8.02 (m, 1H), 7.78 (m, 2H), 7.50–7.47 (m, 1H), 7.41 (m, 2H), 7.27–7.06 (m, 3H), 3.81–3.74 (m, 2H), 2.94–2.90 (m, 1H), 2.84–2.79 (m, 1H), 2.38 (s, 3H), 2.07–1.98 (m, 2H).

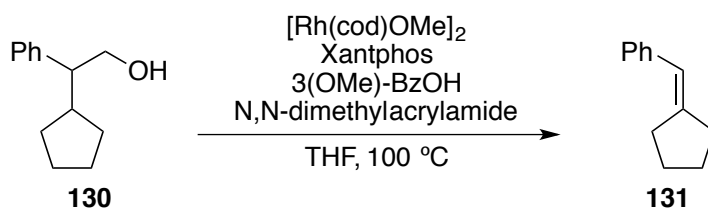
Tandem Oxidation-Dehydroformylation of Primary Alcohols

Allyl Benzene **129**



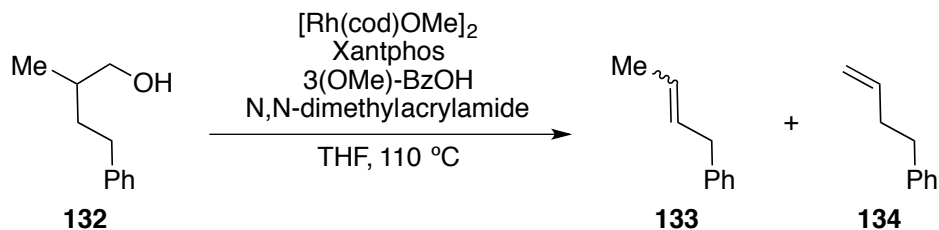
Alcohol **128** (13.6 mg, 0.100 mmol) was subjected to the standard oxidation-dehydroformylation conditions for 24 h. Upon completion of the reaction, the reaction mixture was quenched using standard conditions and was analyzed crude to determine conversion using 1,3,5-trimethoxybenzene as an internal GC/MS standard (95% yield). An example NMR spectrum from a different run of the reaction is included. ^1H NMR (400 MHz, CDCl_3): δ 7.32–7.29 (m, 3H), 7.23–7.19 (m, 3H), 6.02–5.95 (m, 1H), 5.12–5.06 (m, 2H), 3.40 (d, $J = 6.8$ Hz, 2H).

Olefin **131**



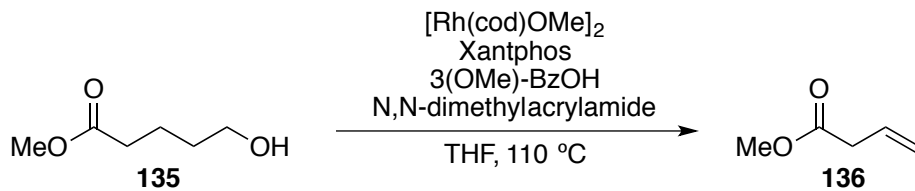
Alcohol **130** (19.0 mg, 0.100 mg) was subjected to the standard oxidation-dehydroformylation conditions for 24 h. Upon completion of the reaction, the reaction mixture was quenched using standard conditions and was analyzed crude to determine yield using 1,3,5-trimethoxybenzene as an internal NMR standard (27% yield). ^1H NMR (400 MHz, CDCl_3): δ 7.33–7.30 (m, 4H), 7.20–7.15 (m, 1H), 6.38 (quintet, $J = 2.4$ Hz, 1H), 2.58–2.54 (m, 2H), 2.52–2.48 (m, 2H), 1.80 (quintet, $J = 7.2$ Hz, 2H), 1.68 (quintet, $J = 6.4$ Hz, 2H).

Olefins **133** and **134**



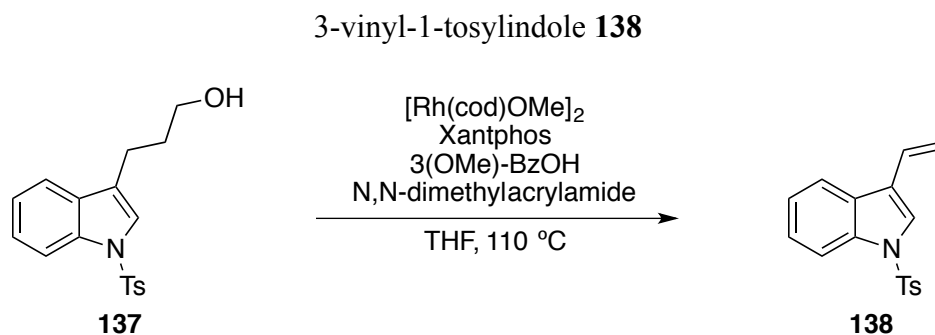
Alcohol **132** (16.4 mg, 0.100 mmol) was subjected to the standard oxidation-dehydroformylation conditions for 24 h. Upon completion of the reaction, the reaction mixture was quenched using standard conditions and was analyzed crude to determine conversion using 1,3,5-trimethoxybenzene as an internal NMR standard. Overall, 58% yield, 62:38 mixture of **133** and **134**, with 63% of the **133** being trans and 37% of **133** being cis. ^1H NMR (400 MHz; CDCl_3): for **133**, δ 7.33–7.29 (m, 2H), 7.23–7.15 (m, 3H), 5.63–5.49 (m, 2H), 3.43 (d, $J = 5.2$ Hz, 2H, cis), 3.41 (d, $J = 6.3$ Hz, 2H, trans), 1.71–1.69 (m, 3H, cis), 1.67–1.69 (m, 3H, trans); for **134**, δ 7.33–7.29 (m, 2H), 7.23–7.19 (m, 3H), 5.88–5.78 (m, 1H), 5.04–4.93 (m, 2H), 2.68 (t, $J = 7.8$ Hz, 2H) 2.37–2.35 (m, 2H).

Methyl 4-butenolate **136**

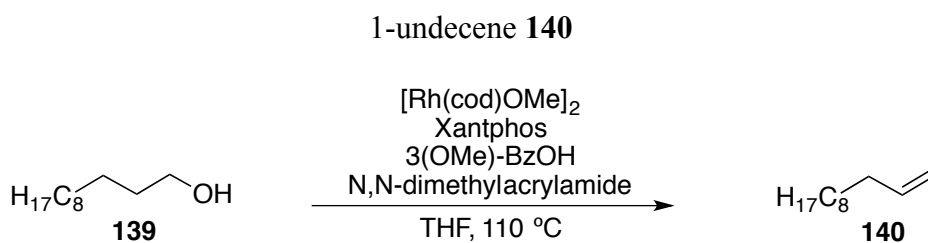


Alcohol **134** (13.2 mg, 0.100 mmol) was subjected to the standard oxidation-dehydroformylation conditions for 24 h. Upon completion of the reaction, the reaction mixture was quenched using standard conditions and was analyzed crude to determine conversion using

1,3,5-trimethoxybenzene as an internal NMR standard. ^1H NMR (400 MHz, CDCl_3): δ 6.99–6.90 (m, 2H), 5.84–5.79 (m, 1 H), 3.06 (s, 3H), 2.30 (d, $J = 3.6$ Hz, 2H).



Alcohol **138** (32.9 mg, 0.100 mmol) was subjected to the standard oxidation-dehydroformylation conditions for 24 h. Upon completion of the reaction, the reaction mixture was quenched using standard conditions and was analyzed crude to determine conversion using 1,3,5-trimethoxybenzene as an internal NMR standard. ^1H NMR (400 MHz; CDCl_3): δ 8.01 (d, $J = 8.2$ Hz, 1H), 7.79–7.73 (m, 3H), 7.62 (s, 1H), 7.34 (ddd, $J = 8.2, 7.2, 1.1$ Hz, 1H), 7.26 (s, 1H), 7.22–7.19 (m, 2H), 6.78 (ddd, $J = 17.8, 11.3, 0.7$ Hz, 1H), 5.80 (dt, $J = 17.8, 0.6$ Hz, 1H), 5.35 (dd, $J = 11.3, 1.1$ Hz, 1H), 2.32 (s, 3H).



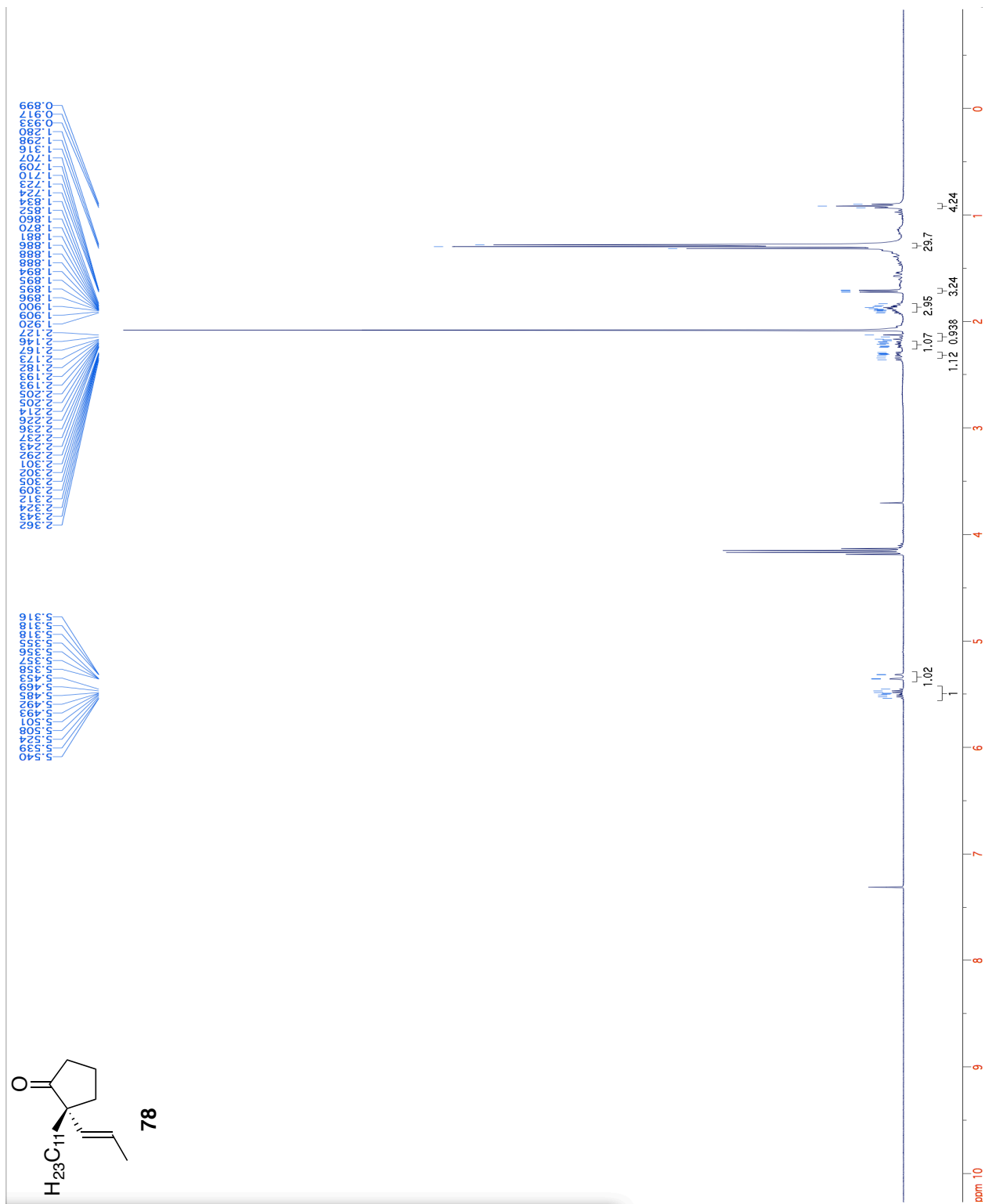
Alcohol **140** (17.2 mg, 0.100 mmol) was subjected to the standard oxidation-dehydroformylation conditions for 24 h. Upon completion of the reaction, the reaction mixture was quenched using standard conditions and was analyzed crude to determine conversion using 1,3,5-trimethoxybenzene as an internal NMR standard. ^1H NMR (400 MHz; CDCl_3): δ 5.76–5.71

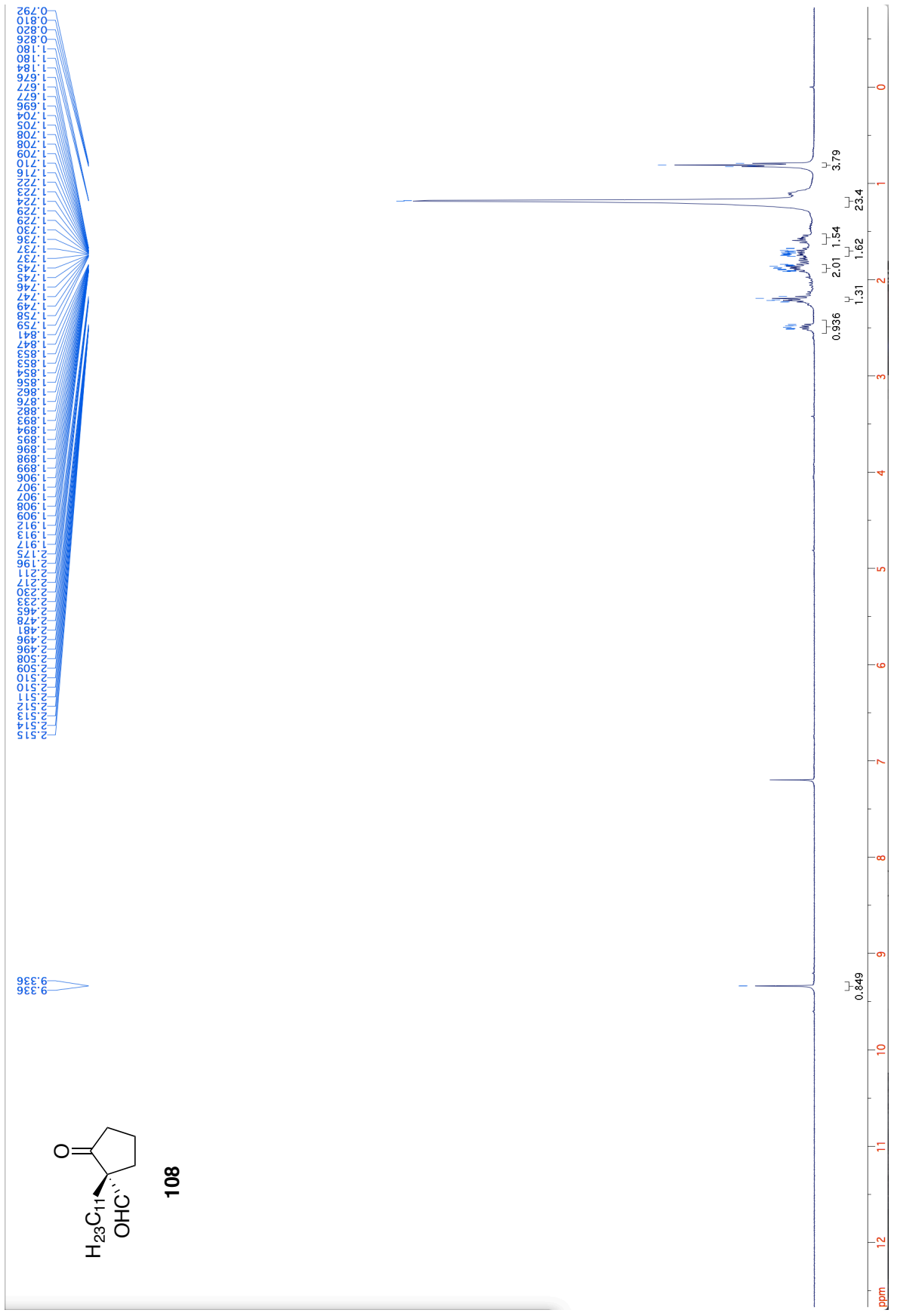
(m, 1H), 4.93 (dt, $J = 17.3, 0.8$ Hz, 1H), 4.86 (dt, $J = 8, 0.8$ Hz, 1H), 1.99–1.96 (m, 2H), 1.81–1.78 (m, 14H), 0.82 (t, $J = 6.8$ Hz, 3H).

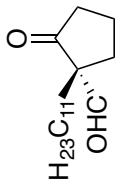
2.5 References

31. (a) Willis, M. C., Transition Metal Catalyzed Alkene and Alkyne Hydroacylation. *Chemical Reviews* **2010**, *110* (2), 725-748; (b) Tsuji, J.; Ohno, K., Organic syntheses by means of noble metal compounds XXI. Decarbonylation of aldehydes using rhodium complex. *Tetrahedron Letters* **1965**, *6* (44), 3969-3971; (c) Kreis, M.; Palmelund, A.; Bunch, L.; Madsen, R., A General and Convenient Method for the Rhodium-Catalyzed Decarbonylation of Aldehydes. *Advanced Synthesis & Catalysis* **2006**, *348* (15), 2148-2154.
32. Lepesheva, G. I.; Waterman, M. R., Sterol 14 α -demethylase cytochrome P450 (CYP51), a P450 in all biological kingdoms. *Biochimica et Biophysica Acta (BBA) - General Subjects* **2007**, *1770* (3), 467-477.
33. Murphy, S. K.; Park, J.-W.; Cruz, F. A.; Dong, V. M., Rh-catalyzed C-C bond cleavage by transfer hydroformylation. *Science* **2015**, *347* (6217), 56-60.
34. (a) Ho, S. K., The Thermal Decomposition of Aliphatic Aldehydes. *Proceedings of the Royal Society of London A: Mathematical, Physical and Engineering Sciences* **1963**, *276* (1365), 278-292; (b) Grela, M. A.; Colussi, A. J., Kinetics and mechanism of the thermal decomposition of unsaturated aldehydes: benzaldehyde, 2-butenal, and 2-furaldehyde. *The Journal of Physical Chemistry* **1986**, *90* (3), 434-437; (c) Norrish, R. G. W., Bamford, C. H., Photodecomposition of Aldehydes and Ketones. *Nature* **1936**, *138*, 1016.
35. (a) Jun, C.-H.; Huh, C.-W.; Na, S.-J., Direct Synthesis of Ketones from Primary Alcohols and 1-Alkenes. *Angewandte Chemie International Edition* **1998**, *37* (1-2), 145-147; (b) Dobreiner, G. E.; Crabtree, R. H., Dehydrogenation as a Substrate-Activating Strategy in Homogeneous Transition-Metal Catalysis. *Chemical Reviews* **2010**, *110* (2), 681-703.
36. Liu, Y.; Kim, K. E.; Herbert, M. B.; Fedorov, A.; Grubbs, R. H.; Stoltz, B. M., Palladium-Catalyzed Decarbonylative Dehydration of Fatty Acids for the Production of Linear Alpha Olefins. *Advanced Synthesis & Catalysis* **2014**, *356* (1), 130-136.
37. Takahashi, M.; Oshima, K.; Matsubara, S., Hydrogen transfer type oxidation of alcohols by rhodium and ruthenium catalyst under microwave irradiation. *Tetrahedron Letters* **2003**, *44* (51), 9201-9203.
38. Shvo, Y.; Hazum, E., A new method for the synthesis of organic iron carbonyl complexes. *Journal of the Chemical Society, Chemical Communications* **1975**, (20), 829-830.
39. Cato, M. A., *Frontiers in Organometallic Chemistry*. Nova Science Publishers: New York, 2006.

Appendix A: Spectral Information





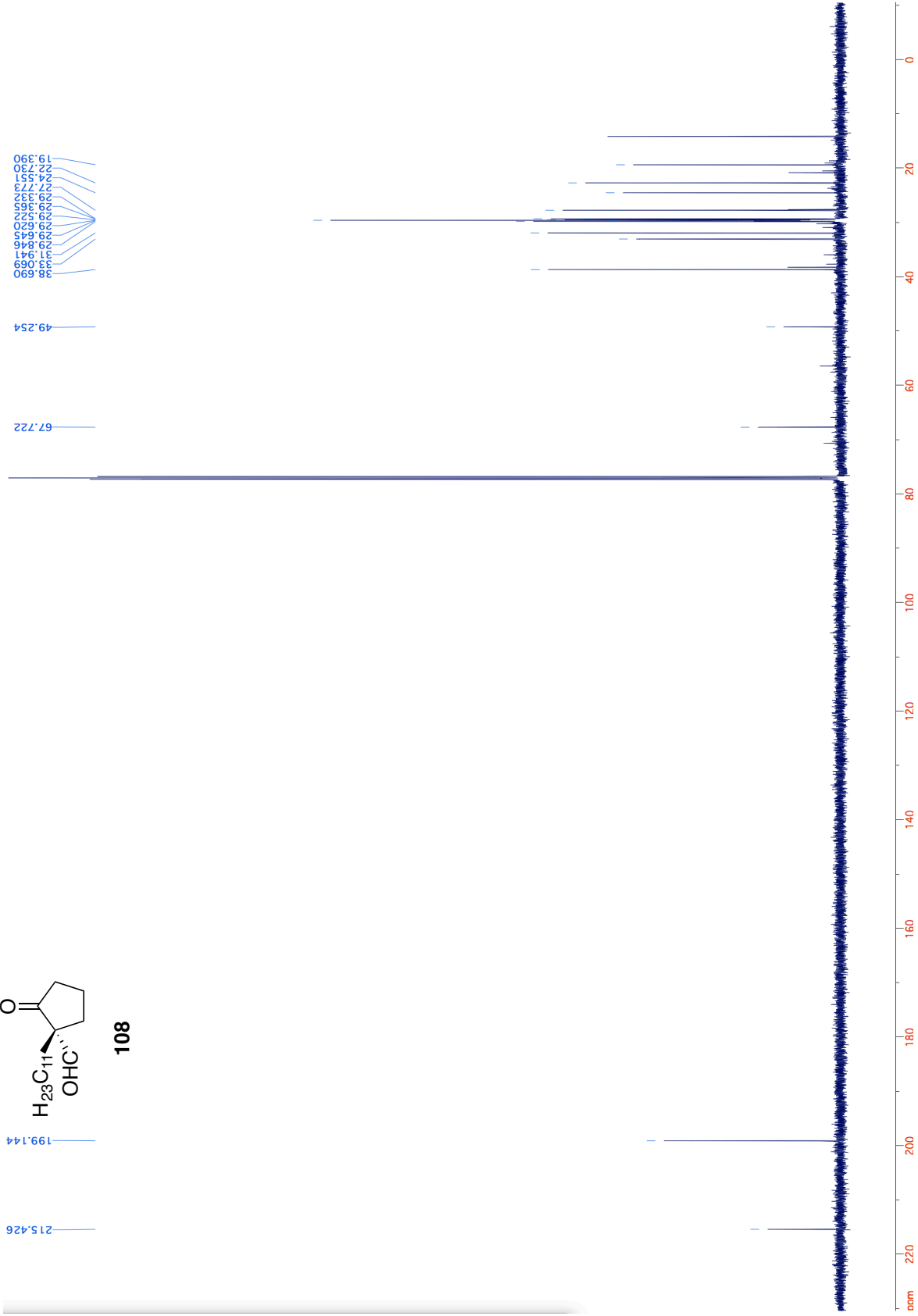


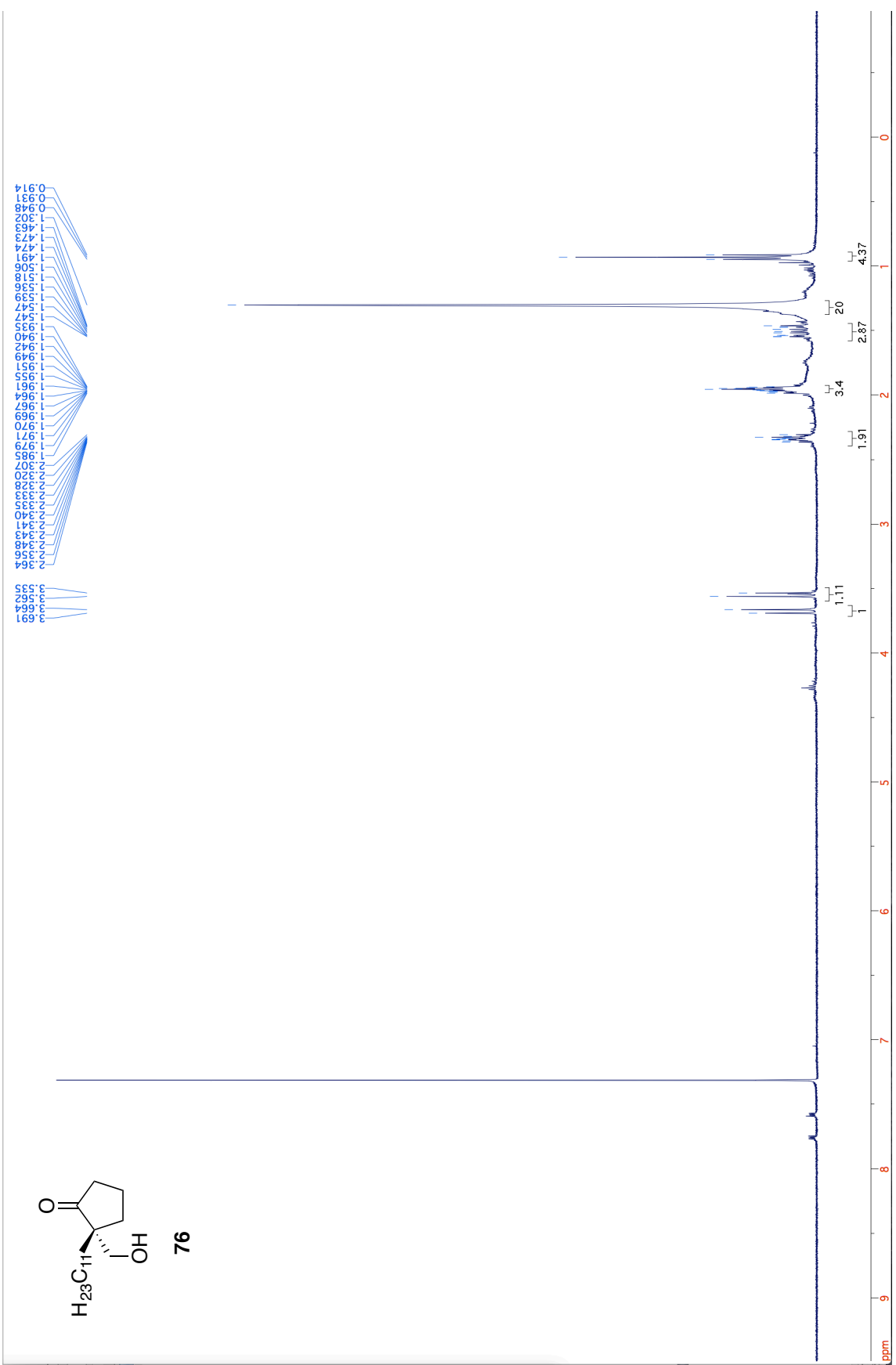
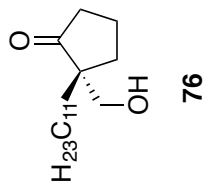
108

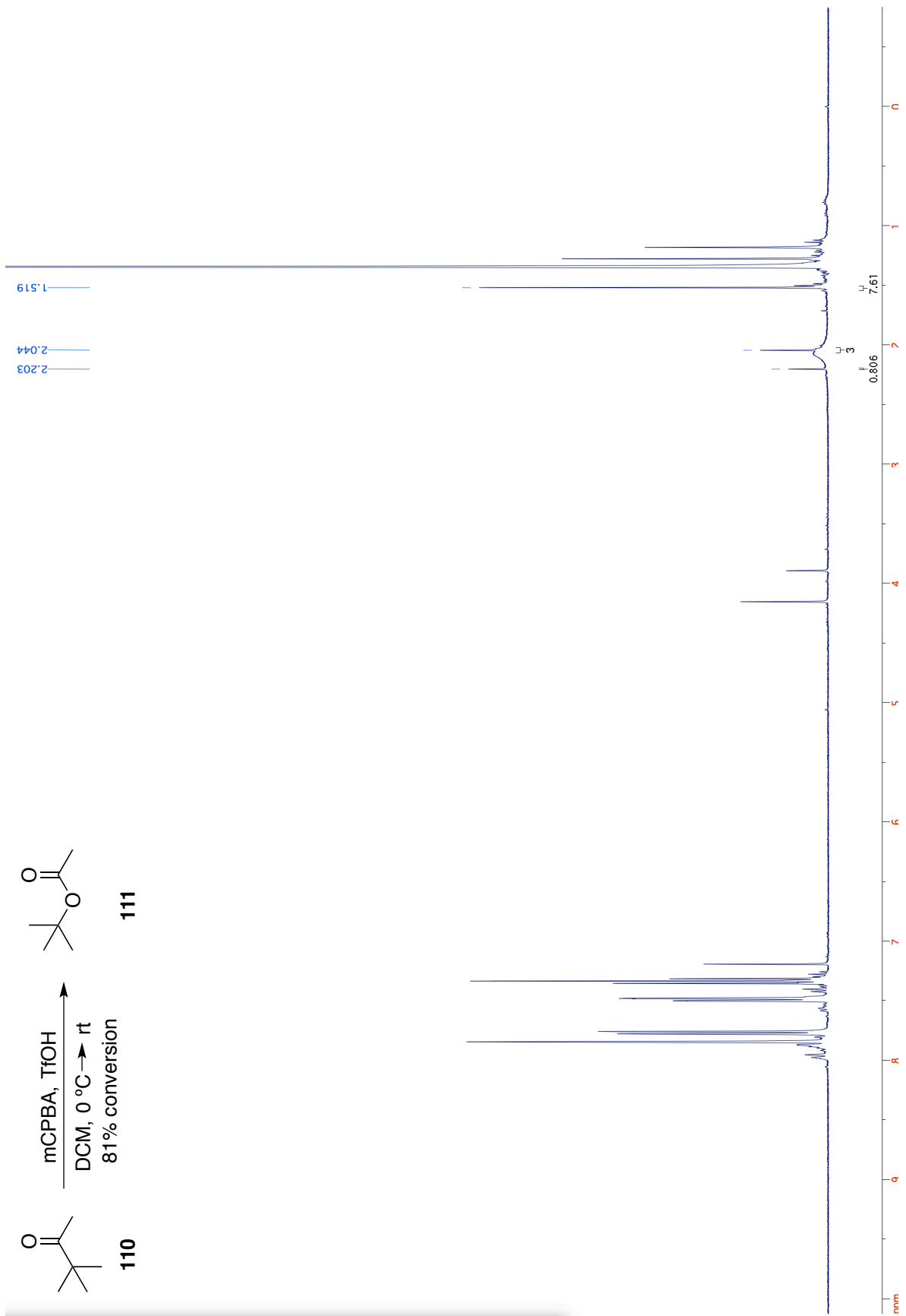
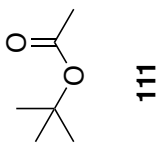
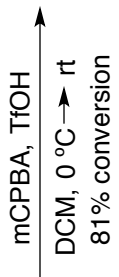
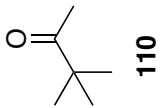
199.144
215.426

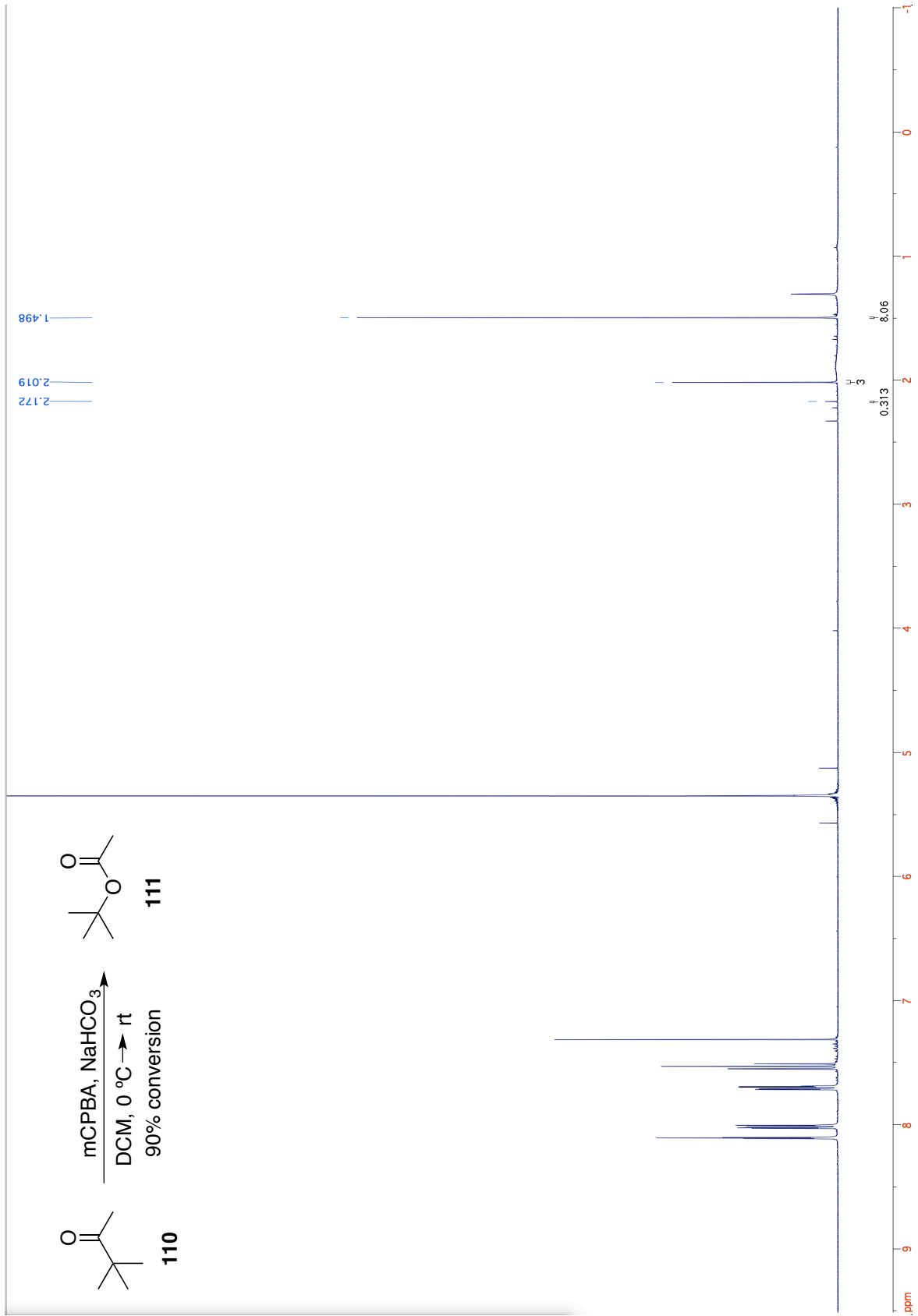
38.690
33.069
31.941
29.846
29.645
29.620
29.522
29.365
29.332
27.773
24.531
22.730
19.390

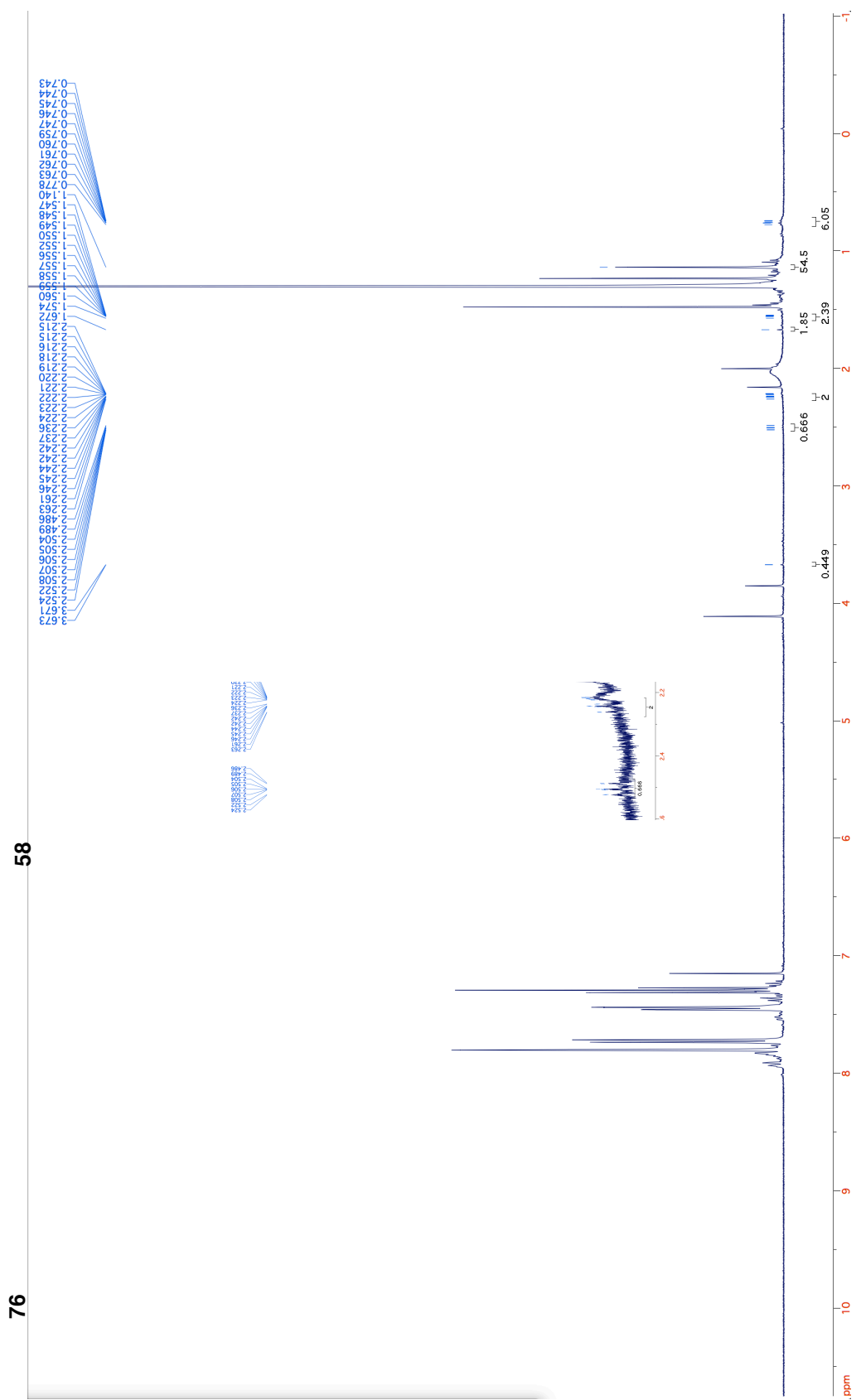
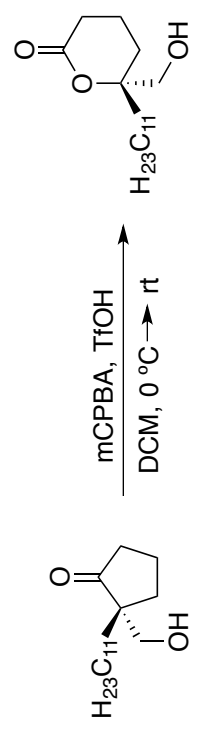
49.254
67.722

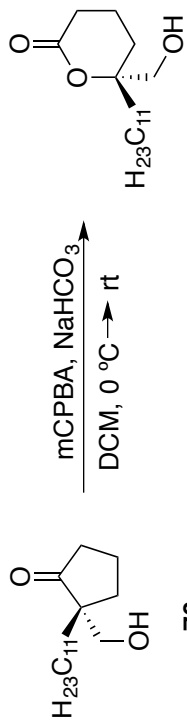












76

58

